TÉCNICO LISBOA

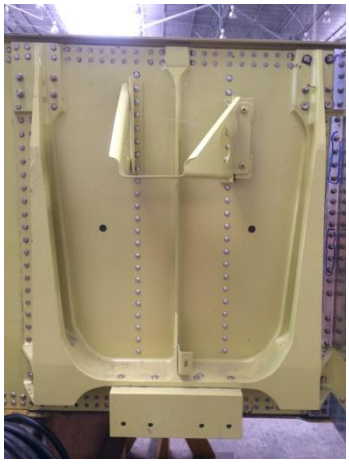

Sealant Joints in Aircraft Integral Fuel Tanks

João Pedro Róis Policarpo

Thesis to obtain the Master of Science Degree in

Aerospace Engineering

Supervisor: Prof. Luís Filipe Galrão dos Reis

Examination Committee

Chairperson: Prof. Fernando José Parracho Lau

Supervisor: Prof. Luís Filipe Galrão dos Reis

Members of the Committee: Prof. Filipe Szolnoky Ramos Pinto Cunha

Eng. Marco Frederico Espanhol

November 2014

Acknowledgements

I would like to express my gratitude to my Professor Luis Reis and my supervisor Engineer Marco Espanhol for their valuable advice, encouragement and availability throughout this research. I also would like to thank Engineers Carlos Rodrigues and Andreia Mendonça for their important input and time serving as well as valuable advice in performing experimental work.

A special thanks to all my friends and teachers who directly or indirectly contributed towards this study.

Above all, my sincere gratitude to my parents, family and my girlfriend for their encouragement, support, patience and love that arouses me each day to continue my investigation.

Abstract

Leaks arising from aircraft fuel tanks have constantly represented a problem for aircraft manufacturers, operators and maintenance crews. The integral fuel tanks within aircraft structures are in general located within the wings and they rely on sealant materials to prevent leakage through joints and fasteners. However, aircraft integral fuel tanks are designed from a structural point of view first and as a fuel tank second. There are numerous potential leak paths for the fuel on these complex wing structures.

The overall aim of the current research was to reduce the fuel leaks in the aircraft fuel tanks at the delivery. Following this approach a company background analysis was performed in order to find out the regions in the fuel tanks susceptible of fuel leaks. A Finite Element Analysis (FEA) of a critical structural member was done to investigate the structural behavior and propose structural improvements. A workcard with instructions to perform a nondestructive inspection (NDI) in the identified structural member was developed.

A research and test of new sealants products was accomplished. The main goal was to initiate a research and test of potential sealants products in order to conduct a future proposal to the Lockheed Martin. A maintenance instructions manual was developed in respect to the procedure to inspect, clean and seal the fuel tanks. It was introduced simplified maintenance instructions to all the technicians in order to make possible an accurate sealing of the fuel tanks.

Keywords: Aircraft, External Fuel Tank, Pylon Fitting, Structural Analysis, Sealants, Maintenance Instructions.

Resumo

As fugas provenientes dos tanques de combustível das aeronaves estão associadas a inúmeros problemas para os fabricantes, operadores e equipas de manutenção. Os tanques de combustível integrais compreendidos no interior da estrutura da aeronave são, geralmente, localizados no interior das asas e dependem de materiais selantes para evitar fugas através das articulações e elementos de ligação. No entanto, os tanques de combustível integrais são projectados primeiramente do ponto de vista estrutural e só depois como tanque de combustível, resultando assim em inúmeras possibilidades de fugas.

O principal objectivo consistiu em reduzir as fugas de combustível nos tanques das aeronaves na fase de entrega. De forma a determinar as zonas dos tanques de combustível mais susceptíveis a fugas, efectuou-se uma análise ao histórico da empresa. Com base nesses resultados e de forma a investigar o comportamento estrutural e propor melhorias, foi realizada uma análise de elementos finitos (FEA) a um membro estrutural crítico. Foi também desenvolvida uma carta de inspecção com instruções para executar uma inspecção não destrutiva (NDI) no elemento identificado.

Seguidamente realizou-se uma pesquisa e testes a novos selantes. Teve-se como objectivo iniciar uma investigação de potenciais produtos para propor futuramente à Lockheed Martin. Foi desenvolvido um manual de instruções de manutenção relativamente ao procedimento de inspecção, limpeza e selagem dos tanques de combustível. Nesse manual foram introduzidas instruções simplificadas de manutenção de forma a tornar possível uma selagem eficaz nos tanques de combustível.

Palavras-chave: Aeronave, Tanque Combustível Externo, Pylon Fitting, Análise Estrutural, Selantes, Instruções de Manutenção.

List of contents

List of Figures

List of Tables

Abbreviations, Acronyms and Nomenclature

In this document, the Imperial System is used, as required by OGMA – Indústria Aeronáutica de Portugal, S.A.

Acronyms

Acronym	***Meaning***
AMS	Aerospace Material Specification
APDL	ANSYS Parametric Design Language
ASTM	American Society for Testing and Materials
CAD	Computer–aided design
FEA	Finite Element Analysis
FEM	Finite Element Model
FOD	Foreign Object Damage
IGES	Initial Graphics Exchange Specification
JP	Jet Propellant
LEL	Lower Explosive Limit
MFW	Maximum Fuel Weight
MIL	Military Specification
MMA	Military Aircraft Maintenance
MMPDS	Metallic Materials Properties Development and Standardization
MPC	Multipoint Constraints
MTOW	Maximum Take–off Weight
NDI	Nondestructive Inspection
OEM	Original Equipment Manufacturer
OWS	Outer Wing Station
RBE	Rigid Body Elements
SA	Anonymous Society
SCF	Stress Concentration Factor
SF	Safety Factor

Nomenclature

Variable	*Meaning*	*Variable*	*Meaning*
A_{cross}	Cross section of the fastener	K_t	Stress concentration factor,
A_{net}	Net area	$\rho_{20000\,ft}$	Air density 20000ft
$C_{D_{Pylon}}$	Drag coefficient Pylon	$\sigma_{applied}$	Applied Stress
$C_{D_{Tank}}$	Drag coefficient External Fuel Tank	σ_{bru}	Ultimate bearing stress
C_D	Drag coefficient	σ_{bry}	Yield bearing stress
CG	Center of Gravity	σ_{local}	Local Stress
D_1	Drag force components front Fitting	$\sigma_{nominal}$	Nominal Stress
D_2	Drag force components rear Fitting	σ_{su}	Ultimate shear stress
$Drag_{ExternalTank}$	External Tank Drag force	σ_{tu}	Ultimate tensile stress
$Drag_{Installation}$	Installation Drag force	σ_{ty}	Yield tensile stress
$Drag_{Pylon}$	Pylon Drag force	$\sigma_{ultimate}$	Ultimate Stress
E_{fast}	Modulus of elasticity of the fastener material	A	Tom Swift's equation constant in function of the fasteners material
E_{skin}	Young modulus of the skin	B	Tom Swift's equation constant in function of the fasteners material
F_i	Force ‘i’	c	Pylon length
K_x	Fasteners spring constant in the 'x' direction	c/t	Length–to–height ratio
K_y	Fasteners spring constant in the 'y' direction	d	External Tank maximum diameter
K_z	Fasteners spring constant in the 'z' direction	l	External Tank length
L_{fast}	Fastener length	l/d	Length–to–diameter ratio or fineness ratio
M_D	Moment created by the Drag force	MFW	Maximum fuel weight
M_i	Moment ‘i’	MS	Margin of safety
P_{brg}	Bearing failure load	MS_1	Margin of safety considering the maximum 1st Principal Stress
P_{fs}	Fastener Shear failure load	MS_2	Margin of safety considering the maximum 2st Principal Stress
P_{net}	Ultimate design net tensile failure load	MS_3	Margin of safety considering the maximum 3st Principal Stress

$P_{tearout}$	Tear–out failure load	$MS_{Bearing}$	Margin of safety considering the maximum bearing
R_1	Vertical reaction created at the front Fitting	MS_{Force}	Margin of safety considering the maximum tensile and shear force
R_{1w}	Vertical reaction created at the front Fitting considering only W	MTOW	Maximum take–off weight
R_2	Vertical reaction created at the rear Fitting	S_1	Principal Stress in the direction 1
R_{2w}	Vertical reaction created at the rear Fitting considering only W	S_2	Principal Stress in the direction 2
S_{Pylon}	Front effective surface of the Pylon	S_3	Principal Stress in the direction 3
S_{tank}	Front effective surface of the fuel tank	t	Pylon height
S_{wet}	Wet Surface	ρ	Density
U_x	‘x’ degree of freedom	D	Fastener diameter
U_y	‘y’ degree of freedom	E	Material Modulus of elasticity
U_z	‘z’ degree of freedom	H	Vertical distance components R1 or R2 to the CG
$V_{20000\,ft}$	Free air stream speed 20000ft	W	Gravitational force
d_1	Horizontal distance between the component R1 and the CG	e	Edge margin
d_2	Horizontal distance between the component R2 and the CG	n	Load factor
$t_{doubler}$	Doubler thickness	t	Thickness of the particular member
t_{skin}	Skin thickness	θ	Banked angle
F_x	Banked turn ‘x’ force component	υ	Material Poisson's ratio
F_y	Banked turn ‘y’ force component		

1. Introduction

1.1. Background

Aircraft fuel tanks correspond to a constant source of problems for aircraft designers and users. The integrity of sealed joints in the integral fuel tanks of military and civil aircraft has important cost, operational, safety and environmental implications. Integral fuel tanks within aircraft structures are typically located within the wings. Usually, aircraft integral fuel tanks are designed from a structural point of view first and as a fuel tank second. The skin of the wing is attached to the inner structure of the wing and the joints connecting the internal structure and the skin has to be sealed to avoid leakage of fuel. The structures on an aircraft as the C–130 are designed and manufactured with the use of machined parts that, if sealed correctly, perform both as a load bearing structural element and as an integral fuel tank. Unfortunately, inside the wings of an aircraft there are innumerable potential leak pathways for the fuel ranging from those between inter–faying surfaces, those from skin joints, those from the fasteners themselves, those from conduits (housing electric cables) and those from pipes and hoses (for fuel, hydraulic and de–icing fluids). It can also be added the special effects of flight stress fatigue, temperature, contaminants (water, deicer fluid and microbiological attack), the fuel itself and application failures on original assembly and at following repairs. It can therefore be appreciated that the potential for leaks is vast.

The operational life of an aircraft can be more than 30 years with no considerable operational leaks, but after a certainly period it starts to emerges several problems that increases the cost of maintenance and the current aircraft is no longer viable to operate.

In a single typical wing of a military aircraft it is likely that there is about 660 lbs of sealant substance. This is applied and has to stick to prepared, coated and anodized aluminum in current aircraft. As a result a sealed joint system comprises the sealant, basic coverage coating(s) and the parent skin material (figures. 1.1 and 1.2) [1], [2].

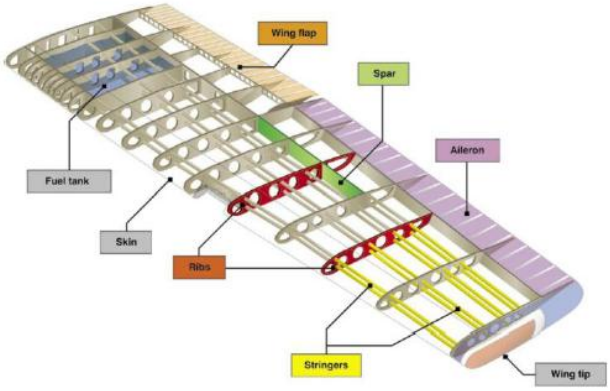

Figure 1.1 – Internal wing components [3]

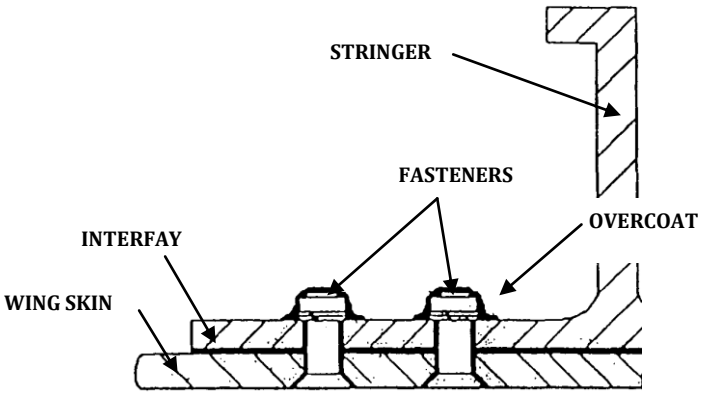

Figure 1.2 – Cross section through the wing skin and stringer. Application of the overcoat [1]

Current approaches to sealant assessment embrace a range of different tests at different conditions, of both bulk sealant samples and sealed joints, as well as the normal lap shear and peel tests. The investigation for new sealants has to be an active project in the current aerospace industry.

1.2. Purpose of Research Work

Integral fuel tank sealing methods presently employed by the major aerospace companies are faying surface and fillet sealing with the wet installation and over–coating of fasteners (Figure 1.2). The most common sealing materials are based on polysulfide compounds, which have been used by the aircraft industry for over 50 years. When polysulfide materials are applied carefully within the manufacturing process requirements of the aircraft constructor, they provide a reliable sealing method against fuel leakage. However, in–service experience with sealing integral fuel tanks has been far from satisfactory. This may be due to the possible influence of combined dynamic and environmental factors on sealant performance and sealant degradation. A key concept for the future evaluation of sealant materials for military or commercial aircraft is to expose realistic samples or sealed joint systems to typical environmental parameters representative of maintenance conditions.

The development and update of a procedure to inspecting, cleaning, sterilizing and sealing fuel tanks is an essential requirement of this research program. The investigation for new sealants has also to be part of this project in order to reduce the fuel leaks. In addition a finite element analysis (FEA) of a critical structural member in terms of fuel leaks is crucial to understand the behavior of it when subjected to different load conditions.

There are several factors that became the driving force behind this research project. The first is that the numbers of fuel leaks that appear during the delivery of the aircraft have been increasing in the last years (chapter 3). Secondly, due to this delay the schedule performed previously has to be readjusted and it probably interferes with the customer's program. Thirdly, the maintenance and operational costs increase substantial which have a negative impact in the company.

Frequently asked questions and factors that should be considered and addressed as the cause of leaks in fuel tanks are:

- Is the correct sealant used?
- What are the procedures for applying the sealant and are they correct?
- What surface preparation is used and is this adequate?
- Are the test conditions and methods (temperature, pressure, fatigue, etc) adequate?
- Are the sealants used in the joint compatible with each other?
- Are the substrates and fasteners compatible?
- The design of the joint itself (tolerances, corrosion and assembly stress).

1.3. Aims and Objectives

This thesis has been developed at the MMA (military aircraft maintenance) department of the company OGMA – Indústria Aeronáutica de Portugal, SA. The company is official approved by Lockheed Martin Corporation to perform maintenance to all C–130 aircraft models (except the new C–130J) following the procedures included in the manuals and operate with approved products and materials. However, the use of new products or a structural modification in some element requires the OEM (Original Equipment Manufacturer) approval.

The overall aim of the current research was to mitigate or reduce the fuel leaks in the aircraft fuel tanks at the delivery. A research and test for new sealants products were performed and the maintenance instructions manual developed, evaluated and updated in respect to the procedure to inspect, clean and seal the fuel tanks. Following this approach a FEA of a critical structural member was done to investigate the structural behavior.

These outputs are going to be used by OGMA – Indústria Aeronáutica de Portugal, SA. The main target is to propose new sealant products and an updated maintenance instructions manual as well as a workcard with instructions to inspect the identified critical locations. The direct result of the developed work is to reduce the maintenance hours and avoid delays in the aircraft delivering, contributing to optimize the costs of the company.

The main objectives are:

- To study a structural member and use FEA to analyze and propose structural improvements;
- Develop and update a workcard with instructions to perform a nondestructive inspection (NDI) in the identified structural member, in specific areas.
- To research and test for new sealants products;
- To develop, evaluate and update the maintenance instructions manual;

1.4. Thesis Structure

The current thesis comprises 7 chapters. The first of them is the introduction, where the general scope of the thesis is presented.

The second chapter consists in the Literature review of aircraft wing design and integral fuel tank technology as well as some theoretical relevant concepts concerning the static analysis.

The third chapter presents the historical analysis, where it's reviewed the historical data of fuel leaks in the C–130 aircraft fleet based on a company database.

The fourth chapter presents the Pylon Fitting analysis. The purpose of this chapter is to evaluate the static behavior of the Pylon Fitting component under ultimate loads to determine the critical areas on the structure and propose structural improvements. In the same chapter it is also developed and updated a workcard with instructions to perform a nondestructive inspection.

The fifth chapter presents the sealants and sealant testing. This chapter considers the geometrical and material considerations that govern a typical sealed joint and the sealants tests performed.

The sixth chapter considers the maintenance instructions where it's presented a brief resume of the general sealing instructions and methods to identify leaks sources in integral tanks.

The seventh chapter contains the main conclusions extracted from that project, and a future work suggestion.

2. Literature Review

The purpose of this chapter is to review the aircraft wing design and integral fuel tank technology as well as some theoretical relevant concepts concerning the static analysis.

2.1. General Wing Design Considerations

2.1.1. Structural Principles

The wings have to incorporate aerodynamic shapes, in some aircraft serve as fuel tanks and support the engine structures. They must withstand the effects of inclement weather (rain, hail, lightning strikes and FOD “Foreign Object Damage”) and must be durable and serviceable with the minimum of maintenance. Structural integrity is a major factor in aircraft design and construction. An aircraft structure in flight is subjected to many, and different, stresses due to the varying loads that may be imposed. The problem is trying to anticipate the possible stresses which the structure will have to withstand, and to build it sufficiently robustly to resist these. This issue is aggravated by the fact of the aircraft structure must be obviously light as well as strong. Current production aircraft are constructed of various materials, the primary one being aluminum alloys. Rivets, bolts, screws and adhesives are used to hold all parts in place. A comprehensive review of airframe design is given by [4] and [5].

2.1.2. Types of Structural Stress

The structure of an aircraft is required to support two distinct classes of load:

- Ground loads; including all loads during movement or transportation on the ground such as taxiing and landing loads, towing and hoisting loads
- Air loads; comprising loads imposed in the structure during flight by maneuvers and gusts.

The two classes of loads can be further divided into surface forces (e.g. aerodynamic) and body forces which act over the volume of the structure and are produced by gravitational and inertial effects. These loads will result in stresses being experienced by the aircraft's structure.

Limit loads are the maximum loads anticipated on the airframe during its life and the airframe should be capable of supporting these loads without permanent deformation. Ultimate loads are the load at which complete failure occurs. The ultimate load is normally related to the limit load by the following formula [4]:

$$Ultimate\ load = Limit\ Load\ \times Safety\ factor \quad (2.1)$$

In general, the safety factor is 1.5 [4].

2.1.3. Wing Construction

Wing construction is basically the same in all types of aircraft. To maintain the aerodynamic shape, a wing must be designed and built to hold its shape even under extreme stress. Basically, the wing is a framework composed chiefly of spars, ribs, stringers and skin (Figure. 1.1). Spars are the main members of the wing. They extend lengthwise along the wing (crosswise to the fuselage). The entire load carried by the wing is ultimately taken by the spars and skin. In flight, the force of the air acts against the skin. From the skin, this force is transmitted to the ribs and then to the spars.

Most wing structures have two spars, the front spar and the rear spar. The front spar is found near the leading edge while the rear spar is located about two thirds of the distance towards the trailing edge.

The ribs are the parts of a wing which support the covering and provide the aerofoil shape. These ribs are called forming ribs. Their primary purpose is to provide shape. Some may have an additional purpose of bearing flight stress, and these are called compression ribs. The ribs are formed and have flanges around their edges to enable the skin and spar webs to be fastened to them. Cut–outs around their edges allow the span–wise stringers to go through them. Stringers are machined and connect the wing skin panels to the rib/spar structure by the use of fasteners and the aforementioned flanges. They also give stiffness and form to the skin as they run longitudinally from root to wing tip.

The strongest wing structure is the full cantilever which is attached directly to the fuselage, via the carry–through structure, and does not have any type of external, stress–bearing structures (figure 2.1) [6].

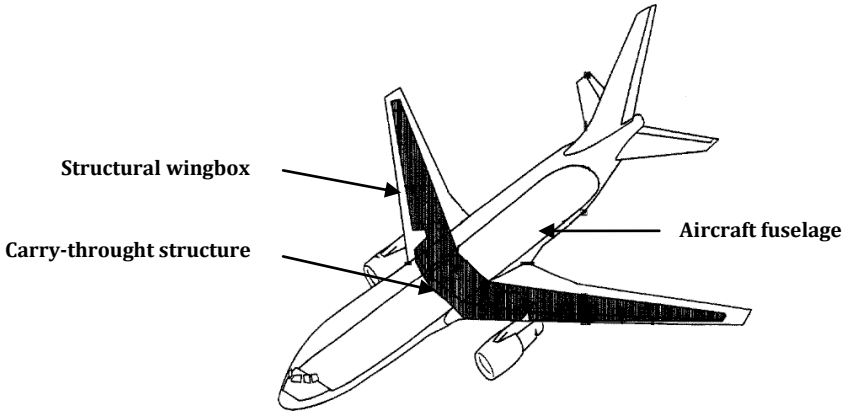

Figure 2.1 – Wing carry–through structure [7]

2.1.4. Design Parameters

The flying surfaces as typified by the wing are essentially cantilever beams (figure 2.1). Cantilever wings must resist all loads with their own internal structure. The aircraft weight tends to bend the wing and the bending load is carried primarily by the spars. Attached to the spars are ribs that give the aerodynamic shape to the wing (figure 1.1). The skin is attached to all the structural members and carries part of the wing loads and stresses.

In addition to acting as a beam to resist span wise loads, the wing must also carry considerable torsion loads and provide sufficient stiffness to prevent excessive twist. This load arises primarily from the flaps and control surfaces. A reduction in the thickness/chord ratio (the ratio between the thickness of a wing section and the chord, which is the distance between the leading and trailing edge) is critical since the bending strength is proportional to this dimension. The aspect ratio of a wing is defined to be the square of the span divided by the wing area. This ratio is a measure of how long and slender a wing is from tip to tip. A reduced aspect ratio thus reduces both bending moment and twist and this is structurally advantageous. During flight, stresses are transmitted first to the wing skin, then to the ribs, and finally to the spars. Spars also must carry loads distributed by the fuselage, landing gear and any nacelles (terminology for any part that is joined to the structure of the wing, such as the engines and pylons). As has been mentioned previously, most aircraft use the area between the spars as a fuel tank. The mass of the fuel acts in the opposite direction to wing lift, thus reducing wing bending moment and, hence, stress. The amount and disposition of the fuel weight in the wing is particularly important as it can provide bending relief during flight. Placing fuel as far outboard as possible and using fuel from the most outboard tanks last would appear to provide the optimum arrangement for wing bending during flight [4]. However, if one considers the large inertia effects of the fuel and the resultant bending of the wing in a downward direction in the event of a hard landing, for example, to avoid aquaplaning on a wet runway, this arrangement of the fuel is not necessarily the best solution and can cause excessive stresses on the wing structure. From this it can be seen how important fuel management during flight is.

Fuel in an aircraft is redistributed in the fuel tank for several reasons besides bending relief. Fuel tapped from the engine high pressure fuel line cools the engine oil. This, in turn, heats the fuel and from this a recirculation system returns part of the heated fuel to the wing tanks to prevent frosting.

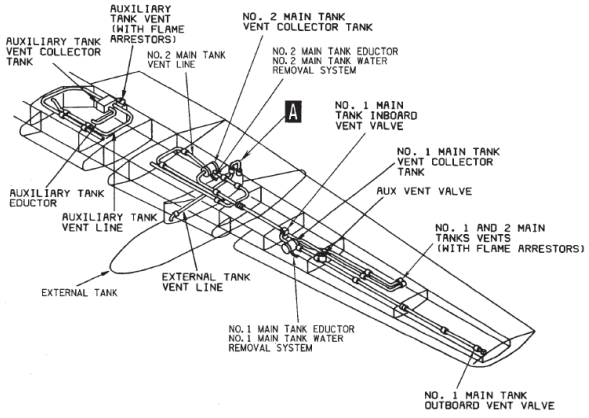

Figure 2.2 – Figure schematic of fuel tank vent system components [1]

The fuel system also allows for ventilation and surge (figure 2.2). The fuel venting system prevents over stressing of the tank structure by maintaining near ambient air pressure between tanks during re–fuelling and fuel use, engine consumption, fuel tank transfer and also during climb and descent. Each fuel tank is vented through vent lines into a surge tank [1].

2.2. Types of Fuel Tanks and Integral Fuel Tank Technology

2.2.1. Types of Aircraft Fuel Tanks

Aircraft typically use three types of fuel tanks: integral, rigid removable and bladder [3].

- Integral tanks are areas inside the aircraft structure that have been sealed to allow fuel storage. This type of fuel tank is presented in depth next since it is object of study in this thesis. In the present study the tanks 1, 2, 3 and 4 represents tanks of this type (figure 2.3) [8].

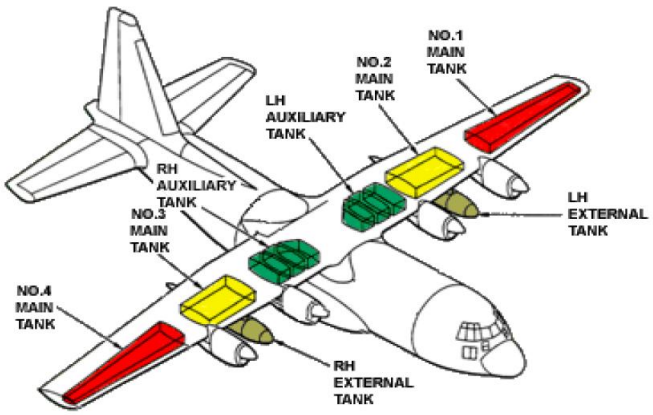

Figure 2.3 – Fuel tank locations [8]

- Rigid removable tanks are installed in a compartment designed to accommodate the tank. They are typically of metal construction, and may be removed for inspection, replacement, or repair. The aircraft does not rely on the tank for structural integrity. These tanks are not found in the C–130 but are commonly found in smaller general aviation aircraft, such as the Cessna 172 (figure 2.4).

Figure 2.4 – Example of rigid removable tank [3]

- Bladder tanks are reinforced rubberized bags installed in a section of aircraft structure designed to accommodate the weight of the fuel. The bladder is rolled up and installed into the compartment through the fuel filler neck or access panel, and is secured by means of metal buttons or snaps inside the compartment. Many high–performance light aircraft, helicopters and some smaller turboprops use bladder tanks. One major down–side to this type of tank is the tendencies for materials to work harden through extensive use making them brittle causing cracks. Examples of this type are the L/R auxiliary tanks in (figure 2.3).

2.2.2. Integral Fuel Tank Technology

2.2.2.1. Principles

The wing structure comprising a main load carrying box structure made up of upper and lower skins, front and rear spars. The upper and lower skins consist of machined plates stiffened by internal span–wise stringers. There are span–wise butt joints in the upper and lower skins formed by a butt–strap and stringer combination (figure 2.5). The fuel tank is integral with the wing box structure. Each wing tank is divided into cells by sealed ribs. The ribs act as web baffles to stop the fuel surging during maneuvers which would make the aircraft unstable and difficult to control (figure 1.1). The joints between the ribs, spars etc. and skin are sealed to prevent fuel leakage and internally treated against corrosion. The number of parts in the wing–box walls and floors should be kept to a minimum. If there are fewer parts then there are fewer joints and seams to potentially leak. A surge box is formed in the inboard end of the tank in which fuel is collected if discharged from the tank vent system. Removable access panels are placed along the upper wing surface for access during maintenance. There are external attachments to the wing box including trailing edge aerodynamic control surfaces. Those attachments to the wing box penetrate the integral fuel tank by several fasteners. Almost elements in the primary structure of the wing use interference fit–type fasteners which improve the fatigue life and ensure adequate sealing of the fuel tanks [9].

Figure 2.5 – The inner components of a C–130 wing (ribs, stringers, skin and the removable access panels)

The joint integrity must be maintained from the static load condition through to the dynamic condition of temperature and pressure cycling and aircraft flexure in flight.

2.2.2.2. Fuel

In the 1940s, the turbine or jet engine emerged and progressively took over from piston driven engines. The principal difference between piston and jet engines is that combustion is intermittent in a piston engine and continuous in a jet engine. As a result, the engines have different fuel combustion quality requirements. In piston engines, combustion timing is critical to high–quality performance.

The fuel used in the first aircraft turbine engines was kerosene because the engines were thought to be relatively insensitive to fuel properties. After the World War II a new mixture of hydrocarbon and kerosene JP–4 was used extensively. However, compared to a kerosene–type fuel, this jet fuel was found to have operational disadvantages due to its higher volatility:

- Superior risk of fire during handling on the ground;
- Losses due to evaporation greater at high altitudes;
- It was recorded less survivable crashes of planes fuelled with wide–cut fuel.

Approximately in 1970 military services initiated a reversion back to kerosene type fuels and they have basically completed the procedure of converting from JP–4 to kerosene–type JP–8 fuels chosen due to the best combinations of properties. Currently JP–8 is the fuel used in C–130 but JP–4 is still used in some parts of Canada and Alaska because it is suited to cold climates [10].

2.3. Theoretical Concepts concerning the Static Analysis

2.3.1. Introduction

The static analysis of any element requires a detailed attention to several aspects. The tensile, shear, bearing stresses or loads of the metallic plates and fasteners have to be determined and evaluated considering the materials properties. Some theoretical relevant concepts are shown in these sections below.

2.3.2. Stress Concentration Factor

A dimensionless factor, known as stress concentration factor K_t is used to quantify how "concentrated" the stress is. Mechanical components should preserve constant section, or its modification should be smooth, otherwise stress concentration will arise. It is defined as the ratio of the local tension in the element to the reference stress (nominal stress) [4], [11].

$$K_t = \frac{\sigma_{local}}{\sigma_{nominal}} \tag{2.2}$$

Stress concentration factor, K_t can be determined by theoretical formulas, computational methods or testing. The index near *K* stands for theoretical, because it is determined recurring to the elastic theory. In the figure 2.6 is an example of stress concentration.

Usually, the nature of stress distribution and the values of stress at concentration sites could be determined by several methods. Theoretical method is through the elastic theory, computational is through the finite element method and testing is made using photo–elasticity or lacquer coatings. [12]

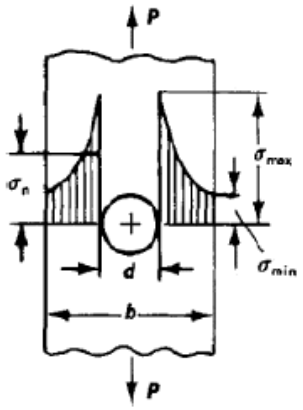

Figure 2.6 – Example of stress concentration near a hole [4]

The analysis of this parameter is very important to evaluate crack initiation and propagation. A crack usually appears due to stress concentration on the crack's tip. As a result, design engineers should try to avoid stress concentration on the components in order to prevent failures.

Stress concentration around fastener holes is one of the most critical aspects leading to failure in aircraft. As so, its comprehension and determination is of great importance [7].

2.3.3. Joint Failure Modes

Joints are the most common source of failure for airframes as well as other structures and there are numerous joint failures modes that will dictate the overall capability of a joint. The overall capability is determined by calculating or testing for the allowable load associated with each failure mode. The lowest allowable load amongst all of the failure modes is equal to the overall joint capability.

The three dominant failure modes that can be encountered are net–tension, shear–out, and bearing, as shown in figures 2.7, 2.8 and 2.9. Although a combined failure mode is also possible. Whereas the net–tension and shear–out are considered as catastrophic failure resulting in total separation of the structural parts, the bearing mode creates a localized damage that is governed by the compressive strength of the material. Besides the loading condition, the element geometry including the holes locations can also influence the joints failure mode. While the net–tension and shear–out failure modes can be avoided through proper geometric modifications, the bearing damage may not. The references [4] and [7] have been used.

2.3.3.1. Net Tension

Net tension failure is defined as a plate tensile failure that occurs between two fasteners along a plane normal to the applied load. When there is a hole the net area reduces and thus the tension reaches higher values if it has to carry the same load than before. In the figure 2.7 that effect is illustrated.

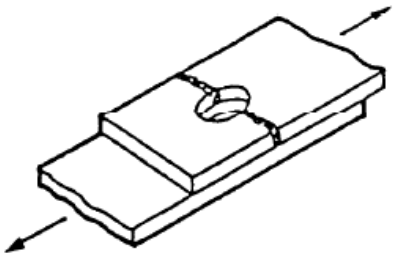

Figure 2.7 – Net tension failure mode [4]

The maximum load that meets both limit and ultimate criteria for net tension is designated as P_{net}. The equation needed to estimate that P_{net} is the equation (2.3) [7]. The variable σ_{tu} represents the ultimate tensile stress, σ_{ty} is the tensile yield stress, A_{net} is the net area of the hole section.

$$P_{net} = Lesser\ of\ (\sigma_{tu} \times A_{net})\ or\ (1.5 \times \sigma_{ty} \times A_{net}) \quad (2.3)$$

2.3.3.2. Tearing out

Tear out failure is a plate shear failure that occurs along two planes parallel to the applied load. Figure 2.8 show that failure mode. The equation for tear out should only be used when test data is not applicable to a given edge margin condition.

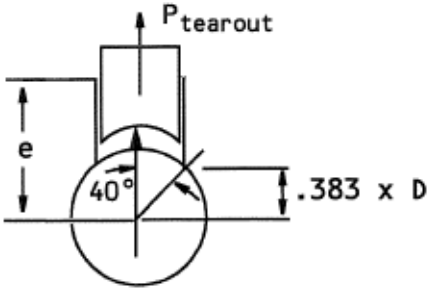

Figure 2.8 – Tearing out failure mode [4]

The maximum load that meets the ultimate criteria for tear out is designed as $P_{tearout}$. The expression for assessing the $P_{tearout}$ is the (2.4) [7]. The variable σ_{tu} represents the ultimate tensile stress, t is the thickness of the sheet, D is the fastener diameter, and e is the edge margin.

$$P_{tearout} = \sigma_{tu}.t\ (2e - .766D) \quad (2.4)$$

2.3.3.3. Bearing Failure

The bearing failure is defined as the hole plastic deformation associated with the maximum load a plate specimen can withstand. That deformation will typically be in the form of hole elongation. Figure 2.9 show that failure mode.

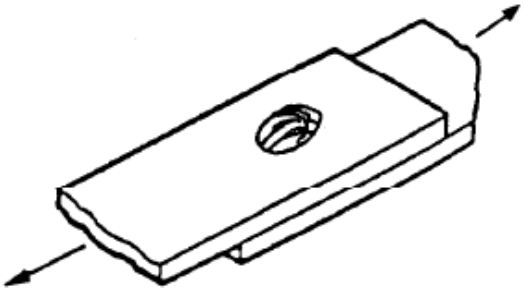

Figure 2.9 – Bearing failure mode [4]

The maximum bearing load that will meet both limit and ultimate criterion is designed as (P_{brg}). From the reference [4] requirements, the bearing load (P_{brg}) can be calculated with the equation (2.5) [7]. The variable (σ_{bru}) is the ultimate bearing stress, and (σ_{bry}) is the bearing yield stress.

$$P_{brg} = Lesser\ of\ (\sigma_{bru} \times D \times t)\ or\ (1.5 \times \sigma_{bry} \times D \times t) \tag{2.5}$$

2.3.3.4. Fastener Shear Failure

Fastener shear failure is a shear failure of the fastener shank. The maximum load (P_{fs}) that meets the ultimate criteria for the fastener shear is defined by the expression (2.6) [7].

$$P_{fs} = \sigma_{su} \times \pi \times D^2/4 \tag{2.6}$$

The variable (σ_{su}) is the ultimate shear stress. Figure 2.10 show that failure mode.

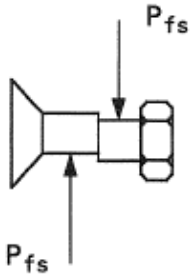

Figure 2.10 – Fastener shear failure mode [4]

2.3.3.5. Transitional Failure

Transitional failures include all other failure modes. Any fastener mechanism failure other than the previous presented is considered a transitional failure. One illustration of transitional failure would be

the fastener pull through. This typically occurs in thin sheets where the fastener head is pulled through the material sheet.

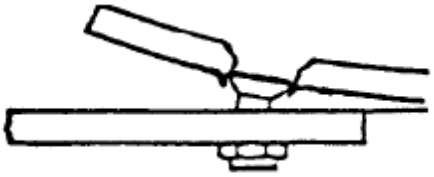

Figure 2.11 – Fastener pull–through failure mode [4]

2.3.3.6. Requirements to Avoid Failure

Usually it is not necessary to calculate the tear out load. There are some specifications to avoid that kind of failure mode at the edge margin of a sheet and most of them are contained in ASTM Standards (American Society for Testing and Materials). Therefore rivet placement on the structure is a major concern for the designer, and the distances between rivets and to the margin of the plate are regulated by these specifications. The conventional rule for spacing of rivets is that they may be no less than 4 diameters apart and no less than 2 diameters to the margin of the plate. Rivets cannot be closer together, since then there would be no room for the riveting tools. Rivets cannot be spaced too widely, which would allow thin plates to gap and not close together firmly. In addition rivets placed in normal parallel rows have different behaviors than staggered ones (figure 2.12). These parameters are mainly defined through the fastener diameter and can be found in tables, such as table 2.1 [4].

Fastener Diameter	***Pattern***	***A***	***B***	***C***	$e = 2D$
$\mathrm{D} = \frac{5}{32} = 0.156''$	Normal Rows	0.63	0.55	–	0.34
	Staggered Rows	1.0	0.39	0.63	0.34
$\mathrm{D} = \frac{3}{16} = 0.188''$	Normal Rows	0.75	0.66	–	0.41
	Staggered Rows	1.18	0.47	0.75	0.41

Table 2.1 – Minimum distance between rivets (inches)

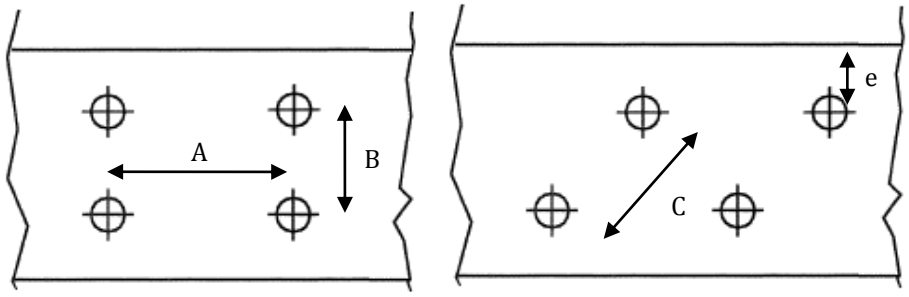

Figure 2.12 – a) Normal row; b) Staggered row

2.3.3.7. Correlation Method

It is difficult to model the behavior of a fastener in a joint, how it receives and transfers the load. The deflection of the fastener due to shear and bending must be analyzed and correlated with test data. The correlation method relates test data through equations and is proven to have excellent results. It models both fasteners and plates with springs, and through a displacement analysis the transfer loads are determined. In order to do so, Swift, T. proposed equation (2.7) to describe the fastener spring constant. The following formula is for single shear. [4].

$$K_x = K_y = \frac{E_{skin}\, D}{A + B\left(\frac{D}{t_{skin}} + \frac{D}{t_{doubler}}\right)} \quad for \begin{cases} Steelfastener A = 1{,}667; B = 0{,}86 \\ Aluminium fastener A = 5; B = 0{,}8 \end{cases} \tag{2.7}$$

It is observed that the K_x and K_y are the fasteners spring constant (lbs./in.) for single shear and D is the fastener diameter. Other hypothetical equations, more accurate, to determine the spring constant are used by Boeing and Airbus, but these equations are protected by exclusive rights and thus cannot be used in this project. Although, Swift's formula presents a conservative value for this constant, and thus safety is guaranteed [4].

For the axial direction, using the equation below, where A_{cross} is the cross sectional area of the fastener and L_{fast} is the fastener length, the spring constant that represents the axial behavior of the rivets is determined through:

$$K_z = \frac{A_{cross}\, E_{fast}}{L_{fast}} \tag{2.8}$$

3. Historical Analysis

3.1. Introduction

This chapter reviews the historical data of fuel leaks in the C 130 aircraft fleet based on a company database. These archives are organized with the company patterns and they include the process ID, task performed, aircraft ID, discrepancy and location, and its corrective action among others. These files were developed and adapted to a suitable format and the information required was organized in *Excel* file. The data available are from 2003 until May 2014.

The information and conclusions presented in this chapter allowed the identification of several regions in the fuel tanks susceptible of fuel leaks. This analysis started with an evaluation of total fuel leaks per aircraft followed by a comparison between the men–Hours of work per aircraft. Next it is presented a graph showing the fuel leaks per tank followed by the comparison of number of leaks per year over the last years, adimensionalized by the number of aircraft inspected during each year. The last evaluation was the number of fuel leaks per location on the wing/tank. The analysis allowed the identification of critical points or regions on the fuel tanks based on the record as well as the aircraft with more problems over the time evaluated.

The chapter initiates with a brief presentation of the aircraft and the most relevant parameters.

3.2. Presentation of the Lockheed C–130

The Lockheed C–130 Hercules is a four–engine turboprop, medium–size utility aircraft which has proven to be one of the most well–known and versatile Aircraft ever built. The C–130 was a historical relevance and represent the bulk of the military work at OGMA. Since the flight of its first prototype in 1954 in California 40 different models of this aircraft have been built. The C–130 is the only military aircraft remaining in continuous production for over 50 years with its original customer. The general views are presented in figure 3.1 [13].

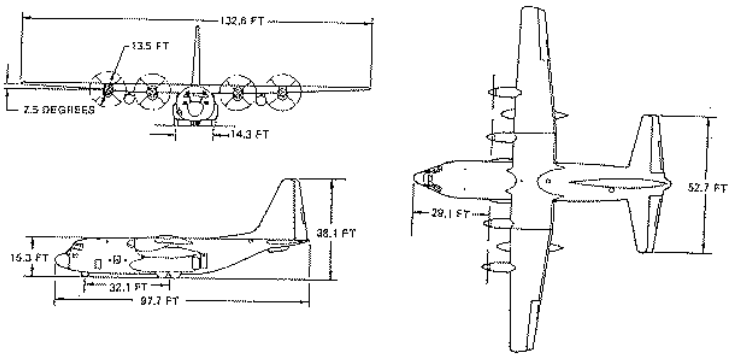

Figure 3.1 – Three views of the C–130H aircraft [8]

3.2.1. Lockheed C–130 Specifications

In order to perform several evaluations developed throughout this study, a number of inputs variables must be known. In the table 3.1 it is possible to find the most relevant parameters of the C–130H [13].

General characteristics	
MTOW (Lbs)	155 000
Empty Weight (Lbs)	75 800
Payload (Lbs)	45 000
Length (ft)	97.2
Wingspan (ft)	132.6
Height (ft)	38.1
Wing area (ft^2)	1745
Power Plant	4 × Allison T56–A–15 Turboprops
Performance	
Maximum Speed (Knot)	320 at 20,000 ft
Cruise Speed (Knot)	292
Range (Nmi)	2 050
Service ceiling (ft)	33 000
Rate of climb (ft/min)	1.83
Takeoff distance (ft)	3 586 (MTOW)

Table 3.1 – Lockheed C–130 general specifications

3.3. Analysis and Results

Fuel Leaks/Aircraft

The first result of the analysis was the graphic below, fuel leaks per aircraft. This relates the number of fuel leaks per aircraft during the consider time period.

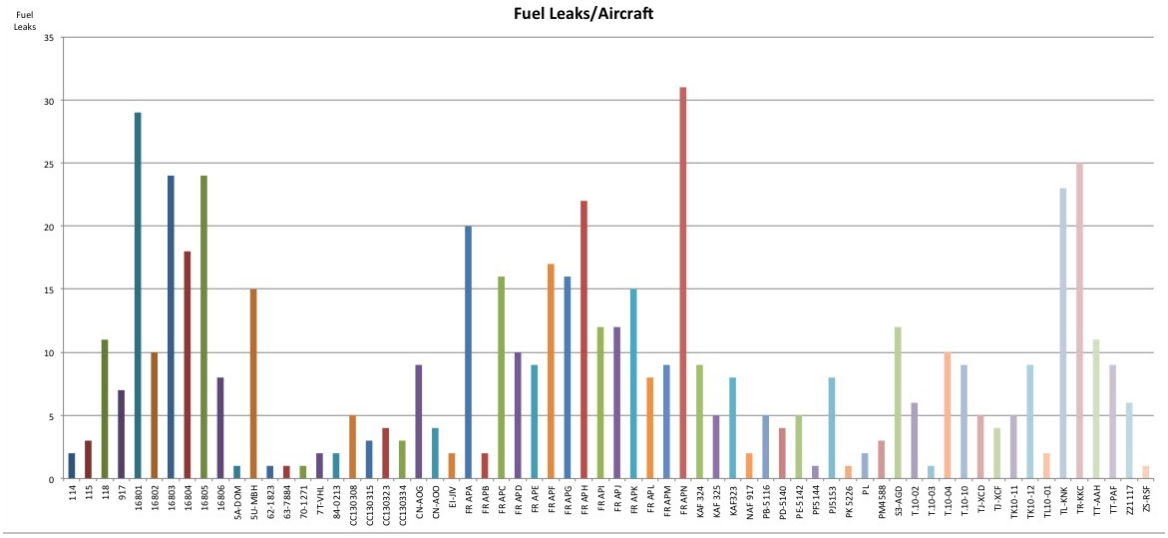

Figure 3.2 – Fuel leaks/aircraft

Men–Hours/Aircraft

In the same line it is also interesting to present the evaluation of men–hours per aircraft. It relates the number of work hours effectively employed repairing the leaks problems in each aircraft.

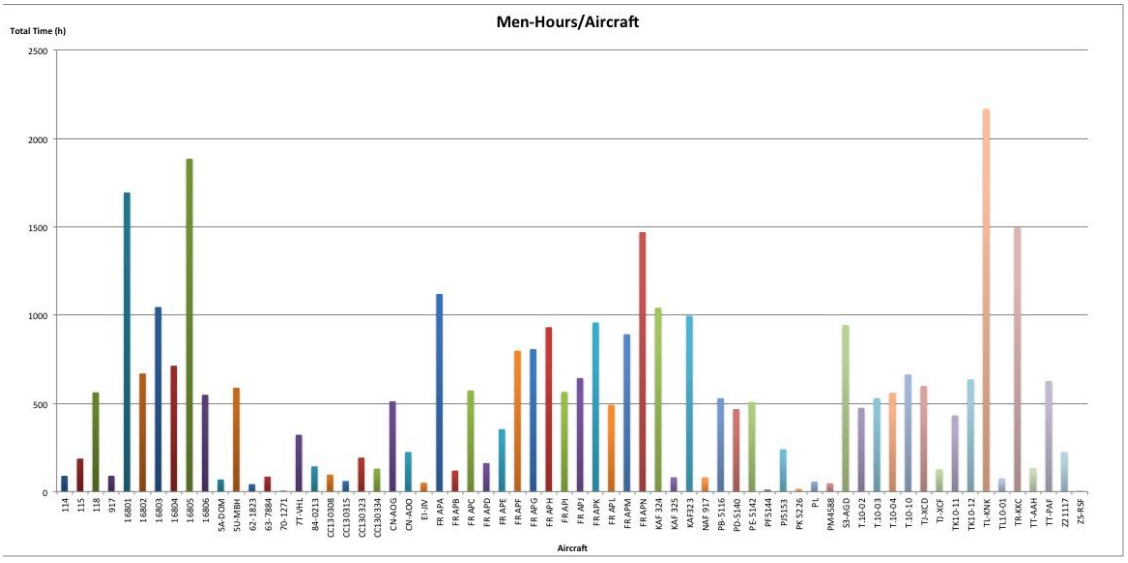

Figure 3.3 – Men–hours/aircraft

- The first record from the previous figures was that the aircraft with more fuel leaks/longer working hours were the A and B series (first manufactured) as well as the ones that are effectively employed in special operations. Among those involved in special operations, it should be noted that they are subject to critical conditions such as hot and humid environments or limit loads maneuvers.

Fuel Leaks/Tank

The second evaluation on this analysis was the tanks in which more fuel leaks were detected.

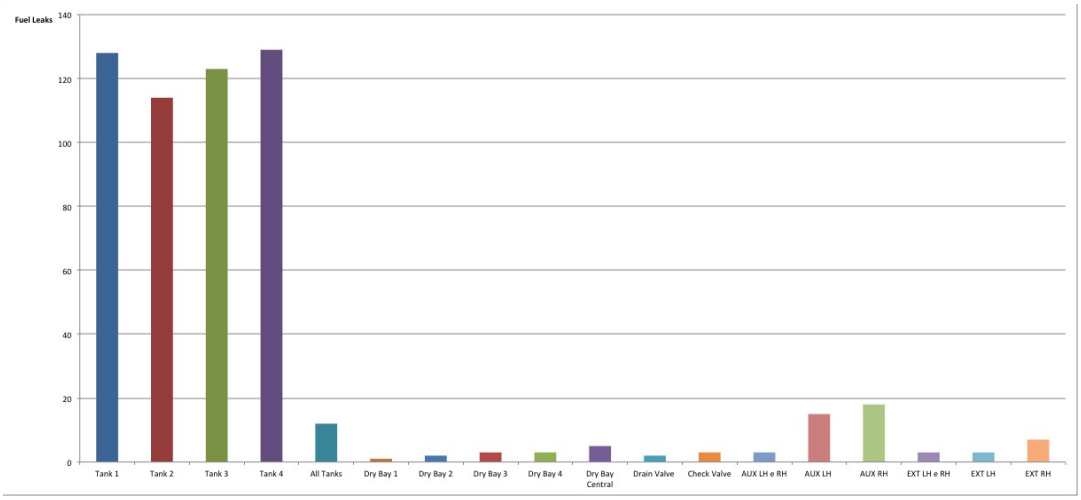

Figure 3.4 – Fuel leaks/tank

- It can be noticed from the figure above a notable difference between the integral tanks and the others. Following this comparison it was found that the main tanks are the mainly affected followed by the auxiliary tanks but with a considerable difference. This result was totally expected based on the technicians and engineers experience among integral fuel tanks.

Fuel Leaks (adimensional)/Year

The third comparison was carried out to observe the patterns of the number of leaks over the last years. The data provided is from January 2007 until May 2014. A graphic was created relating the number of leaks with the year of aircraft delivered. It should be noted that the number of leaks was adimensional by the total number of aircraft delivered this year. The result of this evaluation is in the figure below:

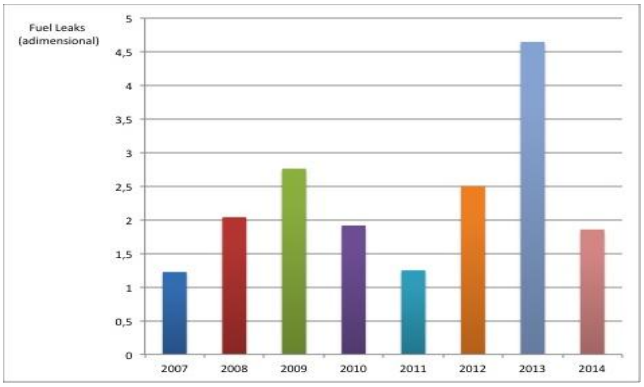

Figure 3.5 – Fuel leaks/year

- It was observed that 2013 was the year with the maximum of fuel leaks over the last eight years with a significant difference among others. It is perceptible a pattern in the chart noticing a rise to a peak followed by a decrease to a minimum, then increased again. This is consequence of the well–defined intervals of time between checks A, B and C on the aircraft.

Fuel Leaks/Location

The last result includes the relation between the fuel leaks and its location on the wing. This is presented in the following figure:

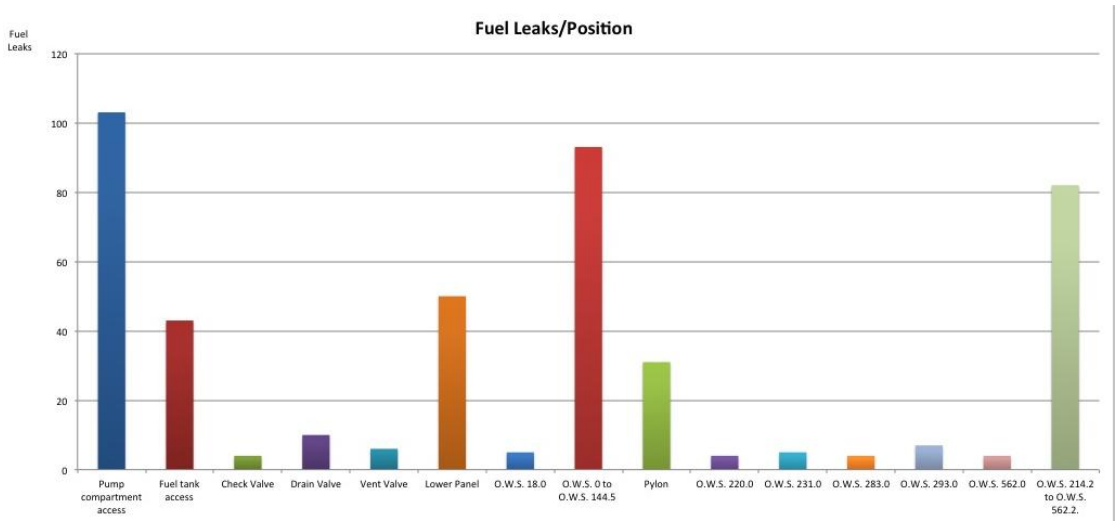

Figure 3.6 – Fuel leaks/location

- From the last result it was evident that the most problematic part/region is the pump compartment access followed by the O.W.S (Outer Wing Station) 0 to 144.5 and the O.W.S 214.2 to 562.2. This acronym O.W.S indicates the position in the wing measured from the outer wing root to the tip in inches.
- The pump compartment access is a partition inside the fuel tank that protects the pump and has no structural load function.
- Focusing on the structural function members, the ones highlighted were the Lower Panel and the Pylon Fitting. There were noticed several fuel leaks in these members and both have structural load contribution to the wing. In addition, a certain number of fuel leaks, presented on the O.W.S 0 to 144.5 could be also from the Lower Panel or Pylon Fitting which reinforce the previous assumption.

3.4. Conclusion

Considering the previous analysis and the last results, the ones highlighted were the Lower Panel and the Pylon Fitting. The Lower Panel is an especially large structural member (approx. 600 in.) with many iterations to simulate as well as to define boundary conditions and loads. It would result in an extremely complex model which could compromise the results obtained. On the other hand the Fitting member is substantial smaller and more accurate to reproduce. The boundary and loads conditions are comparatively more objective to reproduce considering the external tank installation.

As a result in this project a FEA of the Pylon Fitting will be considered. It is a structural member and an evaluation of its behavior under certain conditions could be interesting to propose structural improvements in order to reduce fuel leaks in this area.

Figure 3.7 – External tank with Pylon (green) and Fitting (yellow)

4. Pylon Fitting Analysis

4.1. Aerodynamic Analysis

4.1.1. Introduction

In this section, the contributions of the aerodynamic forces are evaluated. An external tank is a component with its own mass, and which is attached to the wing web through the Pylon and Fitting installation. Since the external tank is a component with significant dimensions there is a significant contribution of this to the aerodynamics forces acting on the Pylon Fitting. The most important forces which act over it are the gravitational and the aerodynamic forces. The following procedure defines some simplifications of the structure in order to make it possible to use analytic formulas to determine the loads.

4.1.2. Theoretical Background

Assumptions:

- The external fuel tank is considered a cylindrical body in axial flow (conservative assumption);
- The cylinder diameter is considered the external tank maximum diameter (conservative assumption);
- The cylinder length is considered the total external tank length (conservative assumption);
- The Pylon is considered of “rectangular” section in axial flow;
- The Pylon height is considered the average between the front and rear height.

The previous assumptions results from the difficult to found experimental or computational data with rounded or streamlined head forms (figure 4.1).

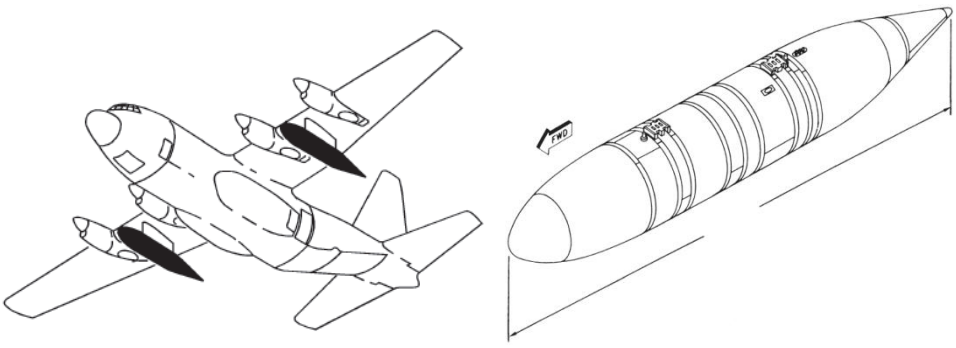

Figure 4.1 – External fuel tanks [1]

The drag coefficient for a cone pointed into the airflow is a bit more complex since it depends on the cone's shape. In particular, the drag will vary depending on how steep the angle of the cone is. The referenced angle is called the half–vertex angle, ε, measured from the centerline of the cone to one of its walls. The larger this angle becomes, the higher the drag of the cone is. As a result the external fuel tank was considered a cylindrical body in axial flow (conservative assumption).

These estimates for the drag coefficient considering a cylinder in axial flow can be found in [14]. This simplification has performed considering the fuel tank a cylinder with *d* (external tank maximum diameter) and the *l* (external tank length). This assumption is conservative once the C_D calculated for this case is substantial superior.

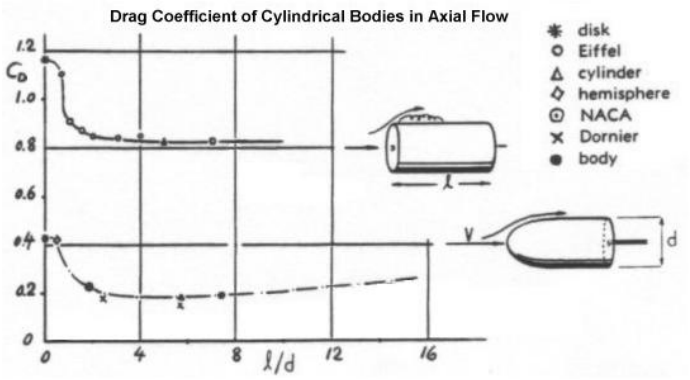

Figure 4.2 – Drag coefficients of cylindrical bodies in axial flow, with blunt shape (upper component) and with rounded or streamlined head form (lower component) [14]

External Tank Data	
l (in.)	308.4
d (in.)	45
l/d	6.85
S_{wet} (in.^{2})	1590.43
C_D	0.81

Table 4.1 – External Tank Data

Plotted in figure 4.2 are the drag coefficients of a number of cylindrical bodies in axial flow. The drag of these shapes essentially consists of that of the forebody and the base drag originating at the blunt rear end. According to the previous graph, the coefficient of drag for a cylinder in this orientation is about 0.81 so long as the l/d (length–to–diameter ratio or fineness ratio) is greater than 2. The table 4.1 contents the external tank dimensions and aerodynamics data, where the S_{wet} is the wet surface of the external tank.

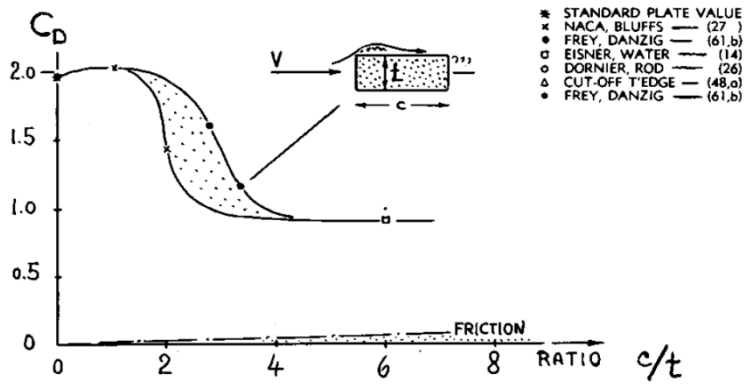

Figure 4.3 – Drag coefficients of “rectangular” section in axial flow [14]

Pylon Data	
c (in.)	78.2
t (in.)	21.45
c/t	3.65
S_{wet} (in.^{2})	211.2
C_D	1.2

Table 4.2 – Pylon Data

Plotted in figure 4.3 are the drag coefficients of “rectangular” section in axial flow. The drag of these shapes essentially consists of that of the forebody and the base drag originating at the blunt rear end. According to the previous graph, the coefficient of drag for a “rectangular” section in this orientation is about 1.2 for a c/t (length–to–height ratio) of 3.65, where the S_{wet} is the wet surface of the “rectangular” section.

4.1.3. Analytic Analysis

The external fuel tank installation shape was designed to support the high loads during operation not to be aerodynamic in order to soft the extra load transmitted to the aircraft. Consequently, there are always non–ignorable drag forces, which can be estimated analytically.

Drag forces are defined as those loads encountered during flight at maximum design airspeed due to the shape and size of externally–mounted equipment. To estimate the drag coefficient from the fuel tank installation geometry and using the basic formulas following was assessing the drag, where (ρ) is the air density, (V) is the free air stream speed, (S) the front effective surface of the fuel tank or Pylon, and (C_D) the drag coefficients [15].

$$Drag_{ExternalTank} = 0.5\rho V^2 S_{tank} C_{D_{Tank}} \quad (4.1)$$

$$Drag_{Pylon} = 0.5\rho V^2 S_{Pylon} C_{D_{Pylon}} \quad (4.2)$$

$$Drag_{Installation} = Drag_{ExternalTank} + Drag_{Pylon} \quad (4.3)$$

The table 4.3 presents the drag components determined previously.

Components	
$\rho = \rho_{20000\,ft\ (\frac{lbs}{in^3})}$	8.803e–2
$V = V_{20000\,ft\ (knot)}$	320
$S_{tank}\ (in.^2)$	1590.4
$S_{Pylon}\ (in.^2)$	211.2
$C_{D_{Tank}}$	0.81
$C_{D_{Pylon}}$	1.2
$Drag_{ExternalTank}\ (lbf)$	2674.63
$Drag_{Pylon}\ (lbf)$	526.15
$Drag_{Installation}\ (lbf)$	3200.8

Table 4.3 – Drag components

4.2. Structural Analysis

4.2.1. Introduction

The purpose of this section is to evaluate the behavior of the Pylon Fitting component under ultimate loads that the aircraft is subject in three different flight conditions. The Fitting structure layout is presented, as well as the external tank installation scheme on the wing and the materials. Then, the fasteners enrolled are exposed. Finally, a detailed finite element model of the Fitting has been built and analyzed to verify the design of the structure and the critical regions.

All the loads acting on the structure are supposed to be only from the external fuel tank installation. This part of the structure has had in–service several fuel leak problems and has reasonably straightforward loading conditions as was previously noticed. The structure member is shown in figure 4.4.

Figure 4.4 – Pylon Fitting (Front web)

Lockheed's C–130 internal structure is conceived to obtain maximum strength to embraces the most critical situations. It is common to find margins of safety indicating "very high" in some company reports, representing the high strength of the aircraft. The structure that is object of study is attached to the wing front spar. The spars are the most important structural component of the wings, since they carry the air loads during flight and the wing weight while on the ground. The figure below shows the external tank installation scheme.

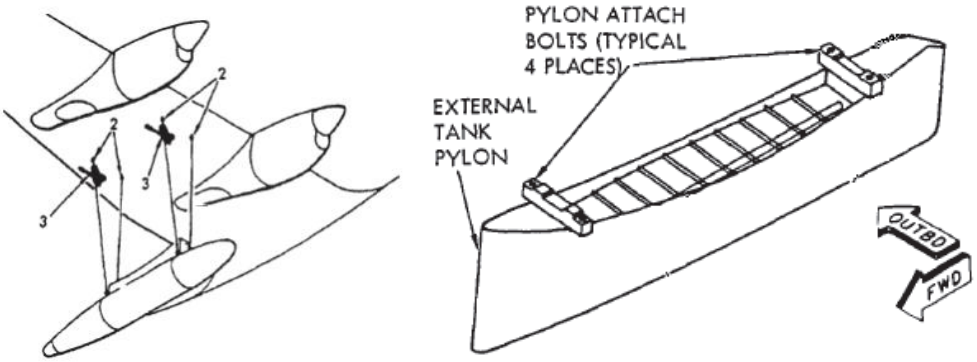

Figure 4.5 – External tank installation scheme [1]

The Pylon attachment bolts and nuts have special characteristics; the nut is designed to spread the load through a circumferential shape. The figure 4.6 presents a bolt and a nut.

Figure 4.6 – Pylon attach bolt and nut

4.2.2. Determination of Loads

The simplification adopted consists of assessing the reactions R_1 and R_2 in the front and rear Fitting, respectively. The forces applied are the drag and the gravitational of the two components. Figure 4.7 presents a scheme of the free–body diagram. The variable (R_1) is the vertical reaction created at the front Fitting, (R_2) is the vertical reaction created at the rear Fitting. (D_1, D_2) and (W) are the drag force components and the gravitational force, respectively. The (R_{D1} and R_{D2}) are the reactions created due to the drag force components. The (M_D) is the moment created by the drag force, applied in the rear Fitting. The distance (d_1) is the horizontal distance between the component R_1 and the center of mass, (d_2) is the horizontal distance between the component R_2 and the center of mass, and (H) is the vertical distance between the components R_1 and R_2 to the center of mass.

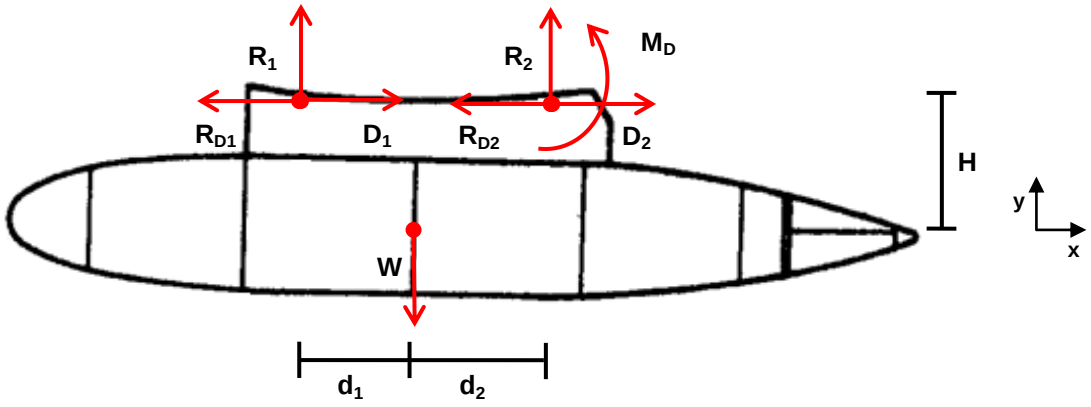

Figure 4.7 – External tank installation simplification (Free–body diagram)

Hypothesis:

- Aerodynamic and gravitational loads are totally absorbed by the Fittings fixing points.
- The center of mass of the total installation (external tank and Pylon) is considered in the center of the cylinder (figure 4.7).
- The drag force is supported by the front and rear joint (D_1 and D_2);
- The moment created by the drag force is applied in the rear joint and is only supported by the front Fitting (conservative).

The total weight of the Pylon tank installation (considering the fuel) was obtained considering the several weights individually (table 4.4) [1].

Component	
Wing Pylon support (Lbs)	135
Lockheed external tank (dry) (Lbs)	656
Fuel tank capacity (US gallons/ liters)	1360/5148
Fuel density (Lbs/gal(US) / Kg/L)	6.7 / 0.81
MFW – Maximum fuel weight (Ext. Tank) (Lbs)	9109
Total Pylon tank installation (Full) (Lbs)	9900

Table 4.4 – Total weight of the Pylon tank installation

The reactions created by the two components to the Fittings are obtained through forces and moment equilibrium. The equation signs are taken based on figure 4.7 scheme.

$$D_1 = D_2 = \frac{Drag_{Installation}}{2} \tag{4.4}$$

$$M_D = Drag_{Installation}\ H \tag{4.5}$$

$$\sum F_i = 0 \overset{i}{\Leftrightarrow} R_2 = W - R_1 \tag{4.6}$$

$$\sum M_i = 0 \overset{i}{\Leftrightarrow} R_1 = \frac{W d_2 + M_D}{d_1 + d_2} \tag{4.7}$$

The distance components and the values for the reactions determined previously are shown in the table 4.5. Note that the index *w* indicates the components considering only the gravitational force.

Components	
d_1 (in.)	32.95
d_2 (in.)	45.25
H (in.)	44.5
W (Lbs.)	9900.0
R_{1w} (lbf)	5728.58
R_{2w} (lbf)	4171.42
R_1 (lbf)	7551.93
R_2 (lbf)	4171.42

Table 4.5 – Distances components and reactions

In the table 4.5 are listed the reactions components calculated considering the aerodynamic and gravitational forces of the external fuel tank installation. These reactions were estimated considering the static case. For this study the component R_1 corresponds to the front Fitting and it is observed that it supports about two times more load than the rear Fitting. This difference is due to the center of mass of the tank is positioned forward within the specified limits established by the aircraft manufacturer.

4.2.2.1. Load Requirements

When performing a structural load analysis, one of the most important concerns is the so–called flight envelope. The different load conditions that an aircraft may be subjected during flight are represented in a chart called flight envelope, or $V - n$ diagram. The aircraft's flight envelope is the sum of the flight maneuvering envelope and the gust envelope. This diagram reports the limit load factors as a function of the aircraft speed. The load factor n is defined as the ratio between the lift L generated by the wings during a particular maneuver and the aircraft maximum weight W. Thus, the limit load factor is a measure of the acceleration that the aircraft must be able to withstand during different flight conditions. In order to clearly understand the combined effect of these two contributions the flight envelope is created. This flight envelope enables the structural loads engineer – as well as specialists in other fields of expertise, to have a much better understanding about the effects that the loads have on the aircraft's structure [6]. The aircraft is considered in 'symmetric' flight, which means, no side–slipping, rolling or yawing. Just pitching and balanced turning maneuvers are considered.

The gust envelope gives the range of loadings generated by gusts at various speeds which the aircraft must also withstand. In–flight gust loads are defined as the loads resulting from turbulence. Combining these two envelopes originate the aircraft flight envelope. This is the most relevant plot, since it does establish the true limit loads that the aircraft's structure may experience in the advent of being subject to gust loads coming from any direction and on any flight condition [6]. Notice that both the maneuvering and gust envelopes are calculated with the aircraft at its projected maximum take–off weight (MTOW). The figure 4.8 presents an example of a combined flight envelope.

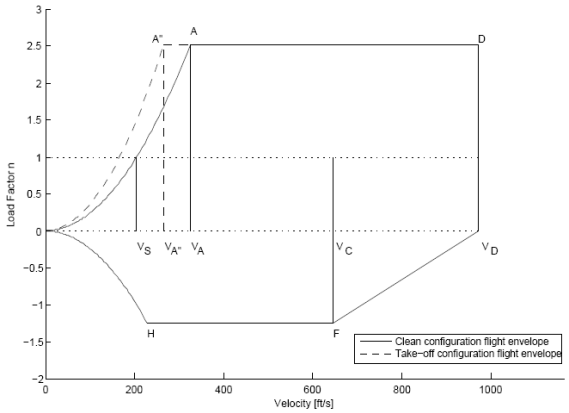

Figure 4.8 – Combined Flight Envelope

In this analysis, the design load criteria are from aircraft manufacturer–approved data and/or airworthiness authority. All externally–mounted equipment and supporting structure that attaches to external hard–points on the aircraft must be designed for the airspeed (lift and drag) loads and the in–flight gust loads. For the C–130 these criteria are [13]:

- Airspeed – 320 knot at 20000ft conditions;
- Flight gust loads – 8.25 g down;
- Banked turn with θ=60 degrees and 3 g down.

These critical points are the extremes for the C–130 and these values are the ones used to evaluate the behavior of the Pylon Fitting under extreme conditions.

4.2.3. Materials Properties

This section considers all of the materials used in the structure analyzed. Component parts must be made of carefully selected materials because of their importance in maintaining integrity of the aircraft under expected stress and loading. The same holds true for fasteners such as bolts and rivets. It is essential that these parts do not fail or weaken with exposure to stress and weather elements.

Corrosion must also be considered. A Fitting made of one metal cannot be secured to the structure with a bolt or fastener made of another metal without measures being taken to prevent dissimilar metal corrosion (galvanic corrosion). Over a period of time dissimilar metal corrosion can result in a weakening of the assembly to the extent that the assembly is rendered unsafe.

In the table 4.6 are the materials used in the structure and fasteners (attachment A) [16], [17], [18], [19], [20].

Elements	***Fitting***	***Fasteners***		
		Solid Rivets	Hi–Locks	Bolts
Material	Aluminium 7075–T6	Aluminium 2117–T4	Nickel Alloy 400	Steel 4140
Density [lb/in^3]	0.101	0.0994	0.318	0.284
Modulus of Elasticity. *E* [*Ksi*]	10300	10300	26000	29700
Poisson's ratio ν	0.33	0.33	0.3	0.3
Yield Strength [*Psi*]	72000	24000	35000	142000
Tensile Strength, Ultimate [*Psi*]	78000	43000	75000	160000
Shear Strength [*Psi*]	47000	26000	49000	96000
Rivet tensile strength *[Lbs]*	–	1187	2071	18100
Rivet shear strength *[Lbs]*	–	596	1353	10860

Table 4.6 – Fitting and fasteners materials properties

4.2.4. Finite Element Analysis

The analysis of a complex member such as the Pylon Fitting requires a finite element model on which the constraints, loads and elements characteristics will be applied in order to obtain a solution. Three load conditions will be investigated, corresponding to extremes of the aircraft operating. The software that has been used in the analysis is ANSYS ® APDL interface, which allows to create an input code in a form of a programming language, granting a more immediate user–control than, for example, the ANSYS Workbench interface [21], [22].

4.2.4.1. Modeling and Elements Setup

The ADPL interface allows the user to create a 3D model of the structure, giving keypoints in input. These keypoints are then used to make lines, areas and volumes that will form the model on which the mesh will be built. However, the ADPL modeler is not so handy when it comes to complex parts. For this cases, a CAD model is created with an external software (such as SolidWorks ®) and then exported in the *IGES* format, that the APDL interface can easily read converting the entities to keypoints, lines, areas and volumes.

4.2.4.1.1. Assumptions and Simplifications

The modeling and finite element analyze were simplified by some assumptions and simplifications that are listed below.

Fitting model

- The bottom surface of the Fitting was modeled using shell elements once it has a reduced thickness. This is an advantage, because gives the possibility to obtain a less complex model which requires much less memory to calculate keeping a close relationship with the real behavior of the structure.

    - Following the previous approach only the solid component was modeled in SolidWorks ®. Then the model was exported to ANSYS, which is represented below (left).
    - After, the bottom and the holes were created using the solid keypoints and the two components merged. The final configuration is represented at right:

Figure 4.9 – Model created in SolidWorks ® and the Fitting model created and assembled in ANSYS ®

Fasteners (rivets)

- Once it is difficult to model the behavior of a fastener in a joint (how it receives and transfers the load), the rivets were simplified by performing a replacement by springs representing the three degrees of freedom (Ux, Uy, Uz). It is possible to neglect the rotation in the nodes because the ratio between the length and the diameter of the rivet is less than 2 [23].

    - The rivets locations were replaced by points where the spring elements will connect. The distribution of keypoints are represented next (red box indicate keypoints where springs connect):

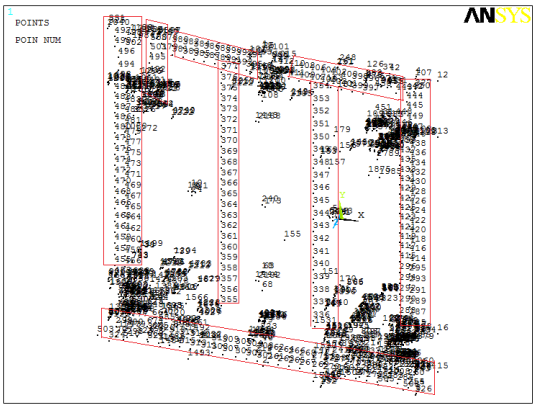

Figure 4.10 – Distribution of spring elements keypoints ANSYS

- The points created previously were identified as “Master” keypoints. Each “Master” keypoint is placed in the previous rivet location and connects to three “Slave” keypoints through a spring element. Each “Slave” keypoint is placed in one of each spatial direction (X, Y or Z aligned with the coordinate system).

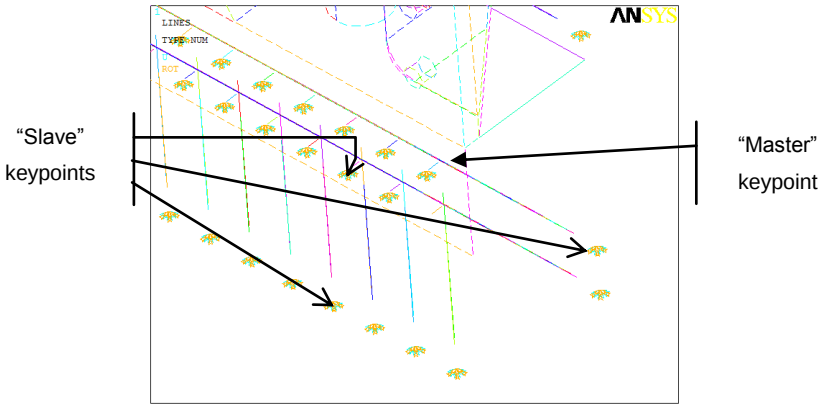

Figure 4.11 – “Slave” & “Master” keypoints – ANSYS

Fasteners (shear bolts)

- The shear bolts require a different analysis due to their larger diameter and were modeled by multipoint constraints method. Bolt head behavior was modeled by rigid body elements (RBE3) and the bolt stud by beam element**.** This method allows defining various contact assemblies and kinematic constraints. The program builds MPC equations internally based on the contact kinematics and the analysis become more realistic in the interface between the part and the bolts [24].

  - Contact in the bolted joint was addressed using surface–surface elements. In REB bolt simulation element BEAM 188 was used to represent the stud and RBE elements

were used to represent the head. The head are connected in a web–like fashion to the surface (figure 4.13) and transfers all the loads as well as the bending effects. It allows the loads to be distributed to the slave nodes proportional to the weighting factors (equally in this case) and the moment is distributed as forces to the slaves proportional to the distance from the center of gravity of the slave nodes.

- To select “Slave” nodes in the region of the washer four volumes were created that overlapped with the model. This procedure allowed selecting the area where the washers are placed and consequently the nodes presented in these areas.

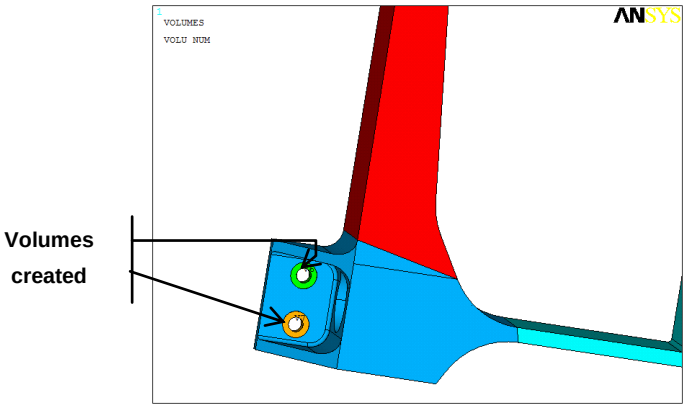

Figure 4.12 – Volumes created in the washer region – ANSYS

- The purple points distributed in the circular area represent the “Slave” nodes and the central point represents the “Master” node. The “Slave” nodes are placed in the washer region and the loads are distributed equally by all the nodes in this region.

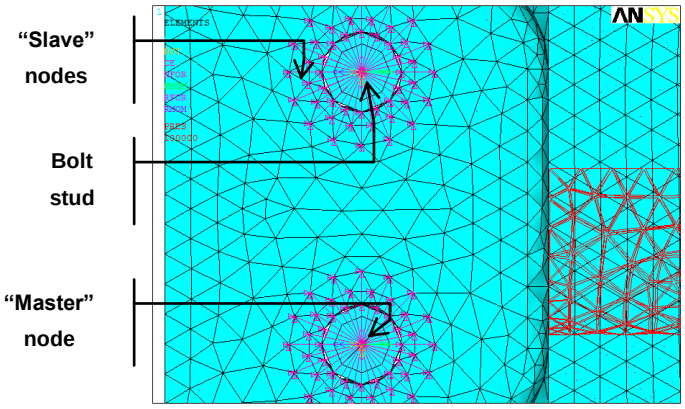

Figure 4.13 – “Slave” & “Master” nodes – ANSYS

4.2.4.1.2. Elements Setup

Four element types were used for this model: the SOLID 285 to model the solid model, SHELL 181 to model the bottom surface, COMBIN14 to model the spring elements, and BEAM 188 to model the bolts [25].

- **SOLID 285** – is a tetrahedic solid, four–node element. The element is defined by four nodes having four degrees of freedom at each node: three translations in the nodal x, y, and z directions, and one hydrostatic pressure (HDSP) for all materials. It is suitable for modeling irregular meshes (such as those generated by various CAD/CAM systems) and general materials (including incompressible materials) and produces enhanced results in very complex geometrical shapes and it is less sensitive to distortion. The element has plasticity, hyper elasticity, creep, stress stiffening, large deflection, and large strain capabilities.

- **SHELL 181** – is a four–node shell element with six degrees of freedom per node: three translations in the nodal x, y, and z directions and three rotation about the nodal x, y, and z axes. It is suitable for analyzing thin to moderately–thick shell structures [25]. The degenerate triangular option is not recommended, since for a triangular element the stress is constant through the entire element, giving non–realistic stress values. However, it can be used for filling small regions of mesh where required. The shell element can be associated with different sections to model different thicknesses. Once it has a reduced thickness which in this situation produces better results.

- **COMBIN14** – has longitudinal or torsional capability in one, two, or three dimensional applications. The longitudinal spring–damper option is a uniaxial tension–compression element with up to three degrees of freedom at each node: translations in the nodal x, y, and z directions. No bending or torsion is considered. The torsional spring–damper option is a purely rotational element with three degrees of freedom at each node: rotations about the nodal x, y, and z axes. No bending or axial loads are considered.

- **BEAM 188** – is a 3D beam with two nodes, with six degrees of freedom at each node, as described above for shell nodes. It is suitable for modeling bolts [24]. The element is based on Timoshenko beam theory, including shear–deformation effects. A quadratic or cubic behavior can be given to the element for a better representation of stresses. The beam element can be associated to different cross–sections.

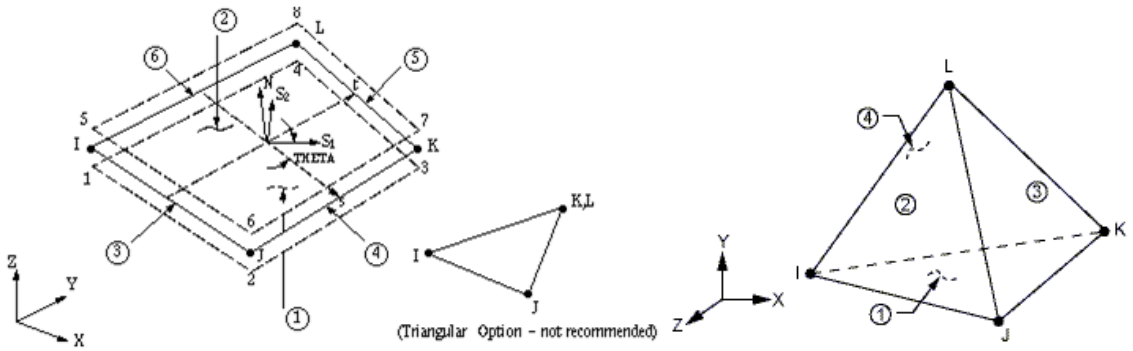

Figure 4.14 – Elements SOLID 285 and SHELL 181 geometries [22]

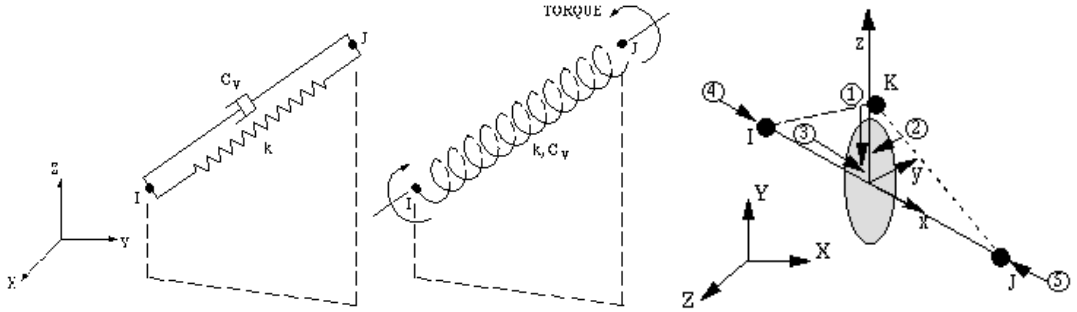

Figure 4.15 – Elements COMBIN14 and BEAM 188 geometries [22]

4.2.4.2. Real Constants

The rivets were simplified by performing a replacement by springs as was present in the chapter 2. The equations in the chapter 2 [4] were used during this process to calculate the spring constants. Different fasteners, thickness or properties of the doublers/skin produce different spring's constants.

- In order to determine these constants an Excel program was created and all the constants determined. This program is presented in the (attachment B).

- In the table 4.7 are shown the spring's constants determined

4.2.4.3. Mesh

The mesh initially produced is shown in the figures bellow. Due to the complexity of this part the mesh was produced using a free mesh. The regions with high curvatures and small angles required special attention and a superior quality of the elements [21].

Load Condition	*Fastener*	*Fastener Diameter (in)*	*Doubler Thickness (in.)*	*Skin Thickness (in.)*	*Spring Constant (Lbs/in.)*
Shear	Solid Rivet	5/32	0.2	0.05	200000
	Hi–lock Rivet	3/16	0.5	0.2	697487
		3/16	0.2	0.05	342210
		3/16	0.2	–0.2	594603
Tension	Solid Rivet	5/32	–	–	1580000
	Hi–lock Rivet	3/16	–	–	6560529

Table 4.7 – Fasteners springs constants

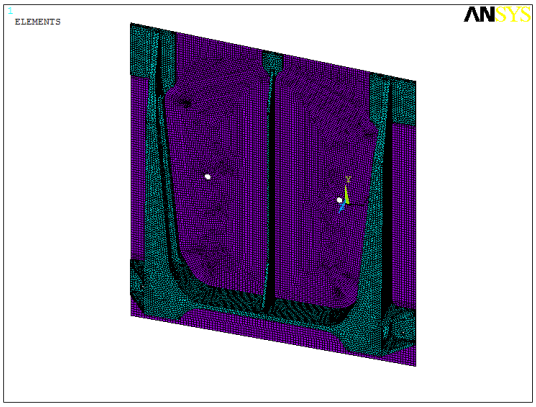

Figure 4.16 – Isometric view mesh

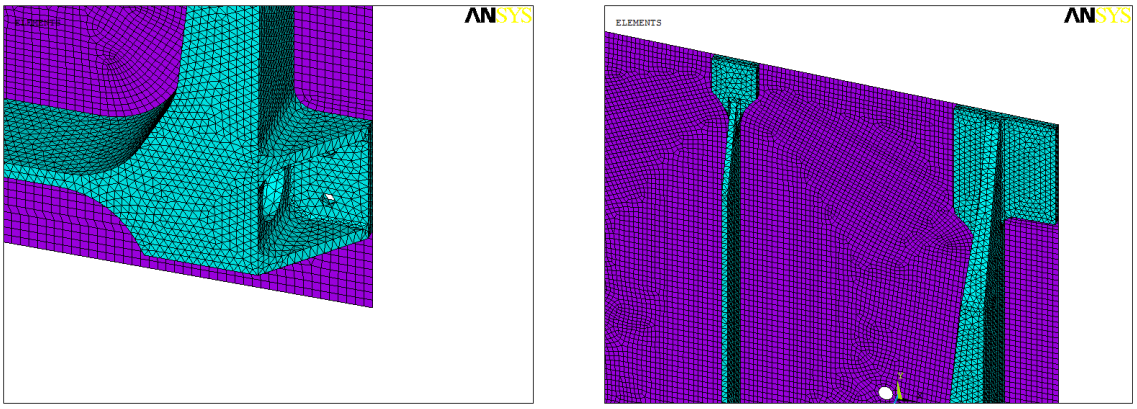

Figure 4.17 – Detailed view pocket and upper surface

Due to numerous problems that appeared during the pre–processor the initial mesh had to be modified. Different regions and volumes were created to permit different mesh refinement along the

structural member. Below is a brief resume of the issues emerged and the solutions found.

- Spring nodes had to be merged with the Fitting nodes. The merge operation is useful for tying separate, but coincident, nodes of different elements together.

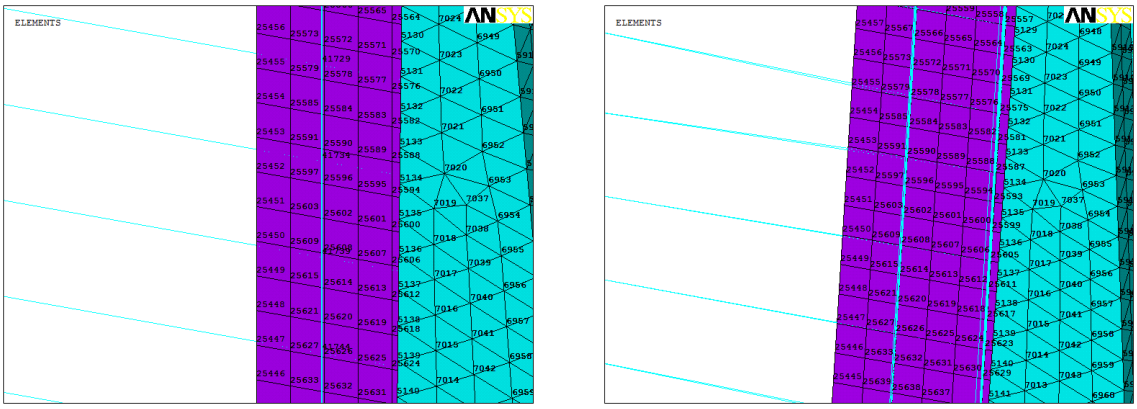

Figure 4.18 – Nodes before and after merging – ANSYS

- This operation was performed in the items selected which allow to introduce different merge parameters in different regions. The parameters introduced include the range of coincidence that is based on the maximum cartesian coordinate difference between nodes. At this point this parameter have to be introduced carefully because if the range is greater than the distance between two nodes of the surface mesh this operation will modify the Fitting mesh and it would bring several errors to the analysis.

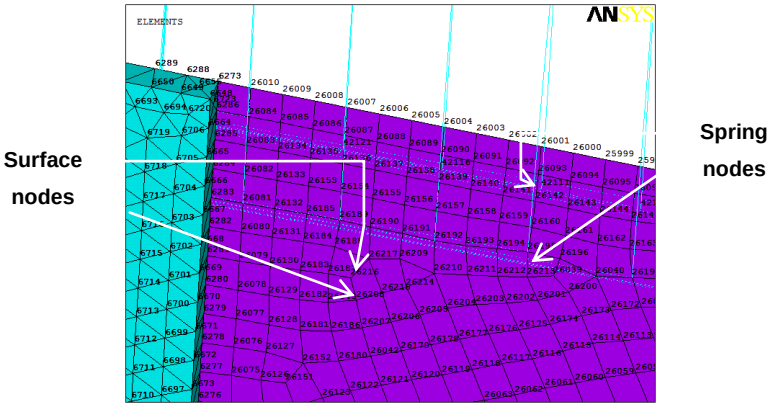

Figure 4.19 – Nodes with a free mesh – ANSYS

- Last figure represents a free mesh. After a geometry check it was found surface nodes closer than some spring and surface nodes what was a limitation to the range parameter. As a result it became impossible to define a parameter to merge the nodes (spring and surface nodes) avoiding merges two or more surface nodes [26].

A procedure followed to solve these problems was to divide the Fitting member in several volumes and areas to permit a different refinement and when possible a mapped mesh was applied.

The next figures present the result of this operation:

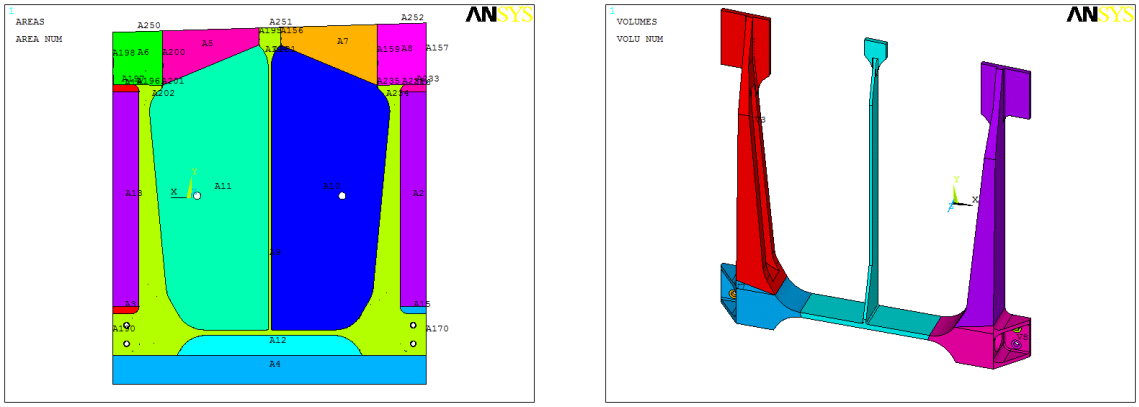

Figure 4.20 – Several surface areas and volumes – ANSYS

The part was re–meshed and the varieties of meshes produced are represented next:

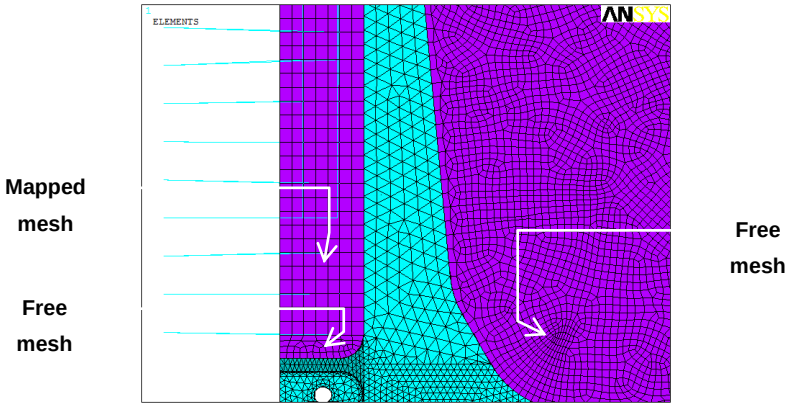

Figure 4.21 – Different surface mesh – ANSYS

- The regions with curvatures and angles were isolated and there were produced free meshes to adjust better to the surface. On the other hand in the regions delimited with straight lines were applied a mapped mesh and consequently avoid problems when merging the nodes.

- The same procedure was adapted to the volumes and the more complex regions were split to create several volumes and different refinement. The regions where the loads were applied had also been taken in account.

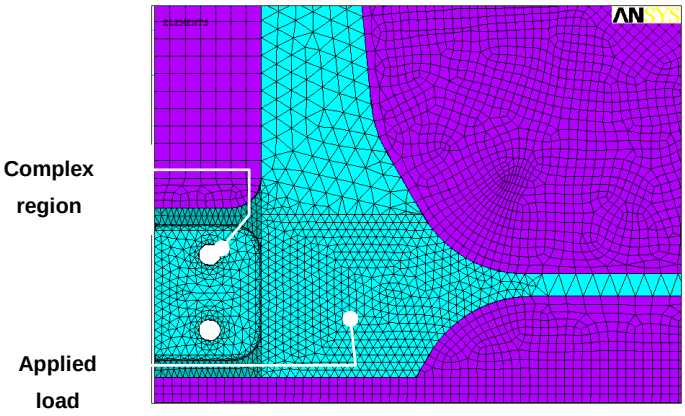

Figure 4.22 – Different volume mesh – ANSYS

4.2.4.4. Loads and Boundary Conditions

The most complicated part when dealing with a structural analysis is related to transferring the boundary conditions and load data from the real problem to the mechanical model.

4.2.4.4.1. Boundary Conditions

The boundary conditions that are applied to the structural model must be chosen accurately in order to obtain the best simulation of the real behavior of the structure. The first important assumption is that the spring and bolts nodes were constrained in all directions. In the model, this corresponds in blocking the UX, UY and UZ displacement of the interested nodes. The next figures present the model constrained.

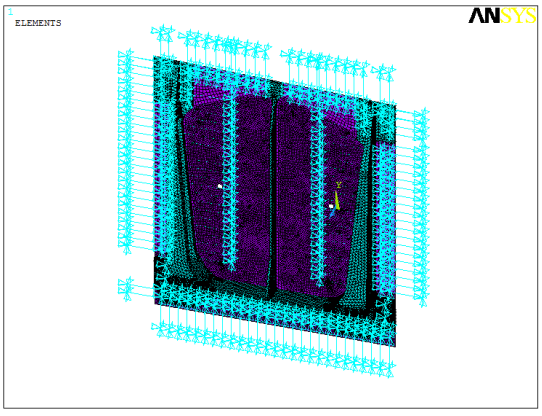

Figure 4.23 – Boundary conditions that simulate the connection between the Fitting and the spar

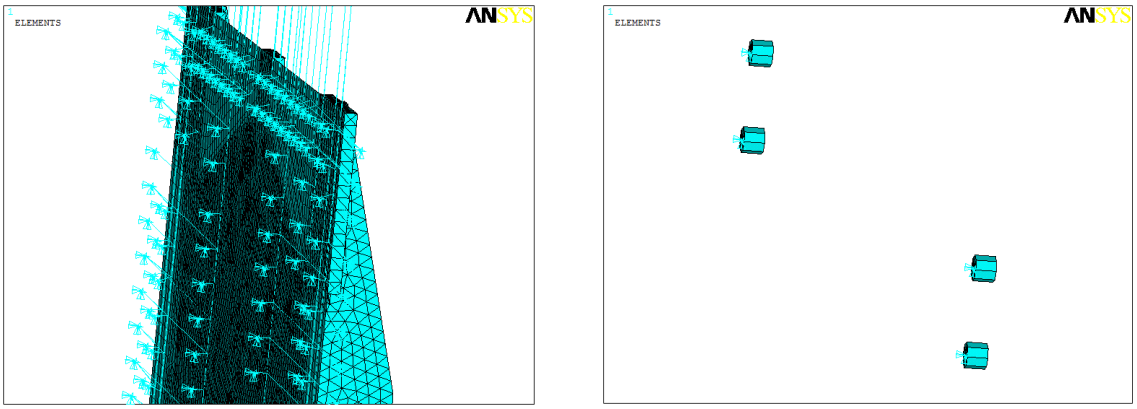

Figure 4.24 – Boundary condition springs and bolts (detailed view)

4.2.4.4.2. Loads

The following step was the application of the loads. From the Lockheed Martin documentation provided by the company and the calculus performed previously the loads applied for the static cases are present in the table 4.5.

- The load applied in each Fitting was considered the components determined early, R_1 and R_2. As observed previously the wing leading edge supports a higher load compared with the trailing edge (R_1>R_2). Consequently the load considered in this section is the R_1, which has in account the weight of the tank installation and the drag force.

- In terms of FEA the load was applied in the area where the barrel nut is introduced. The surface in contact with the nut (figure 4.6) and the model was considered of 120º as is represent in the following figures:

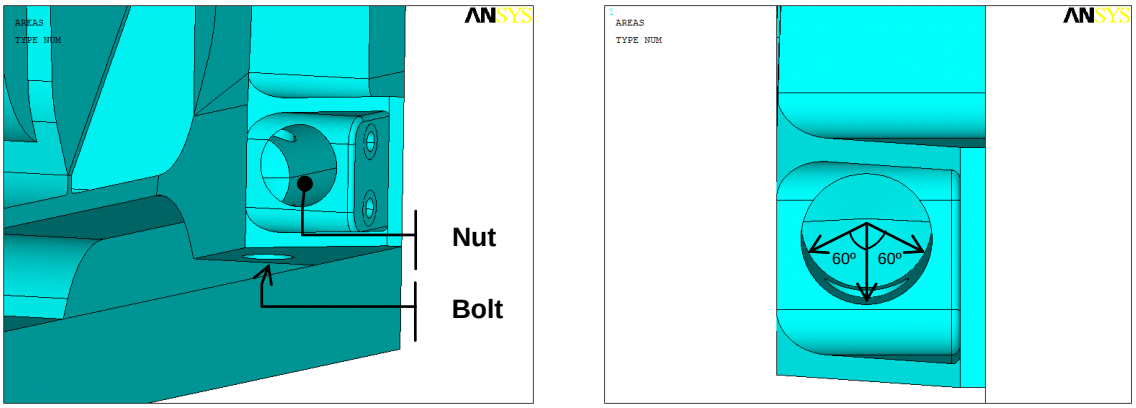

Figure 4.25 – Scheme of the attachment bolt and barrel nut and area of load application

This procedure was followed and the loads were applied in each side of the Fitting as it can be seen in the next figures.

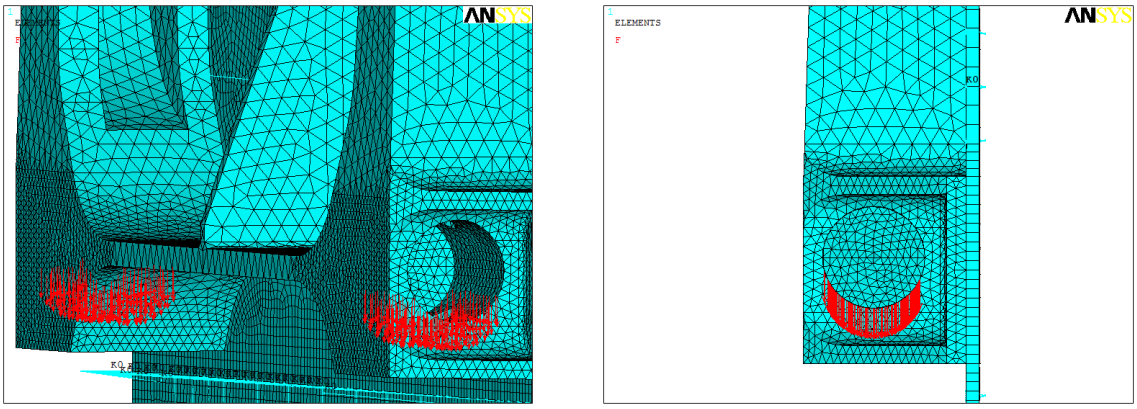

Figure 4.26 – Load applied in each side of the Fitting

It was also considered the case of banked turn with a bank angle of θ=60 degrees and a load factor of n=3. These conditions are critical for the C–130 aircraft operation.

These conditions were applied in the FE model taking in account the Pythagorean Theorem (figure 4.27). The boundaries conditions were the same as for the static case studied previously.

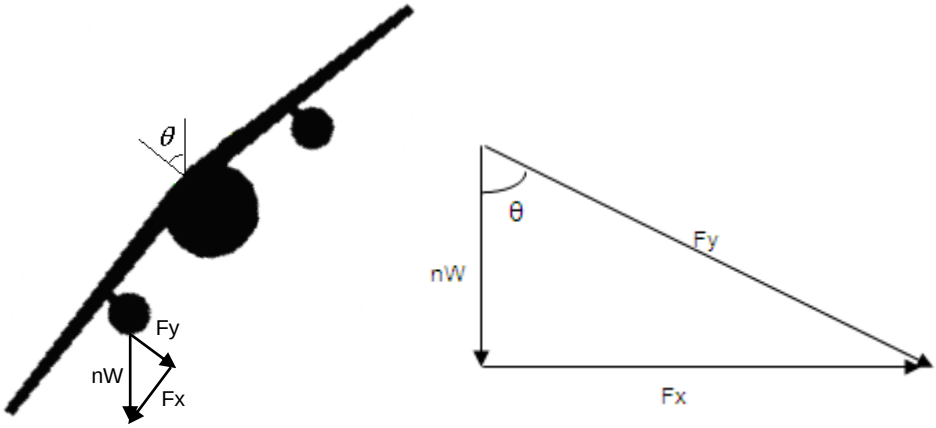

Figure 4.27 – Banked turn and Pythagorean Theorem applied to the forces

$$F_x = nW \sin\theta \tag{4.8}$$

$$F_y = nW \cos\theta \tag{4.9}$$

The Load nW was divided into two components considering the Pythagorean Theorem and the loads applied in the Pylon Fitting. The figure 4.28 illustrates this procedure.

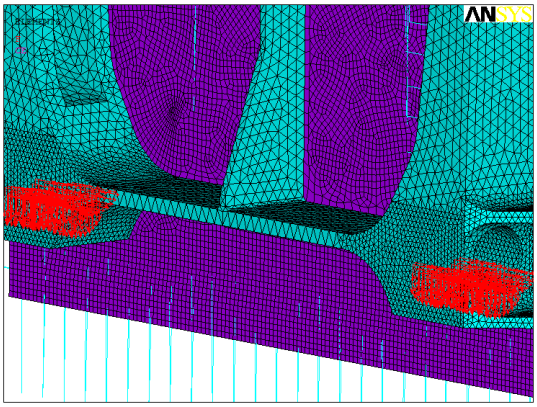

Figure 4.28 – Load applied in each side of the Fitting

4.2.5. FEA Results

4.2.5.1. Static Analysis Procedure

Once the geometrical values, boundaries conditions and load distribution have been introduced in the FE model the static analysis was performed. Three different static analyses were done, each one for a different load condition or flight maneuver. The objective of these analyses was to find several safety margins related with the various elements which define the static behavior of the structure. The list of safety margins is shown in the table 4.8.

Element	***Safety margin***	***Explanation***
Hi–Lock	MS_Shear_F	Indicates the margin of safety considering the fastener Shear failure
	MS_Bearing	Indicates the margin of safety considering the fastener Bearing failure
Solid Rivets	MS_Shear_F	Indicates the margin of safety considering the fastener Shear failure
	MS_Bearing	Indicates the margin of safety considering the fastener Bearing failure
Shear Bolts	MS_Shear_F	Indicates the margin of safety considering the fastener Shear failure
	MS_Bearing	Indicates the margin of safety considering the fastener Bearing failure
Fitting	MS_1	Indicates the margin of safety considering the maximum 1st Principal Stress
	MS_2	Indicates the margin of safety considering the maximum 2st Principal Stress
	MS_3	Indicates the margin of safety considering the maximum 3st Principal Stress

Table 4.8 – Safety margins

The safety margins were determined using the next equation [7]:

$$MS = \frac{\sigma_{ultimate}}{\sigma_{applied}} - 1 \tag{4.10}$$

In order to reach the safety margins an Excel file was developed to implement all the calculus related with the static analysis. The Load conditions presented in the Excel are: The level flight n=1g down, in flight gust loads with load factor n=8.25g down and banked turn (60º) with load factor n=3g down. For each element it was created a similar worksheet to evaluate the behavior under each condition. These results are fundamental to assess the maximum forces and stresses and compare with the ultimate for each element. The bearing failure was also evaluated. These results are in the attachment C.

4.2.5.2. Results Comparison & Developed Software

Considering the results from the previous analyses evaluated in the Excel file (attachment C), the critical case in flight is the vertical gust n=8.25 g down. Taking in attention this case, several critical regions were identified.

Fasteners (Hi–Lock, Solid Rivets, Shear Bolts)

- The fasteners elements were evaluated in the Excel file considering the results provided by the FEA. For each element the shear force component was determined and compared with the ultimate. For the tensile force and the bearing failure the procedure was the same and the results compared with the material data.
- The results indicate that the fasteners elements loaded the most are the shear bolts followed by the Hi–Locks in the Lower Flange.
- The evaluation performed in the Excel concludes that the fasteners are in the safe zone but some MS are close to 0.5 for several elements (Pocket Shear Bolts and Lower Flange fasteners).
- For some Lower Flange fasteners the MS for bearing failure presents to be in a relatively low value which correspond to a possible bearing failure on structural member (Fitting) at these fastener locations.

Fitting Member

Following the principal stresses are presented as well as the identified regions.

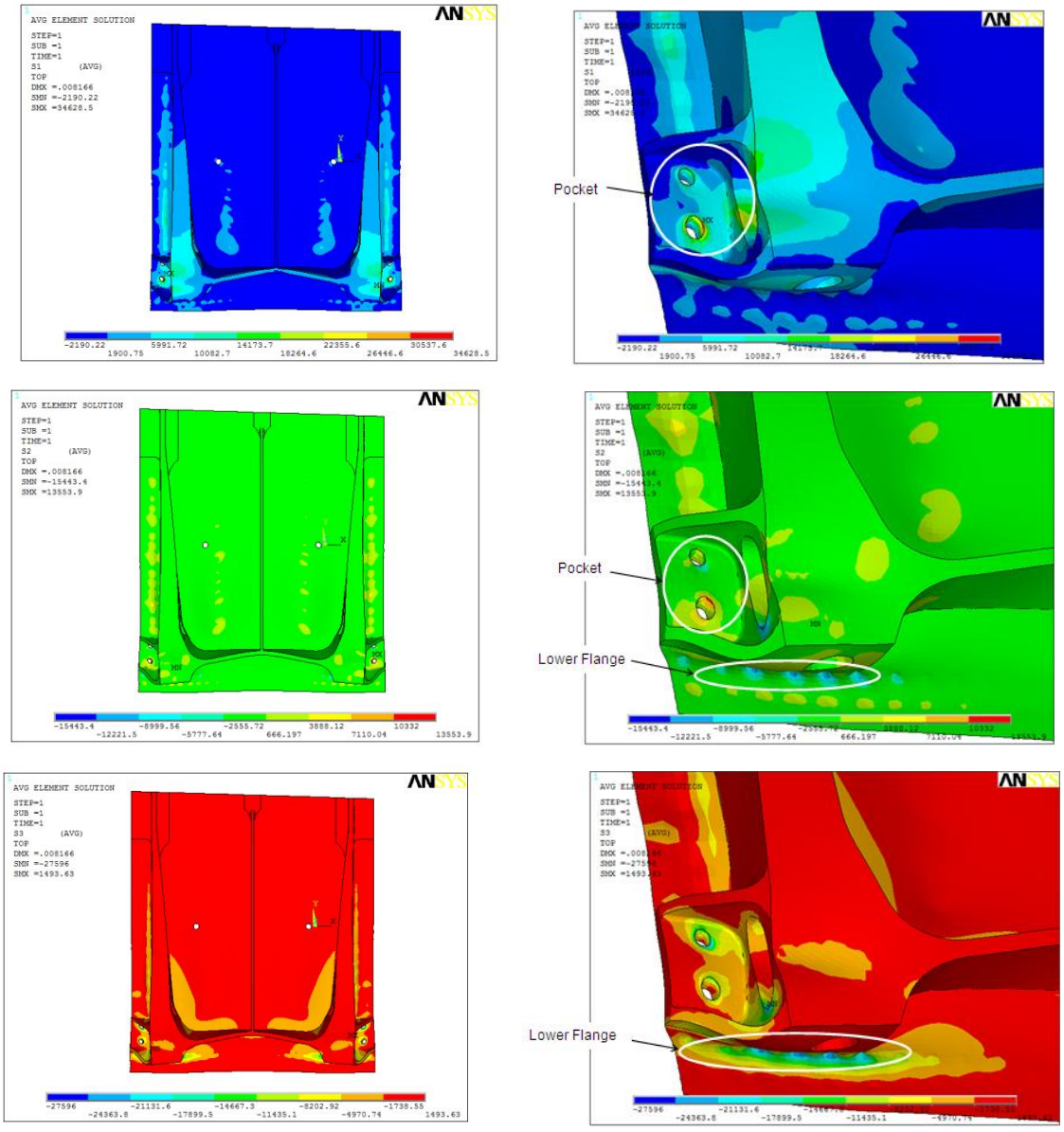

Figure 4.29 – Standard configuration – S1, S2 and S3

In the figure 4.29 are assigned the regions where the maximum stresses were indentified. The region of the Pocket and the first line of fasteners in the Lower Flange are the critical zones. In accordance with aircraft structures design these results were expected once these elements are the first to be loaded and consequently the ones supporting more loads. Fuel leaks result mainly from net tension (cracking) or bearing in the elements. (figures 2.7 and 2.9) [27].

4.2.6. Fitting Upgrades

Once the critical regions were identified several Fitting upgrades were evaluated. The procedure adopted considers a redesign of the Fitting avoiding modifying the shape which is essential to the

assembly on the wing. As a result an effective solution is through the increase of the thickness in the identified regions increasing the net area and thus reducing the stress concentration.

Due to these several modifications the fasteners springs constants had to be modified and the next table presents the new springs constants.

Load Condition	*Fastener*	*Fastener Diameter (in)*	*Doubler Thickness (in.)*	*Skin Thickness (in.)*	*Spring Constant (Lbs/in.)*
Shear	Solid Rivet	5/32	0.3	0.05	260000
	Hi–lock	3/16	0.3	0.05	369149
	Rivet	3/16	0.3	0.2	647679

Table 4.9 – Fasteners springs constants

The improvements considered were the increase of the thickness in the Lower Flange from 0.2in to 0.3in and in the Pocket by 0.1in.

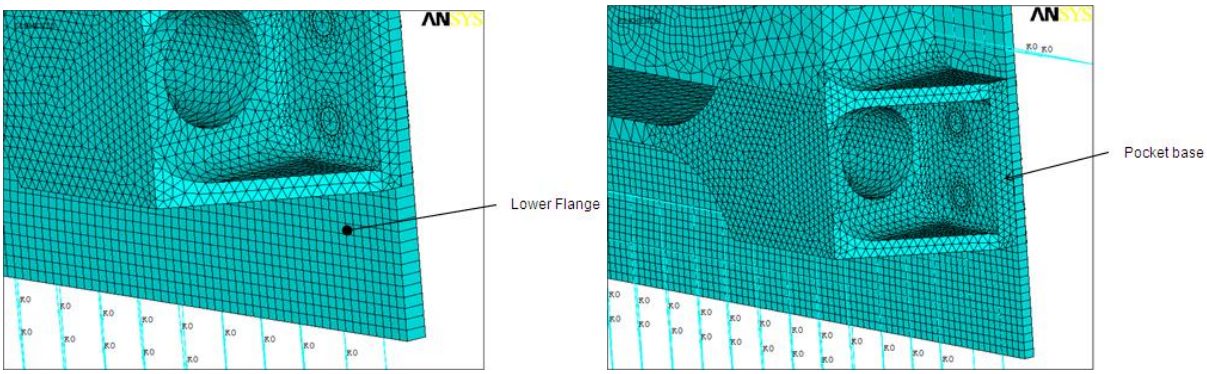

Figure 4.30 – Lower Flange and Pocket thickness increase

The table 4.10 present the results obtained from the FEA considering the improvements performed. These results are compared with the standard configuration considering the load case of n=8.25g. The S1, S2 and S3 are the maximum principal stresses on the Fitting. Bolt FX, FY and FZ are the maximum loads in the bolts. Hi–lock FX, FY and FZ are the maximum loads in the Hi–locks elements and Solid Rivet FX and FY are the maximum loads in the Solid Rivets elements.

Note: The symbol ↓ indicate a lower maximum value compared to the standard configuration, ↑ indicate a higher maximum value and ≈ indicate a value relatively close.

FE Analyses	*S1*	*S2*	*S3*	*Bolt FX*	*Bolt FY*	*Bolt FZ*	*Hi–lock FX*	*Hi–lock FY*	*Hi–lock FZ*	*Solid Rivets FX*	*Solid Rivets FY*
Lower. F.	↓	↓	↓	↓	↓	↓	≈	↑	↑	≈	↓
Pocket	↓	↓	≈	≈	↑	↑	≈	↓	↓	≈	≈

Table 4.10 – Maximum stress and loads FEA upgrades comparison

Lower Flange – This upgrade consists in the increase of the thickness in the Lower Flange.

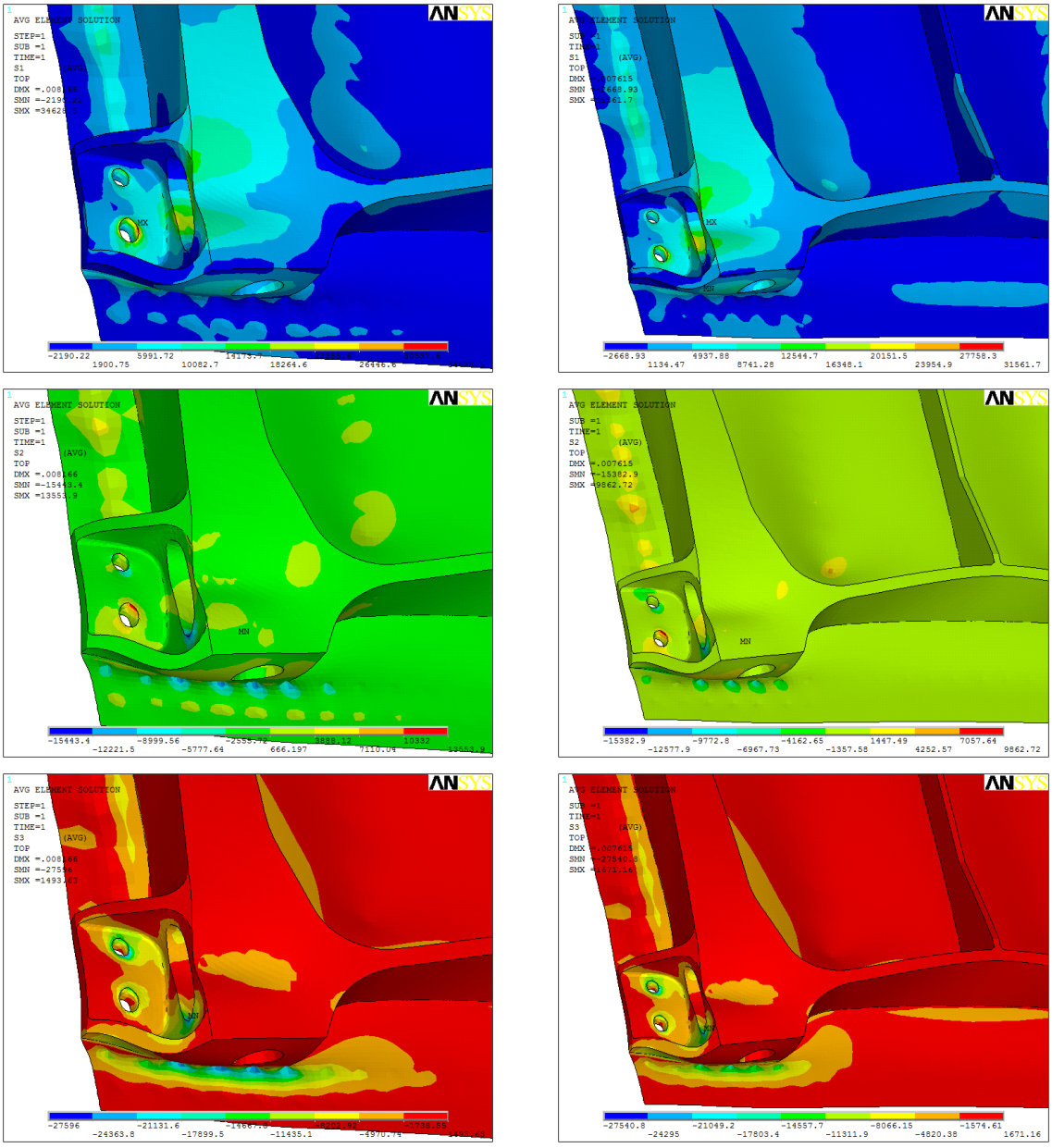

Figure 4.31 – Standard and Lower Flange thickness increase configuration (L & R, respectively) – S1, S2 and S3

From the previous results it is observed that the improvement in the Lower Flange reduced significantly the maximum stresses in the structure but increases the loads transfer by the lower fasteners. This increase is suitable once the load values carried by these fasteners are in the safety zone.

Pocket – This upgrade consists in the increase of the thickness in the Pocket base.

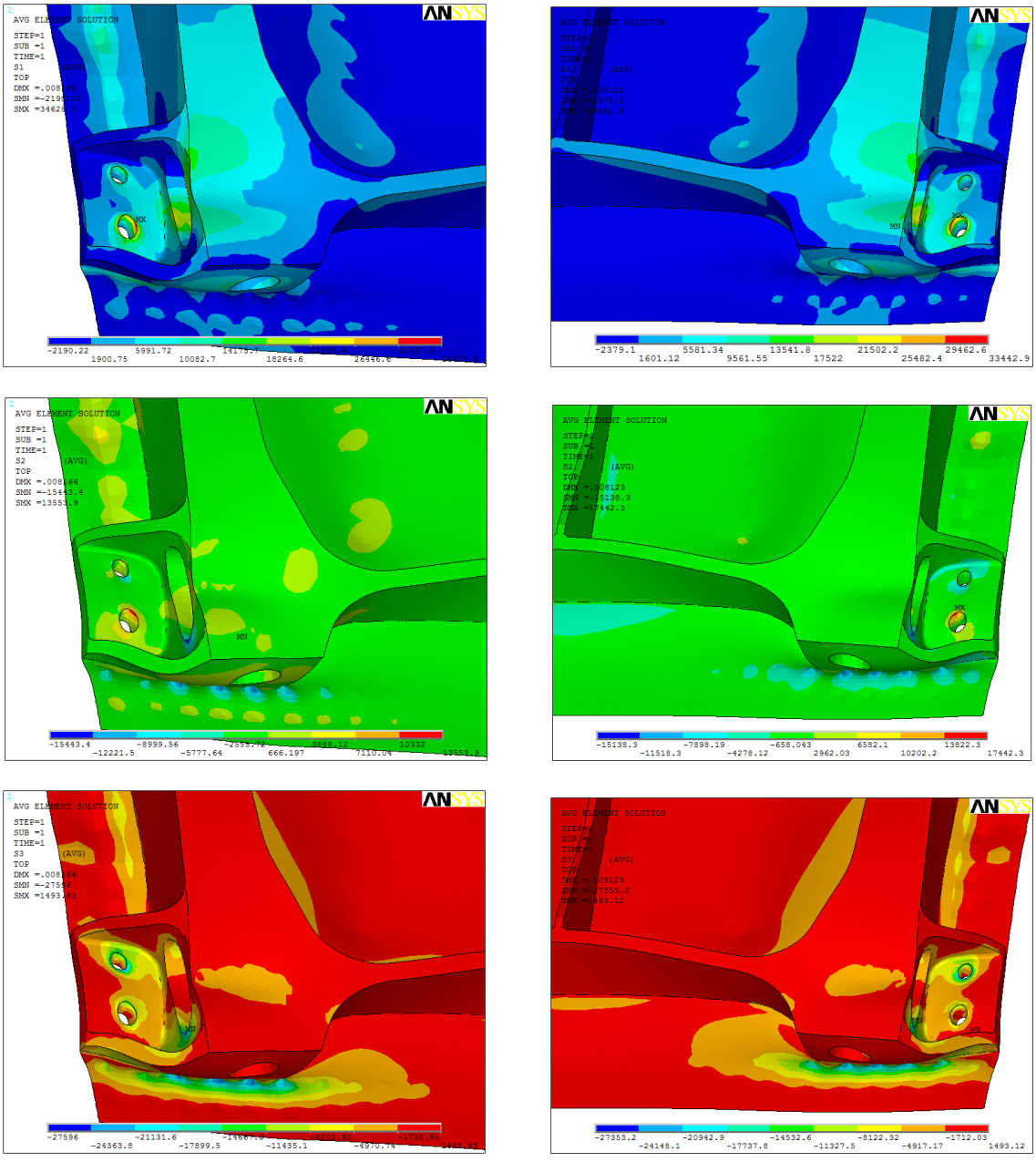

Figure 4.32 – Standard and Pocket base thickness increase configuration (L & R, respectively) – S1, S2 and S3

The modification in the Pocket does not carry significant improvement. Although the maximum principal stresses decreases the stress concentration increases in the Pocket. The Lower Flange fasteners are slightly relieved as observed but the increase of stress in Pocket base is not intended.

Lower Surface – Considering the results obtained with the improvement in the Lower Flange, the same procedure was applied to the Lower, Side and Top flanges as well as the Interior surface.

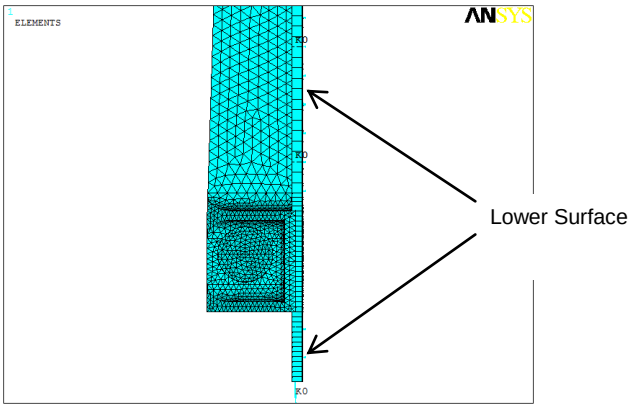

Figure 4.33 – Lower surface thickness increase

The results are compared with the Lower Flange improvement.

FE Analyses	*S1*	*S2*	*S3*	*Bolt FX*	*Bolt FY*	*Bolt FZ*	*Hi–lock FX*	*Hi–lock FY*	*Hi–lock FZ*	*Solid Rivets FX*	*Solid Rivets FY*
Lower surf.	↓	≈	↓	↓	↓	↓	↑	↑	↑	↑	↑

Table 4.11 – Maximum stress and loads FEA upgrades comparison

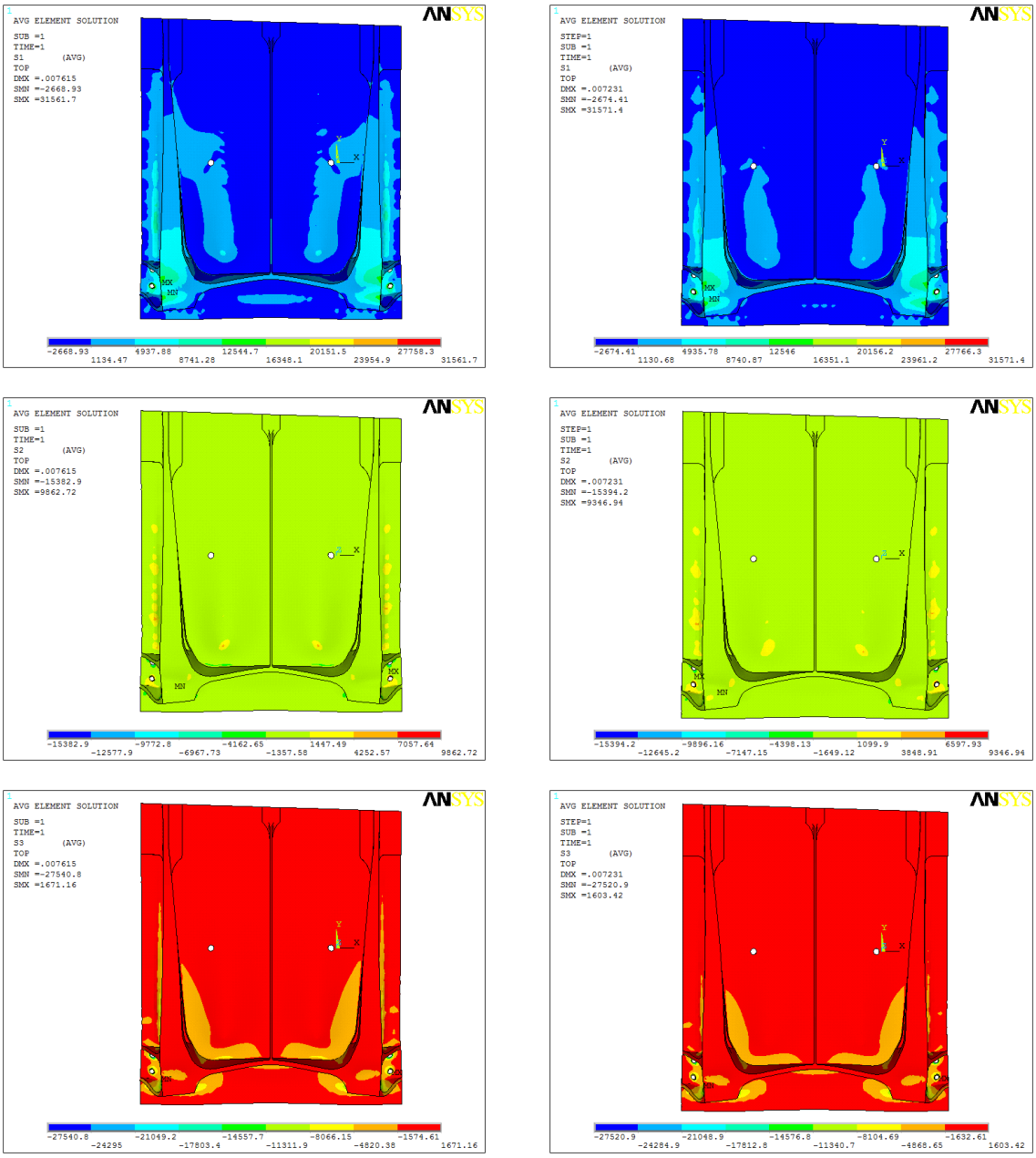

Figure 4.34 – Lower Flange and Lower Surface thickness increase (L & R, respectively) – S1, S2 and S3

This modification introduced reinforcement in such regions resulting in a load transfer from the Pocket and Lower Flange section to the Fitting Side Flanges, Interior and Top. Consequently the Pocket and Lower Flange sections were relieved and the stress concentration decrease in the critical regions.

The previous improvements performed in the Fitting member were evaluated in respect to the weight increase. The table 4.12 presents the detailed weight increase in percentage (%) considering the standard configuration.

Configuration	*Total Weight (Lbs)*	*Weight increase (%)*
Standard	24.32221	0
Lower Flange	24.90145	2.381506
Pocket base	24.39706	0.307706
Lower Surface	28.56482	17.44334

Table 4.12 – Weight increase (%) of the configurations considered

The Lower Surface upgrade increases the Fitting weight by approximately 4.2 lbs. Considering the aircraft empty weight this increase is about 0.005 % (negligible). The manufacture of the new members considering the improvements requires a different forge mold. The cost increase is directly related with the fabrication of new molds which has to be evaluated with the manufacturer.

4.2.7. WorkCard

A workcard with instructions to perform a Nondestructive Inspection (NDI) on the forward and aft Pylon attach Fittings was developed. These inspection procedures are in the SMP 583 [28] and the purpose was to develop and update these procedures in order to inspect the identified zones. These instructions were based on the results from the FEA carried previously.

1. **Purpose** – Perform NDI between the OWS 72 and OWS 90, outer wing forward spar web, forward and aft Pylon attach Fittings, and Pylon attach bolts and barrel nuts for left and right hand sides.
2. **Description** – The spar web is 7075 CLAD aluminum. The forward and aft Pylon attach Fittings are 7075 aluminum. The Pylon attach bolts and barrel nuts are alloy steel.
3. **Defects**
    a. Countersunk fasteners – Forward spar defects looked for in this inspection are fatigue cracks generally running vertically between two countersunk fasteners and above the top fastener.
    b. Shear Bolt holes – Forward and aft Pylon attaches Fitting defects looked for in these parts are fatigue cracks in the bolt holes in the upper portion of hole where barrel nut is installed.
    c. Pylon attaches bolts and barrels nuts – Defects looked for in the Pylon attach bolts and barrels nuts are cracks. The cracks are expected to occur in threaded portions and at sharp radius areas.

In this inspection procedure it is considered three different NDI methods [12]:

- **Eddy Current Surface Scan** – Accurate method for verifying material integrity and conductive material coating thickness. It uses electromagnetic induction to detect flaws in conductive materials.
- **Fluorescent penetrant inspection (FPI)** – A type of dye penetrant inspection in which a fluorescent dye is applied to the surface of a non–porous material in order to detect defects that may compromise the integrity or quality of the part in question. Noted for its low cost and simple process, FPI is used widely in a variety of industries.
- **Wet Fluorescent Magnetic Particle** – A process for detecting surface and slightly subsurface discontinuities in ferromagnetic materials such as iron, nickel, cobalt, and some of their alloys. The process puts a magnetic field into the part.

The procedure to inspect is accessible on the card SMP 583 [28]. The figure 4.35 presents the front Fitting with the scan areas indicated. It includes the Bottom Flange Hi–Locks (countersunk fasteners) and the Pocket holes (Shear Bolt holes). The Pylon attach bolts and barrels nuts are present in the figure 4.6.

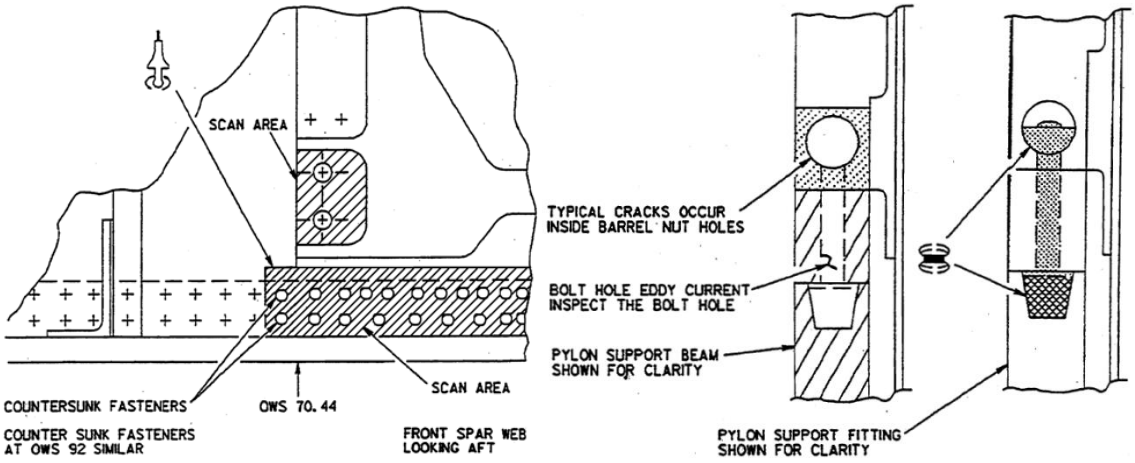

Figure 4.35 – Forward Pylon attach Fitting and Pylon attach bolts and nuts (scan areas) [adapted 28]

4.3. Conclusions

The aims and objectives set out at the beginning of the project with respect to the structural analysis were accomplished. To achieve this, the design, development and evaluation of a Fitting member was successfully carried out. The analysis was accomplished using actual boundary and loading conditions.

A procedure and a Microsoft Excel file supporting the methodology has been developed during the study. The Excel file enables determining the static behavior of the fasteners and the Fitting member as well as the upgrades performed. The methodology principles are explained at the current report.

- The initial objective of perform a historical analysis in order to find out the regions in the fuel tanks susceptible of fuel leaks was completed. From this analysis a structural member was selected.
- A FEA was carried to check and determine the critical zones and fasteners in the structural member selected. The Excel file created was an important tool during this step.
- The region of the Pocket and the first line of fasteners in the Lower Flange were identified as the critical zones. This procedure allowed to decide the upgrades and the location of structural reinforcement applied and verified through FEA.
- The structural reinforcements allowed to decrease the maximum stresses on the Fitting. Although the loads carried by some fasteners increases it did not take any complication since these values are in the safety zone, accordingly to the fasteners data.
- The Lower Surface upgrade is the best option to decrease the stresses on the critical zones. The reinforcement introduced in such regions resulting in a load transfer from the Pocket and Lower Flange section to the Fitting Side Flanges, Interior and Top maintain the structural integrity of the member.
- A workcard with instructions to carry out a Nondestructive Inspection on the forward and aft Pylon attach Fittings was developed. The purpose was to update these procedures in order to inspect the identified zones. These instructions were based on the results from the FEA carried previously.

The next chapters present the sealants and sealant testing as well as the maintenance instructions. The main goal is to research and test new sealants products in order to reduce the fuel leaks. The development, evaluation and update of the maintenance instructions manual introduce correct and simplified maintenance instructions to all the technicians in order to make possible an accurate sealing of the fuel tanks.

5. Sealants and Sealant Testing

This chapter considers the geometrical and material considerations that govern a typical sealed joint in a wingbox integral fuel tank. The purpose of the review is to arrive at the requirements for the tests and the development of the sealing procedures.

5.1. Introduction

One definition of sealant is "a material that isolates one environment from another". For a sealant to be effective in performing its function it must have some essential characteristics: flexibility and fatigue resistance; physical strength, chemical and environmental resistance, and high adhesion to all surfaces to which the sealant is applied. Of these characteristics, adhesion is the most important as a material will lose its ability to "seal" the moment that adhesion is lost. There is no such thing as the "perfect sealant" since no sealant can possess all of the desirable properties for all applications.

Aircraft manufacturers currently use polysulfide based sealants which are resistant to aviation fuels and are therefore useful for sealing fuel tanks. It is produced in the following classifications [29]:

Type I – Sealing material suitable for brush or dip application
Type II – Sealing material suitable for application by extrusion gun or spatula
Type III – Sealing material suitable for spray gun application
Type IV – Sealing material suitable for faying surface application gun or spatula

5.2. Polysulfide Sealant

The first aerospace sealants were two part products based on liquid polysulfide (LP's) polymer cured with lead peroxide. During the 1950's dichromate–cured sealants were used and the late 1960's noticed the introduction of manganese–cured sealants. The latest developments have been in epoxy cured polythioether sealants, which came on the market in the late 1980's.

The polysulfide sealants used in aerospace applications are still mainly two component systems which, on mixing, cure by chemical reaction. Basically, the polysulfide polymer in the base component reacts with an oxidizing agent (for example manganese dioxide) in the curative component. Sometimes the two components are pre–mixed and then stored at very low temperature to stop the reaction. Only at the time of application is the mixed sealant brought to room temperature, applied to the joint, with the cure initiation at the same time. The sealant will cure within a few hours, but the sealant's full physical properties may take several days to develop.

Polysulfides will adhere to metal, glass, fiberglass, wood, or any combination of these. The polysulfides are not resistant to high temperatures, but are all impermeable to fuel and solvent deterioration. This makes them suitable for fuel tanks and fuel systems [2].

5.2.1. Advantages and Disadvantages of Polysulfide Sealants

Some of the key properties in the cured, polysulfide sealant are listed below [2].

Advantages:

1. Superior resistance to swell in aviation fuels
2. Excellent adhesion (in tension, sheer and peel) to aluminum, titanium, other metals and composites (primers and surface treatments may be used for optimum adhesion and durability of adhesion)
3. Low permeation to fuel vapor, water vapor and air
4. Good low temperature flexibility (–50°C and lower)
5. Good heat resistance
6. Good elasticity, reasonable strength (in the presence of fuels), good resilience
7. Good adhesion of new sealant to old sealant (i.e. in repair)
8. Superior application properties (simple to apply)

Limitations:

1. Water and antifreeze absorption, leading to swell and a drop in properties, in particular tear resistance
2. Absorption of water and antifreeze weakens adhesion
3. Attack by bacteria leads to reversion
4. High specific gravity (SG).

5.3. Sealant Joints used in Aircraft Integral Fuel Tanks

The principal application areas are shown in a typical skin butt–strap joint in figure 5.1 [1], [30].

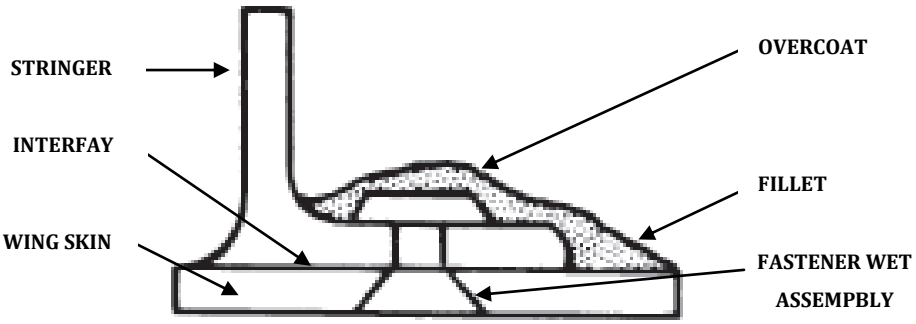

Figure 5.1 – Sealant application used in aircraft integral fuel tanks [adapted 1]

- **Interfay sealing** – Sealing is applied by applying sealant thinly to the whole surface area of both faces of the parts to be assembled. Nominal thickness of the sealant is between 0.01in to 0.015in. When a jointing compound has not been deployed in the assembly, fretting can result. Fretting corrosion refers to corrosion damage at the contact surfaces. Damage can occur at the interface of two highly loaded surfaces which are not designed to move against each other. Interestingly, the concept of using interfay sealant in aircraft construction was driven in the first instance by the need to address fretting and corrosion issues as opposed to achieving fluid sealing.
- **Joint edge sealing** – The sealant is applied as a fillet bead. It is applied when the components are assembled using interfay sealant, and in some cases may be areas where the sealant has been displaced by the pressure exerted by the fasteners. To ensure a perfect sealing a fillet sealant is applied to the edge of the joint.
- **Overcoat** – A layer of sealant is applied over rivet or bolt heads and nuts. The application of the sealant in this method can be compared to applying paint. The part to be sealed is cleaned and a type I sealant is applied with a brush to the component, usually a fastener, to ensure that fluids cannot migrate down the threads or along any small surface imperfections present.
- **Wet assembly** – When one end of a fastener or rivet is to come into contact with the sealed medium (fuel), the fasteners or rivet are assembled using the wet sealant. This ensures that the sealant will fill any imperfections along the fastener length, thread or under the head thus stopping the fuel from finding a leak path.

5.4. Sealant Selection

Sealant selection and the joint design must be developed in agreement. In selecting the proper sealant for a specific application, consideration must be given to such characteristics as modulus, cure time, application parameters, adhesion, weather conditions, chemical resistance and suitability of the sealant to "seal" the chosen sealed environment (gas, fluid etc.).

The sealants employed in integral fuel tanks must attain certain specifications and standards. The general specifications and tests for the sealants used to seal the interior of the tanks (contact with fuel) are established in the Aerospace Material Specification (AMS) AMS–S–88002 (May, 1999) [31]. The sealants used to perform the interface sealing on fuel tanks and during assembly process (without contact with fuel) are presented in the Military Specification (MIL) MIL–PRF–81733D (May, 1998) [29].

5.5. Causes of Sealant Failure in Integral Fuel Tanks

It can be appreciated that the adhesive and cohesive properties of aircraft sealant primer systems and the surfaces to be sealed are influenced by factors such as temperature, fuel contamination and fatigue cycling. The principal causes of failure can be summarized as: [1]

- **Blisters** – Blisters may be caused by air bubbles or cleaning solvents trapped in the sealant when it cures. A blister may break, and thus open the sealant, due to expansion at high altitudes, flexing of the wing structure, or an extreme increase in temperature.
- **Breaks (cracks) in sealant** – Continual excessive flexing of the wing structure in flight, rough landings, or fast taxiing over rough terrain with a heavy fuel load can cause breaks in sealant. Breaks in sealant can also be caused by mechanical damage and shoes or boots of maintenance personnel.
- **Voids or omissions in sealant** – Leaks will result if sealant is omitted from hard–to–get–at–places, or if sealant is not thoroughly worked into all voids along all seams and joints. Injection in injection holes is critical and the sealant must extrude from all openings.
- **Poor adhesion** – Sealant will not adhere if the structure has not been thoroughly cleaned. Dirt, grease, soap film, oil film, moisture trapped in seams and joints, and even fingerprints will reduce adhesion. Poor or no adhesion will result if an attempt is made to apply sealant that is about to exceed its application life.
- **Pinholes in sealant** – Brush sealant, if not worked thoroughly with a brush around each rivet or fastener, may form pinholes as the sealant cures. If base compound and accelerator are not completely mixed, the fuel may dissolve the unmixed accelerator, forming small voids.
- **Deterioration of sealant** – Deteriorated sealant appears chalky and powdery, and will crack easily on flexing. Such sealant may contain pinholes. Deterioration of sealant is caused primarily by fuel. Sealant is normally top–coated to retard this deterioration.
- **Dried–out sealant** – Dried–out sealant topcoat is caused by a tank having been empty for a period beyond the safe limit. When sealant topcoat has been dried out, it hardens and cracks easily, causing leaks. If this condition is found, the entire sealing system of the tank is generally affected. It can be identified by a network of multiple cracks over the sealant surfaces. Drying out can be prevented by coating the O–rings, mechanical seals, and topcoat in the entire tank with 1010 oil.

5.6. Sealants Tests and Results

5.6.1. Introduction

In order to acquire results from the sealants used in aircraft fuel tank maintenance, 4 different sealants (types II) were evaluated, 2 for each specification indicated in the section 5.4. From these sealants 2 are currently employed in fuel tanks sealing at OGMA (1 and 3) and the other 2 are potential products to apply (2 and 4).

The products tested were:

AMS–S–88002

1. PR 1440 B2 (Currently employed at OGMA in C–130)
2. AC 236 B2 (Approved by Lockheed to C–130)

MIL–PRF–81733

3. PS 870 B2 (Currently employed at OGMA in C–130)
4. MC 780 B2 (Not approved by Lockheed to C–130)

The products currently used at OGMA in C–130 (1 and 3) were tested to validate their standard properties considering in the specifications from the manufacturer and to compare with the results from the products not employed at present (2 and 4). Those 2 Sealants are not being used by OGMA because AC 236 B2 has long drying times and MC 780 B2 is not approved by Lockheed Martin. However OGMA already apply it in different Aircraft. It's important to test the product 1 since it is employed as interface sealing. Usually to perform the interfay sealing, sealants type III should be applied, because they are more fluid. However these sealants have longer curing times and during maintenance operation cannot be used. So, maintenance manuals require the application of sealants type II (product 1 or 2) as interference sealant, allowing decrease the sealant cure time. Although AC 236 B2 has longer drying times than the others it is important to test in order to verify if in the same conditions this material have the same adhesion to the metal parts.

Note that the specifications considered specify some exposures in fluids (as aviation fuel) but it was not performed once the sealants products are already certified by the manufacturer to resist aviation fuel.

5.6.2. Sealant Tests

The tests and conditions are presented in the next sections [32]:

5.6.2.1. Standard Test Conditions

Test specimens were prepared at standard laboratory conditions and immediately after completion of preparation, were placed under 25 °C ± 3 and 50% ± 5 relative humidity to cure.

5.6.2.2. Preparation of Sealing Compound

The sealing compound was prepared according to the manufacturer's instructions. The mix ratios between sealant base compound and the curing agent were accomplished as specified by the manufacturer.

Figure 5.2 – Preparation of sealing compound

5.6.2.3. Curing of the Sealing Compound

For qualification tests, the sealing compound must be cured for 14 days at standard conditions. For acceptance tests, the sealing compound shall be given an accelerated cure for 48 hours minimum at standard conditions followed by 48 hours at 50 °C. The second alternative was considered.

5.6.2.4. Application Properties Test Methods

- **Appearance** – The base compound and curing agent shall be of uniform blend and free of skins, lumps, and jelled or coarse particles. There shall be no separation of ingredients which cannot be readily dispersed by mechanical agitation or mixing by hand.

- **Color** – Unless otherwise specified in the contract or order, the color of the sealing compound is as furnished by the manufacturer. The curing agent, if furnished separately, shall be of contrasting color to facilitate mixing.

5.6.2.5. Viscosity of Base Compound

The viscosity of base compound was performed in order to ensure that the sealant is in perfect conditions before mixture.

The viscosity of base compound test used the Brookfield Model RVF viscometer (figure 5.3). The readings obtained were converted to poises. Viscometer spindle size (no. 7) and speed of rotation (2 rpm) used were defined in the material specification for the class and application time of sealing compound under test, according to sealant class. The highest reading was taken after the instrument has run in the fluid for 60 to 70 s (figure 5.3). This procedure was conducted two times and the average value was determined. The average value was then checked for conformance to the sealing material specification (figure 5.3). The results are in the tables 5.1 and 5.2.

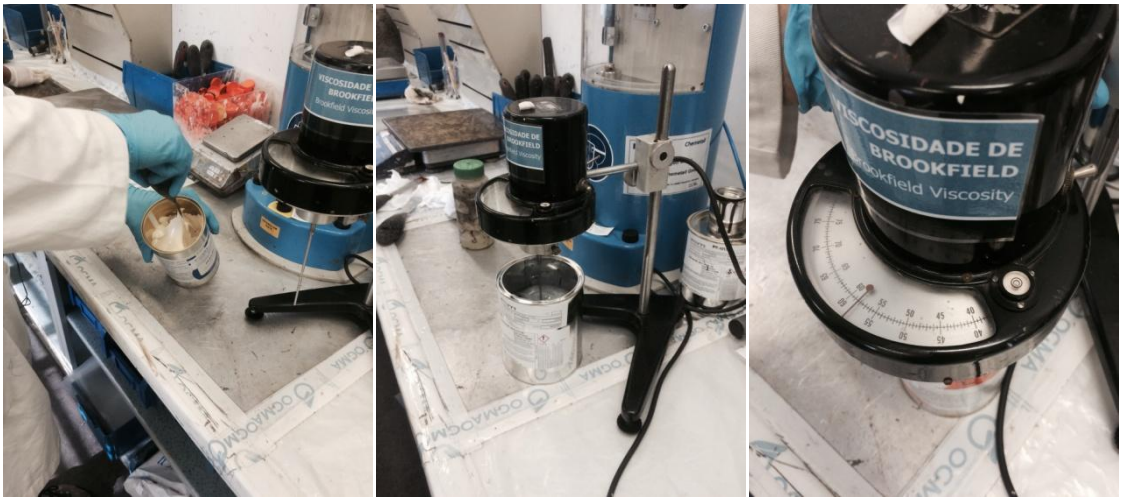

Figure 5.3 – Viscosity of base compound test preparation and result

5.6.2.6. Flow

The flow test is normally applied on sealants Type II, i. e., on sealants to be applied by gun or spatula in order to test the displacement of sealant when applied on a vertical surface (e. g. aircraft fuselage sealing).

The flow test was conducted using a clean flow test jig as shown in figure 5.4. Depth of the fixture plunger is critical and shall be controlled within the tolerance specified in figure 5.4 during all flow testing. The flow jig was placed on a table with the front face upward and the plunger depressed to the limit of its travel. Within 15 min of the beginning of sealant mixing, the mixed sealing compound

(freshly mixed) was extruded to fill the cavity created by the depressed plunger. Then the sealant was leveled with the front surface of the jig. Within 10 s after the leveling operation, the jig was placed upright on its base and the plunger immediately advanced to the limit of its forward travel (figure 5.4).

After that the flow measurement was taken at exactly 30 min after the sealing compound had been applied to the flow test fixture. The flow was measured from the lower edge of the plunger to the extreme point to which flow had advanced. The results are in the tables 5.1 and 5.2.

Figure 5.4 – Flow test fixture and procedure [32]

5.6.2.7. Tack–Free Time

This test was performed to analyze the sealant process cure, i. e. to verify if it was curing as it was expected.

The sealing compound was applied in accordance with material specification requirements and cured at standard conditions for the tack–free time defined in the material specification for the sealing compound under test (figure 5.5).

Figure 5.5 – Sealing compound under test

At the end of the specified tack–free time, 1 in x 7 in strips of low density polyethylene film, cleaned with cloth wipes and clean solvent, were applied to the sealing compound and held in place for 2 min ± 10 s. The strips were then slowly peeled back at right angles to the sealing compound

surface. (The polyethylene came away clean and free of sealing compound). The results are in the tables 5.1 and 5.2.

5.6.2.8. Standard Curing

The standard curing is an important test since it evaluates if the remaining work on the aircraft can be continued without having impact on the process.

The instantaneous hardness was determined using a type A Durometer (figure 5.6) after the sealing compound cured at standard conditions, for the time defined in the sealing compound specification. The reading was taken on three different circular specimens as shown in figure 5.6. The results are in the tables 5.1 and 5.2.

Figure 5.6 – Type A Durometer

5.6.2.9. 14–Day Hardness (Complete cure)

The 14-day hardness was determined as previously, after the sealing compound had been cured for the standard conditions (accordingly to 5.6.2.3.). The reading was taken as described above. The specifications require hardness above 45/50 shore A.

The hardness test aimed to assure that the material was mixed in appropriate mixing ratio to provide cure and elasticity required for this type of material. The results are in the tables 5.1 and 5.2.

5.6.2.10. Shear Strength Test

The shear strength test was performed to test the strength of the sealant against structural failure. Usually this test is performed on sealants type III, a type of sealant more fluid and developed to be applied as an interference sealant. However as referred previously this sealant has longer curing times (some of them more than 14 days) and during maintenance operation cannot be used. So,

maintenance manuals require the application of sealants type II as interference sealant, allowing decrease the sealant cure time.

For this reason it was important to perform this test, even not being a test required to qualify these sealants, in order to test if it is expected adhesion problems using a type II sealant.

The shear strength test required six AMS4049 aluminum alloy test panels (0.040 in x 1 in x 3 in) for each sealant which were coated with alodine. After conversion coating, a coating of sealant 0.010 in to 0.020 in thick was applied to one end of the six panels covering approximately 1 in on each panel. Three shear strength specimens were formed by mating the sealant coated ends using two panels for each assembly, creating a 1 in^2 overlap for each specimen. The fixture shown in figure 5.7 was used to control dimensional tolerances. The excess sealant was squeezed out to reduce the thickness of the sealant to 0.010 in.

Figure 5.7 – Shear strength test fixture [32]

The sealant was then cured at standard conditions for the time defined in the sealing compound specification (figure 5.8).

Figure 5.8 – Shear strength specimen

Shear strength was determined using a tensile test machine operated at a jaw separation speed of 2 in per min (figure 5.9). The results are in the tables 5.1 and 5.2.

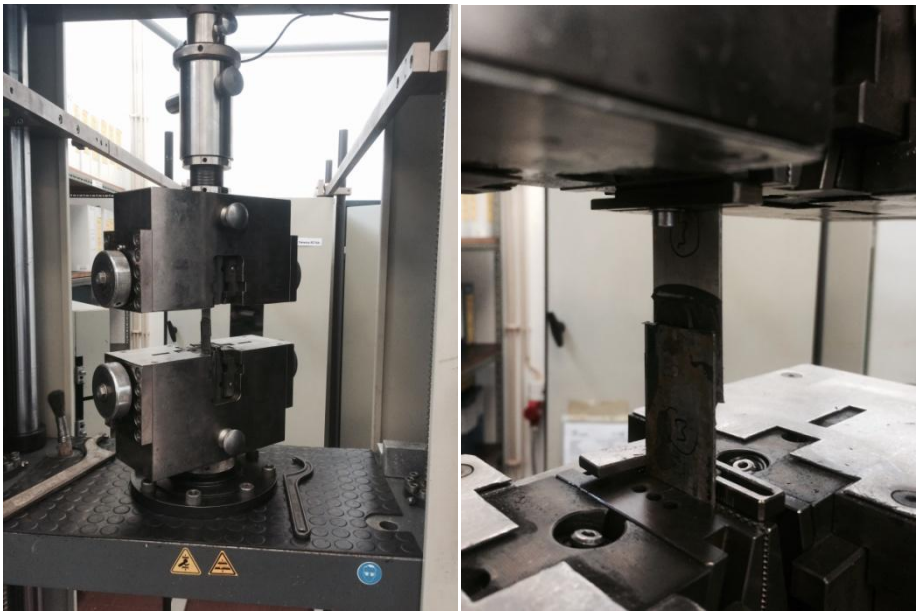

Figure 5.9 – Shear strength test machine

5.6.2.11. Peel Strength Test

Peel strength test panel materials described in the sealing compound specification were prepared and cleaned. Panel dimensions are as shown in figure 5.10. Panel test surfaces were coated with sealing compound as shown in figure 5.11 and to a total sealant thickness of 0.125 in covering approximately 5 in from one end of the test panel.

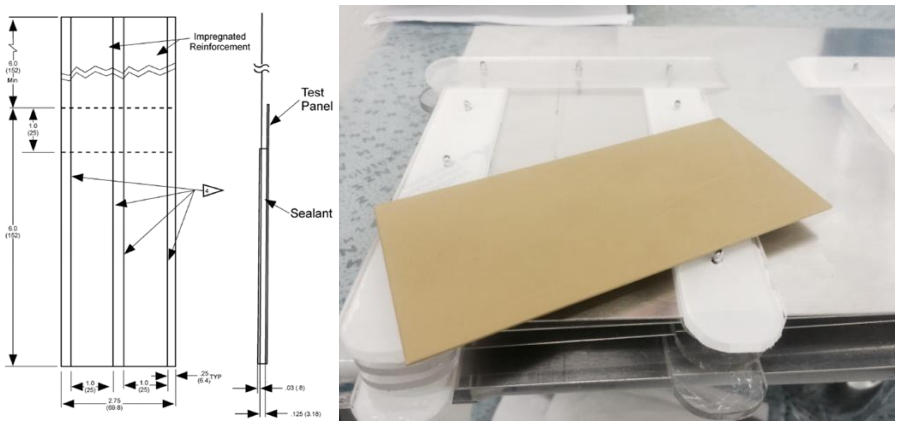

Figure 5.10 – Peel strength specimen configuration (Panel test surfaces after surface treatment) [32]

A reinforcing material was used in the construction of the 180 degree peel strength test panels. A mesh screen of monel metal was cleaned and used as the reinforcement. It was not applied an adhesion promoter during the procedure since during maintenance process this product is not currently applied.

The sealant coated end of the reinforcement was smoothed to the 0.125 in thick layer of sealing compound, ensuring that no air was trapped between the reinforcement and the sealing compound (figure 5.11).

Figure 5.11 – Panel test surfaces coated with sealing compound

An additional coating of sealing compound was then applied over the reinforcement to approximately 0.031 in. thickness. The complete assembly represented in figure 5.12 was cured at standard conditions for the time defined in the sealing compound specification.

The sealing compound peel strength and cohesion to metallic surfaces was determined after complete cure of sealant. Two panels of each sealant to be tested were prepared in accordance with AS5127/1 [32] (figure 5.12).

Figure 5.12 – Peel strength specimen final configuration

The panels were then tested for conformance to the sealing compound specification. Two 1 in wide strips were cut through the reinforcement and sealing compound to the metal surface of the test panel and extended the full length of the wire screen or fabric as shown in figure 5.12. The test panel was installed in a tensile test machine. The upper jaw was clamped to the test panel, and the lower jaw hold the screen reinforcement as shown in figure 5.13.

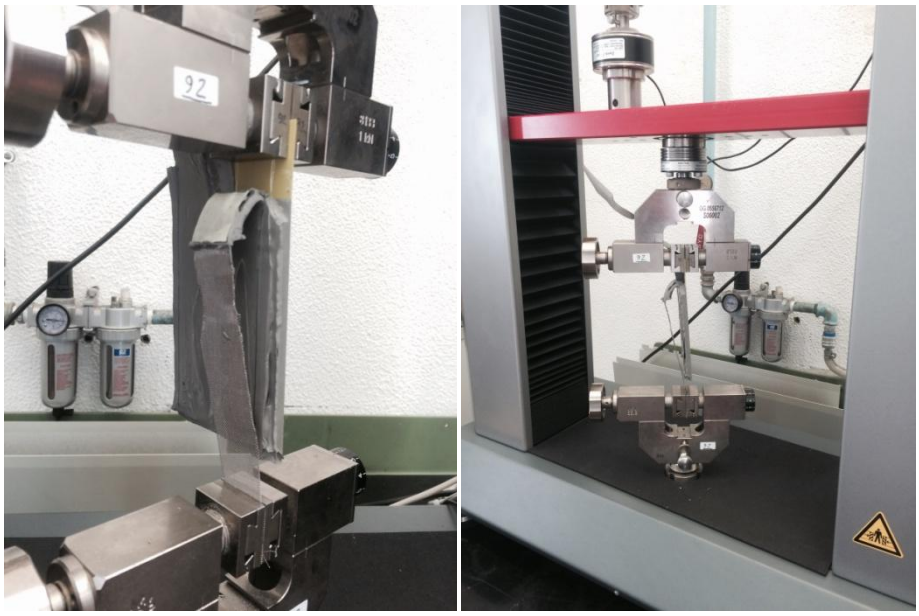

Figure 5.13 – Peel strength test

The specimens were stripped back at an angle of 180 degrees as shown in figure 5.13 to the metal panel in a tensile testing machine having a jaw separation rate of 2 in per min. An initial cut was performed through the sealing compound to the panel. During the peel strength testing, five additional cuts were made in an attempt to promote adhesive failure (figure 5.14). The results were the numerical average of the peak loads during cohesive failure, not including the load due to cutting the specimen. The results are in the tables 5.1 and 5.2.

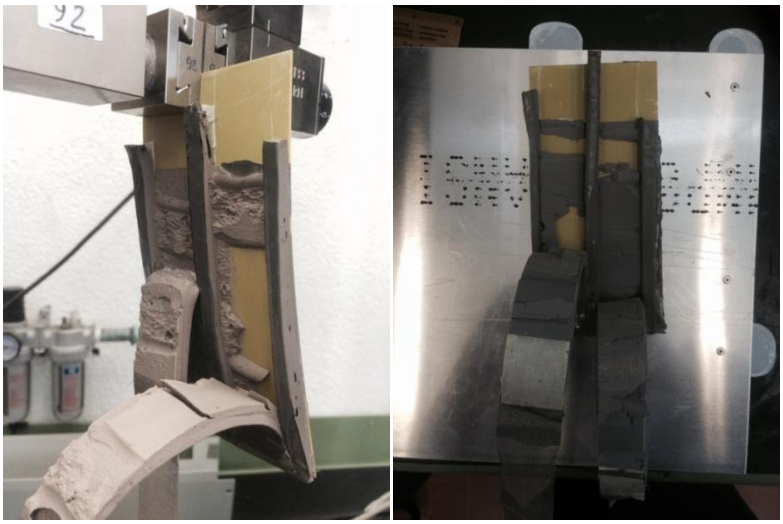

Figure 5.14 – Peel strength result (Adhesive failure)

5.6.3. Sealants Test Results

The results obtained during the previous tests are presented in the table 5.1 and 5.2. It is divided by the products indicated to seal the interior of the tanks (contact with fuel), table 5.1, and the products indicated to perform the interface sealing on fuel tanks and during assembly process (without contact with fuel), table 5.2. The complete results are presented in the attachment D.

AMS–S–88002	*Specification*	***Products***			
Test		**PR 1440 B2**		**AC–236B2**	
		Table value	Real value	Table value	Real value
Appearance	–	–	OK[1]	–	OK[1]
Cured Specific gravity	1.65	1.57	–	1.64	–
Viscosity of Base Compound	9000–14000 poises	10000 poises	10700 Poises	9000–14000 poises	13200 Poises
Flow	0,1–0,75 in.	–	0,1	–	0,1
Application Time	2H	2H	OK[2]	2H	OK[2]
Tack–Free Time	40H	≤8H	OK[3]	≤24H	OK[3]
Standard Cure Time	72H (30 Shore A)	≤11H	OK[4]	≤48H	OK[4]
Complete cure (Shore A)	45–50 Shore A	50 Shore A	OK[5] (51 Shore A)	60 Shore A	OK[5] (49 Shore A)
Shear Strength	200 Psi (95% Cohesive failure)	≥300	295.1* (Co. failure)	≥350	330.31* (Co. failure)
Peel Strength	100% cohesive failure	100% Co. failure	≤100%	100% Co. failure	≤100%

Table 5.1 – Tests results AMS–S–8800

MIL–PRF–81733	*Specification*	***Products***			
Test		**PS870B2**		**MC780B2**	
		Table value	Real value	Table value	Real value
Appearance	–	–	OK[1]	–	OK[1]
Cured Specific gravity	Not specified	1.48	–	1.1	–
Viscosity of Base Compound	6000–16000 poises	10000 poises	11700 Poises	9000–14000 poises	10200 Poises
Flow	0,1–0,75 in.	–	0,1	–	0,1
Application Time	2H	2H	OK[2]	2H	OK[2]
Tack–Free Time	12H	≤14H	OK[3]	≤14H	OK[3]
Standard Cure Time	72H (30 Shore A)	≤20H	OK[4]	≤24H	OK[4]
Complete cure (Shore A)	45–50 Shore A	50 Shore A	OK[5] (47 Shore A)	50 Shore A	OK[5](50 Shore A)
Shear Strength	200 Psi (95% Cohesive failure)	≥358	224.8* (Co. failure)	≥210	195.7* (Co. failure)
Peel Strength	100% Cohesive failure	100% Co. failure	≤100%	100% Co. failure	≤100%

Table 5.2 – Tests results MIL–PRF–81733

[1] – Visual inspection during preparation of sealing compound.

[2] – The application time is defined as the period of time from mixing the base compound with the accelerator until the time that the product should not be applied due to an increase in viscosity. Result OK: the mixture prepared to perform the tests was with adequate viscosity to be handled.

[3] – Tack free time (5.6.2.7.).

[4] – Time to reach 30 Durometer A (30 shore A).

[5] – According to section 5.6.2.9.

* – Indicate the average shear strength value (Complete results in attachment D).

5.7. Conclusions

The aims and objectives set out at the beginning of the chapter were achieved. The complete cure test, described in the section 5.6.2.9, was performed to all the specimens previous to the tests initiation in order to evaluate if the material was at the satisfactory hardness.

In the table 5.1 and 5.2 are presented the cured specific gravity which is an important parameter to evaluate the final weight increase in the aircraft due to the sealant application. Considering the sealants tested the MC780B2 could be an option when the weight increase has a great impact in the aircraft performance.

The viscosity of the base compound test was performed in order to ensure that the sealant was on perfect conditions before mixture. The values obtained are presented in tables 5.1 and 5.2 and as noticed they are all within the range required by specifications.

The flow test was conducted with success and the results obtained were in the acceptable range. Although the flow displacement was lower compared with the sealants type III the values obtained meet the minimum required by the technical documentation. The last results permitted to prove that sealants type II are suitable for the application of aerodynamic chords.

The shear strength test was carried out with success and the results obtained permitted to take several conclusions. It was observed adhesive failure in some points of the specimen (figure D.5 and D.7) consequence of a poor cleaning, degreasing and alodine application before the sealing application (contamination). This test was performed in order to test if it was expected adhesion problems using a type II sealant applied as an interference sealant. It was concluded that the sealants type II, even not being qualified to apply as an interference sealant, had an excellent behavior during the test (attachment D) as well as a similar or even superior shear strength compared to the required by the specifications. Only the product MC780B2 had a shear strength below the value required (2.5% less than the required), all the others presented records above the minimum required. It is important to note that this product is not approved by Lockheed Martin to C–130.

The peel strength test results were not the expected since the sealant had not the expected adhesion over the panel surface (figure 5.14). The specification requires all 100% cohesive failure and a minimum peak load due to cutting the specimen of 20 Lbs (figure D.11). Unfortunately these criteria were not accomplished. Consequently it was not possible to obtain valid results for the peel strength. All the specimens had the same characteristic behavior under test, including the not approved by Lockheed Martin.

The first problem identified was a poor surface preparation. It is especially important to cleaning, degreasing and primer surface reactivation by sanding before sealant application. In addition it is essential to apply adhesion promoter before sealant application. In the current investigation the adhesion promoter was not applied since currently this product is not applied during maintenance process at OGMA.

The results obtained are directly associated with the absence of promoter (or poor surface preparation) before the sealant application and these results are important to advertise the maintenance technicians for the importance of the correct surface preparation. Currently they are not sensitized about this problem.

As noticed previously a correct sealant application has direct influence on the sealant adhesion and long term performance. For this reason it is very important to ensure that maintenance instructions are accomplished during maintenance process. The correct products and procedures to deal with fuel tank sealing repair and application reduce significantly the possibility of fuel leak in future. In the next chapter it is presented a brief resume of the general fuel tanks sealing instructions.

6. Maintenance Instructions (Fuel Systems)

6.1. Introduction

Correct and simplified maintenance instructions must be available to all the technicians in order to make possible an accurate and efficient sealing of the fuel tanks. It is also important that they are aware of the principal causes of leaks and how they can be reduced. In this chapter it is presented a brief resume of the general fuel tanks sealing instructions found in the technical manuals from Lockheed Martin [1], [28], [33].

6.2. Fuel System Sealing

The C–130 airplane is provided with various types of fuel tanks. These are the main integral wing tanks, the auxiliary tanks (bladder cell), the external Pylon–mounted fuel tanks, and the fuselage auxiliary fuel tank (only on the KC–130 tankers) (see figure 6.1). The main fuel tanks are of the integral type and are located in the outer wing. The auxiliary fuel tanks are the bladder type and are located in the center wing. The external fuel tanks are of the streamlined metal type and are Pylon mounted under the outer wing. It was noticed in chapter 4 that it's in main integral fuel tanks that appeared the most part of fuel leaks and consequently those that concern for the study.

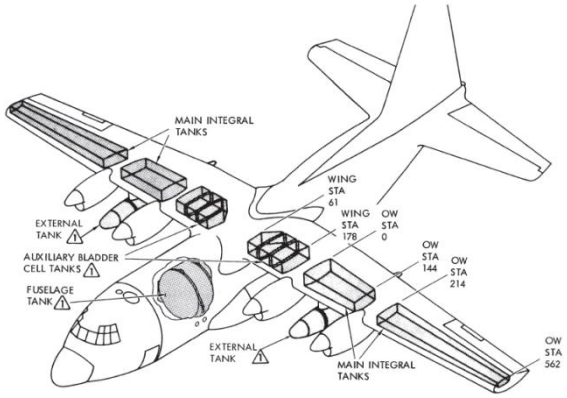

Figure 6.1 – Fuel tank locations [1]

The airplane fuel system is sealed against plumbing leaks by synthetic rubber gaskets, O–rings, packings, seals, and diaphragms. The airplane structure itself is sealed against leakage of fuel, and also against any other liquid, air, or fire, by filling or covering all locations of possible leakage with sealant which cures to a rubbery, fuel–resistant material. Different types of seals and different sealing materials as well as different methods of application are used throughout the airplane to meet specific sealing requirements.

The main tanks are sealed during assembly of the wing structure. Various seals applied at this time become integral parts of the structure assembly for the service life of the airplane, except damage requires breaking these seals to make structural repairs. The purpose of these seals is to prevent channeling of external fuel leakage to a point remote from the internal leak source. If this can be prevented by sealing during structure assembly, future repairs of tank leaks are much simplified. This stage of sealing is known as faying surface sealing.

After the structure has been assembled with these seals, injection sealing is used to fill voids remaining after faying surface sealing. Injection seals are also considered to be integral parts of the structure, though they are applied after the structure has been assembled. They are replaceable only in case of structural repair and/or deterioration.

Fasteners are wet–installed with sealant during the assembly process. All fasteners are covered by two brush coats of sealant and fastener sealant is replaceable during maintenance.

The application of fillet seals follows. Fillet seals avoid fuel from performing contact with faying surface and injection seals by covering the otherwise exposed edges of these seals with a fillet of sealant along all joggles and joints in the structure. The fillet seals are inspected and repaired during maintenance.

Throughout the sealing operation, prevention of corrosion of the structure is incorporated as an essential part of sealing. Before the detail parts are assembled with faying surface seals, each part is coated with a corrosion preventive coating. The corrosion preventive material application differs among serial numbers as its notice in the corrosion protection section. This corrosion protective coating is repairable during maintenance.

At all stages of the sealing and corrosion prevention operations, care should be taken to maintain the interior of the tanks in a perfectly clean condition, both to prevent fuel contamination with foreign matter and to provide the maximum adhesion of the sealant and coatings to the metal surfaces and to the sealants and coatings applied during earlier stages of the process. The same precautions must be taken during field repairs of the sealing and corrosion preventive systems. The preparation for sealing and the sealing process are described in detail in the following paragraphs to provide the maintenance operate with complete information regarding the sealing and corrosion preventive systems in the tanks which must be maintained in condition during the service life of the airplane.

6.3. Exterior Leaks and Recommended Action

If external leakage is reported, the leak should first be observed from the outside before any fuel is drained, or access covers removed. Immediate corrective action is sometimes necessary, due to the rate and/or location of the leak, but in many instances corrective action may be delayed until the aircraft can conveniently be taken out of service for repair. Evaluation of a leak must be careful and impartial to minimize possible flight hazards. For this reason, correct classification of a leak is very important. The following paragraph defines the various types of leaks, and indicates the required action.

6.3.1. Types of Leaks

Fuel leaks are classified in four groups: slow seep, seep, heavy seep and running leak. The locating of the leak, in conjunction with the type of leak governs the action to be taken. The following definitions and notes on leak locations determine if immediate repair is required or whether it may be allowed to continue, under observation, until a scheduled servicing period comes due. The size of the area of the aircraft surface wetted by leaking fuel may be used as an accurate measure of the leak rate. The leak should be observed for 30 minutes, by which time it should be possible to make an accurate identification of the leak type, which will determine what, has to be done. [1]

- **Slow seep** – This is a leak wetting an area of the surface not over 0.75 in. in diameter in 30 minutes. If located in an open area of the surface, a slow seep does not have to be repaired immediately, but should be repaired as soon as the aircraft is down for any other servicing. If the slow seep is in an enclosed area, where fuel from the leak could eventually collect and form a fire hazard, the leak must be repaired before the next flight.
- **Seep** – This is a leak wetting an area of the surface between 0.75 and 1.5 in. in diameter in 30 minutes, and not visibly running, flowing, or dripping. If located on an open area of the surface, repair may be delayed until other servicing work takes the aircraft out of service. If the seep is in an enclosed area, it must be repaired before the next flight.
- **Heavy seep** – This is a leak where fuel appears to spread very slowly and covers an area larger than a seep but does not flow, run or drip. The wet area of a heavy seep does not cover an area over 3 in. in the selected 30 minutes time interval after an area has been wiped clean. Talcum powder should be applied to examine the leak.
- **Running leak** – Fuel drips or runs from the structure from this leak. It must be repaired before the next flight, regardless of location.

6.4. Methods to Identify Leaks Sources

The suitable repair of a leak requires that the true source be found. Appling sealing compound inside the tank on an area that appears from the outside to be the leak source will rarely solve the problem. Although the faying surface seal is specifically designed to minimize channeling, fuel may, under unusual conditions, find leak channels such as skin splices, doublers and spar caps. In such cases personnel must be familiar with the wing structure and must employ a positive method to determine the true source.
Five methods accepted as standard in leak detection are:

1. **Approximate location by fuel level** – In most cases the leak source can be found in the approximate location of the detected leak. One method of determining a leak source, particularly in the forward and aft beams and in the inboard and outboard tank bulkheads, is to

drain the tank in 1,000 Lbs increments until the fuel stops leaking. Stopping the leak indicates that the fuel level is just below the hole in the sealant at the time.

2. **Air–bubble method** – The exterior of the tank structure is covered at the area of the leak with a leak detector fluid. All seams, bolts, rivets, or fillets are blown at the most probable leak source on the inside of the tanks. The check is continued until the leak is located as indicated by bubbling of the leak detector fluid.
3. **Fluid blowback method** – This method is similar to the air–bubble method, except that an isopropyl alcohol is blown from the outside leak point with 10 Psi maximum air pressure. The leak source is identified when the alcohol emerges inside the tank. The alcohol must be blown out from inside before resealing.
4. **Drilled screw method** (see figure 6.2) – For leaks which are particularly difficult to locate, the following method is especially effective:

    a. Prepare a screw of appropriate size, and other equipment as shown in figure 6.2.
    b. Remove the rivet or bolt that is known or suspected to be the leak exit point.
    c. Install the drilled screw, gaskets, washer, and nut as shown.
    d. Paint the suspected area on the inside of the tank with soap solution, or leak detector fluid.
    e. Apply air through the drilled screw under a maximum pressure of 10 Psi. Bubbles in the leak detector fluid will indicate the leak source.

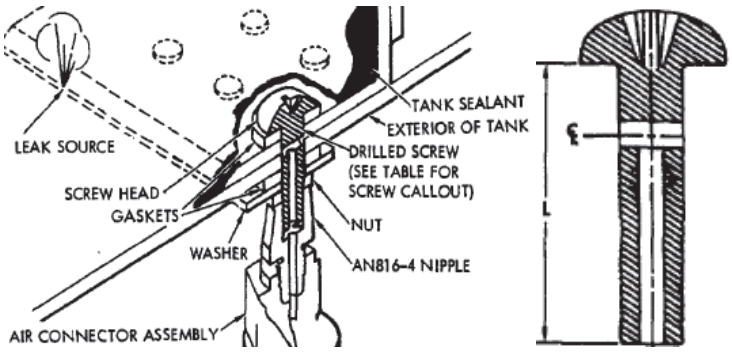

Figure 6.2 – Drilled screw method [1]

5. **Vacuum and fluorescent dye method** – The vacuum and dye (ultraviolet light) method is one of the most accurate methods of locating the leak source on the inside of the tank. When the ultraviolet light source is not available, a colored dye may be used instead of fluorescent dye as a leak tracer. Vacuum is applied on the interior of the tank and dye applied on the exterior leak exit point. The dye solution will emerge at the leak source and can be easily seen with an ultraviolet light.
6. **Pressure test** – Fuel tank air pressure check may be used as a last resort (wing structure is subjected to hoop stress) during the troubleshooting procedure for locating fuel leaks. If the pressure test is used, tanks may be pressurized with air to 3.0 Psi maximum.

6.5. Preparation for Sealing

Before assembly operations are started on the outer wings, all surfaces which are to be sealed are thoroughly cleaned. Contamination of the surfaces, even from fingerprints, can prevent adhesion of corrosion preventive coating and sealants, and cause corrosion and leakage.

6.5.1. Inspecting, Cleaning, and Sterilizing Fuel Tanks

Fuel tanks containing jet fuel are frequently contaminated with the fuel from inadequately maintained fuel supply sources. The most frequent contaminant is water and sometimes the contaminants in dirty water are microbiological growth such as fungus, bacteria, yeast, and associated micro–organisms. Existence of micro–organisms is an indication of a deteriorated coating and corrosion in the interior of the affected tank. Inspection of fuel tanks for microbial contamination must be accomplished on a regular calendar schedule and as frequently as every 60 days.

These procedures are generally made following these steps:

1. **Defueling** – Aircraft fuel tanks must be defueled in accordance with general instructions contained in the instruction manual [33].
2. **Purging and ventilation** – Prior to entering a fuel tank, the tank must be purged in accordance with the procedures contained in the instruction manual [33]. Limited entry into a fuel tank is permissible at a Lower Explosive Limit (LEL) value that is higher than the value required for complete entry. Limited entry is defined as a head and shoulder entry only.
3. **Tank entry** – Access to integral fuel tanks is provided through the bulkhead doors in the dry bays located aft of each of the four engine nacelles and through the upper surface panel doors of the outer wing.
4. **Cleaning fuel tanks** – Each fuel tank must be scrub out with a cleaning solution composed of 38 to 49 °C tap water and MIL–PRF–87937. Soft bristle brushes should be used for scrubbing. Introduce the cleaning solution in a coarse spray under law pressure. Do not let the cleaning solution dry on the surface. Re–spray the cleaning solution as necessary to keep the surfaces wet. Tanks are then forced–air dried to remove all traces of solvent.
5. **Decontamination** – Tanks and cells found to be contaminated with colonies of micro–organisms shall be sterilized after completion of the cleaning operation.

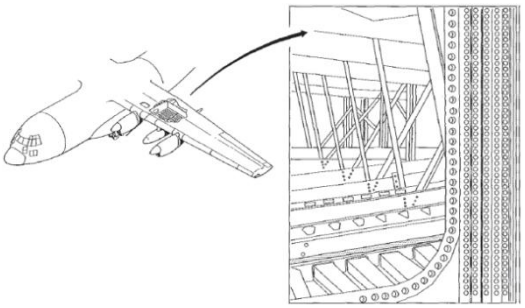

Figure 6.3 – Access to integral fuel tanks [1]

6.6. Sealing Process

6.6.1. Sealing During Assembly

The faying surface seals applied at this stage will become integral parts of the wing structure. Once applied, these seals are inaccessible for any future repair except by disassembling the basic structure of the wing.

1. A 0.010 to 0.015 in. thickness of sealing compound containing a corrosion inhibitor is used to attain a uniform mixture of the two–part sealant. All assembly of fay surface sealed parts is accomplished only during the application life of the sealant.
2. A continuous coat of sealing compound approximately 0.015 in. thick is applied to the clean mating surfaces (bare metal or cured organic coating). Prior to the expiration of the assembly time of the faying surface sealant, the parts are assembled and the fasteners installed.
3. When permanent fasteners cannot be installed within the assembly time, temporary fasteners, setup screws or clamps are used to ensure proper tightening of the joint until the permanent fasteners can be installed.
4. The faying surfaces of the assembled joint are completely filled as evidenced by a continuous bead of sealant on all edges of the joint.
5. All fasteners which pass into the fuel tank boundary are installed wet with sealant.
6. Excess sealant, squeezed from the joints by fastener pressure, is removed with phenolic or wood spatulas, and wiped with a clean rag. This prevents scratching either the corrosion preventive coating or the anodic film.
7. The faying surface seals are then cured under the applicable conditions of time and temperature required by the process specification.

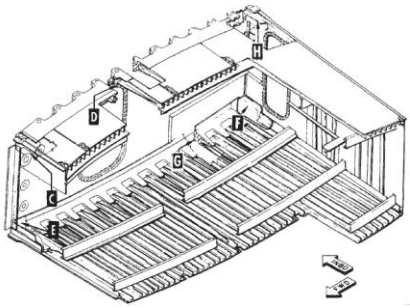

Figure 6.4 – Sealing during assembly illustration [1]

6.6.2. Injection Sealing

All injection sealing is accomplished within the application life of the sealant used to fay surface seal. The sealant is injected into voids in the structure which remain after faying surface sealing and assembly. These voids occur at various places, such as bulkhead corner Fittings, and must be filled with sealant to provide a base for the fillet seals which will be applied in these areas, and to eliminate pockets in the structure in which air could be trapped and later expand and break the integrity of the tank sealing system. Injection holes are used in areas where voids are longer than 1 in.

1. The sealant is injected until it appears at all related holes and openings. Particular attention is given at this time to locations where leaks were found in the pressure test following structure assembly.
2. The injection seals are cured before the next operation is started.
3. When sealant cure is completed, the tanks are leak tested with air at 3.0 Psi, using leak detector solution on the outside. Any leaks found during this check are recorded on a chart for corrective action at a later stage of sealing.

6.6.3. Fillet Sealing

Before application of the fillets, the local areas to which the fillets are to be applied are cleaned to ensure maximum adhesion of the fillets to the corrosion preventive coating.

1. The surfaces which are to be fillet sealed are cleaned, and a coating of adhesion promoter is applied.
2. The fillets are applied with a pressure sealing gun containing sealant.
3. All fillets are made continuous in themselves, or in conjunction with adjacent fillets, so that no gaps exist when this operation has been completed.
4. While the sealant can still be worked, the fillets are smoothed and pressed into place with a phenolic tool or a brush lubricated.

5. This is done within an hour of fillet application.

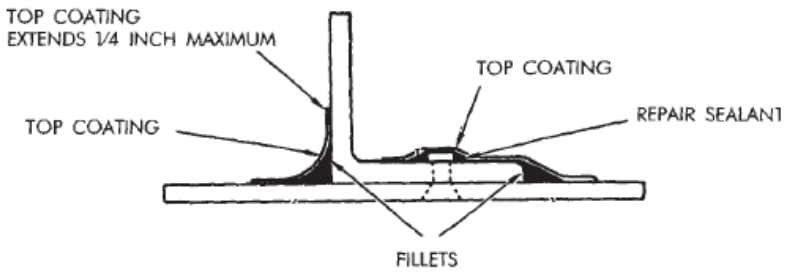

Figure 6.5 – Fillet sealing illustration [1]

6.6.4. Fastener Sealing

All fasteners penetrating the fuel tank boundaries, including the base plate of nuts, are brush sealed on the fuel side of the tank.

1. Fasteners are brush sealed on both ends.

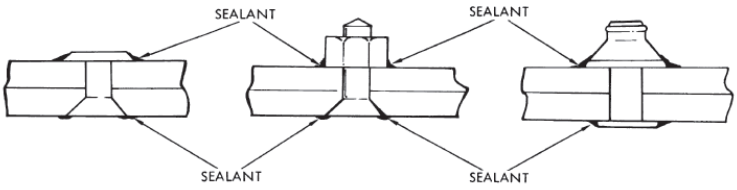

Figure 6.6 – Fastener sealing illustration [1]

6.6.5. Brush Sealing

The surfaces which are to be brush sealed and cleaned, a coating of adhesion promoter is applied.

1. All fasteners on the inside of each tank are covered with a 1/16 in. nominal coat.
2. The fillets and brush seals are then cured for one hour at shop temperature.
3. The sealed areas are inspected for pinholes, bubbles, and thin spots, and retouched as necessary.
4. Sealant is then cured at shop temperature or at elevated temperature of 49°C to 60°C until sealant is tack–free.
5. Tanks are again leak tested by air pressure at 3.0 Psi. Any necessary repairs for leakage are made at this time.

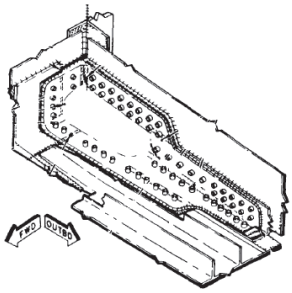

Figure 6.7 – Brush sealing illustration [1]

6.6.6. Sealing Repairs

Sealing repairs in the main fuel tanks are accomplished following the next procedure:

1. Remove defective sealant by cutting and scraping as required to establish a sound base for applying new material. Use nonmetallic knives and scrapers. Clean and dry exposed base sealant and metal surfaces just prior to application of new materials using a lint free cotton cloth moistened with trichloroethane or aliphatic naphtha.
2. Avoid touching cleaned surfaces with uncovered hands or foreign materials that will prevent proper adhesion of sealant.
3. Corrosion inhibiting sealant shall be used in the faying–surface sealing and for wet fastener installations.
4. If corrosion of metal is detected, it should be referred to applicable manual for further instructions.
5. Fuel tank leaks must be repaired with the appropriate sealant and this sealant must only be applied to clean metal or to a factory applied polyurethane coating.
6. Adhesion promoters should be used to improve the surface adherence. The applied coating shall be exposed to air for a minimum of 30 minutes prior to sealant application. Adhesion promoter coatings that have not had the sealant applied to them within 8 hours and have not been protected, shall be re–cleaned and the promoter reapplied.
7. Cure times specified in the product are applicable except if the shop conditions differ enough from curing schedule (elevated temperature – humidity).
8. Those fasteners which penetrate the fuel tanks must be individually wet installed and then post–assembly sealed with one brush–coat.

In the case of the tank has not been completely stripped, the resulting application will interface with the existing polyurethane top coat. Inhibiting sealant can be applied over aged polyurethane if the following preparations are completed; otherwise, the patched overlay will not adhere satisfactorily. Preparation of aged polyurethane (polyurethane with extensive exposure to fuel) shall be accomplished as follows:

1. Rub area to be coated using an A–A–58054, Type I, Class 1, Grade B (fine) abrasive mat dampened with ASTM 0740 Methyl Ethyl Ketone (MEK). Rub until the gloss has been broken from the polyurethane surface. An abrasive cloth can be used as a substitute abrasive material.
2. Clean the surface with a cloth dampened with ASTM 0740 Methy1 Ethyl Ketone (MEK).
3. Adhesion promoters should be used to improve the surface adherence. The instructions presented previously are applied at this stage.
4. Coat the prepared surface (including the surface and the overlapping surface to which the sealant repair is being applied) with a thin film of MIL–PRF–81733, class 1, grade A, type I or II sealant. Use a stiff bristle brush and a scrubbing action to establish complete wetting for maximum adhesion.
5. Repeat the application of additional sealant material using a gun, spatula, or brush. Overfill depressions as required to avoid pockets or low spots capable of trapping water condensates.
6. Overcoat the applied sealant with a coat of MIL–C–83019 clear, flexible polyurethane. This coating may be applied immediately to type III sealant and after one hour to type I sealant. The coating should not overlap the adjacent metal surfaces by more than ½ in.

6.7. Corrosion Protection

6.7.1. Sealing for Corrosion Protection

The following paragraphs describe the variations in the basic protective coatings employed in integral fuel tanks as a function of the chronological development in the state of the technology to date.

1. Early series airplanes were delivered with a spray coating of polysulfide over the inside bottom surfaces of the tanks followed by an application of Buna–N protective coating (figure 6.8). Unfortunately, this coating was found to provide food for micro–organisms entering the tank. Colonies of these micro organisms were found to multiply very rapidly and introduce concentration cells causing corrosion to develop at point of contact with the exposed metal.

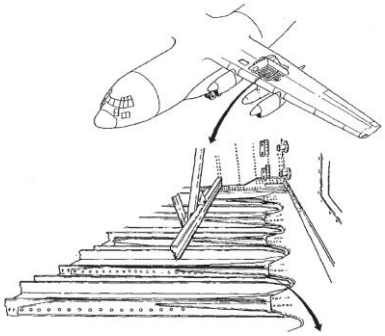

Figure 6.8 – Polysulfide and Buna–N coated fuel tank interior surfaces [33]

2. On airplanes AF63–07813 and up, and airplanes modified by T.O. I.C.–130–1039, a second protective system was introduced to replace the Buna–N system and reduce the problem of microbial corrosion. This second system consisted of a protective coating of polyurethane which offered little or no food value to micro–organisms. Early applications of polyurethane were found to be too brittle for application over sealant and were subsequently changed to include MIL–C–83019 polyurethane over all fillet seal and brush–coat applications. Without this top coat, the base polysulfide tank sealant is degraded by the fuel.
3. On airplanes AF66–00219 through AF72–01298, an overcoat of polyurethane containing a dark green biocidal dye was added to the lower 6 in. of all integral fuel tanks. This dye was introduced as a biocide to kill off the many forms of bacteria encountered in fuel tanks.
4. On airplanes AF73–01580 and up, and airplanes modified by T.O. I.C.–130–1039, a flexible coating of polyurethane containing the dark green biocidal dye was included in the finish specification for structural metal parts contained in the lower portion of the tanks. This finish was applied to each part in detail prior to its being incorporated into the assembly.

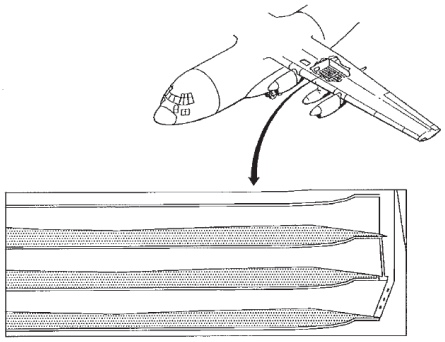

Figure 6.9 – Polyurethane coated fuel tank bottom surface [33]

6.7.2. Inspection for Corrosion Under Sealant

Corrosion blisters can be observed through the polyurethane coating but cannot be observed under polysulfide sealant. The only indication of corrosion presence under polysulfide sealant is its loosening or lack of adhesion. During the maintenance, integral fuel tanks shall be inspected in accordance with the applicable manual.

7. Conclusions and Future Work

The overall aim of the current research was to reduce the fuel leaks in the aircraft fuel tanks at the delivery. Following this approach a FEA of a critical structural member was performed in order to investigate the structural behavior under critical loads. This analysis allowed to decide the upgrades and the location of structural reinforcement applied and verified through FEA.

A workcard with instructions to carry out a nondestructive inspection on the forward and aft Pylon attach Fittings was considered. The purpose was to evaluate and update these procedures in order to inspect the identified zones. These instructions were based on the results from the FEA carried previously. These instructions are also valid for others fuel tank areas.

A research and test of new sealants products were performed. The main goal was to initiate a research and test of potential sealants products in order to make a future recommendation to Lockheed Martin. It was concluded that the results obtained were directly associated with the poor surface preparation (absence of promoter) before the sealant application and these results are important to advertise the maintenance technicians for the importance of the correct surface preparation. A correct sealant application has direct influence on the sealant adhesion and long term performance.

The maintenance instructions manual was developed, evaluated and updated in respect to the procedure to inspect, clean and seal the fuel tanks. It was introduced correct and simplified maintenance instructions to all the technicians in order to make possible an accurate sealing of the fuel tanks.

These outputs are going to be used by OGMA – Indústria Aeronáutica de Portugal, SA. The main target was to initiate a research into alternative sealant products and a complete review of the maintenance instructions manual as well as a workcard with instructions to inspect the identified critical locations. The direct result of the developed work is expected to reduce the maintenance hours and avoid delays in the aircraft delivering, contributing to optimize the costs of the company.

Future developments should be concerned with the introduction of dynamic and environmental parameters representative of actual flight conditions. Almost all tests performed are of a static nature, it is acknowledged that movement (high stressed areas) and poor surface preparation lead to leaks. Thus the missing component of testing is movement coupled with the other key variables.

As a result, the investigation carried in the current thesis can be completed with a study of the Fitting member under fatigue loads considering in flight conditions (e. g. high and low temperatures and pressures).

Future work should also include the sealants tests with a correct surface preparation (surface cleaning and application of promoter) before the sealant application. It will be essential to confirm the previous assumptions.

8. References

[1] Lockheed Martin Aeronautics Company**.** *Maintenance Instructions Fuel Systems*. Lockheed Martin Corporation. 1980.

[2] Petrie, Edward M. *Handbook of Adhesives and Sealants*. McGraw-Hill. 1999.

[3] Whitford, Ray. *Fundamentals of Fighter Design*. The Crowood Press Ltd. 2004.

[4] Niu, Michael C.Y. *Airframe Stress Analysis and Sizing*. Hong Kong Conmilit Press Ltd. 1997.

[5] Niu, Michael C.Y. *Airframe Structural Design*. Hong Kong Conmilit Press Ltd. 1988.

[6] Megson, T.H.G. *Aircraft Structures for Engineering Students*. Butterworth-Heinemann. 2012.

[7] Alteon, Boeing Company. *Aircraft Structural Repair for Engineers*, Part I. 2003.

[8] 3G Aviation. L382 HERCULES (RR 501-D) B1 (Maintenance Training Manual). 3G aviation. 2011.

[9] Advisory Group for Aerospace Research and Development (AGARD). *Fuel Tank Technology* (Report No.771). 1989.

[10] Hemighaus, Greg. *Chevron Aviation Fuels Technical Review (FTR–3)*. Chevron Products Company. 2006.

[11] Pilkey, Walter D. *Stress Concentration Factors.* John Wiley & Sons, Inc. 1997.

[12] NDT Resource center. *NDT Non–Destructive testing*. [Online] 15 September 2014.

[13] FAA. *Metallic Material Properties Development and Standardization 01.* FAA. 2003.

[14] Hoerner, Sighard F. *Fluid dynamic drag (Theoretical, Experimental and Statistical Information)*. Published by the Author. 1965.

[15] Brederode, Vasco D. *Fundamentos de aerodinâmica incompressível*. Ed. Autor. 1997.

[16] Azom. *Material Property Data*. [Online] 05 August 2014.

[17] Department of Defense. *Material Property Data.* [Online] 05 August 2014.

[18] EOL. C–130 Basic Specifications. *C–130 Investigators Handbook*. [Online] 12 July 2014.

[19] Jacquet Export. *Material Property Data*. [Online] 05 August 2014.

[20] MatWeb. *Material Property Data*. [Online] 05 August 2014.

[21] ANSYS, Inc. *Structural Analysis Guide, Release 12.1*. 2009.

[22] ANSYS, Inc. *Theory Reference, Release 12.0*. 2009.

[23] NASA. *Fastener Design Manual*. NASA Publication. 1990.

[24] Montgomery, J. *Methods for Modeling Bolts in the Bolted Joint*. Published by the Author. 2002.

[25] ANSYS, Inc. *Elements Reference, Release 12.1*. 2009.

[26] ANSYS Inc. *Node Merge Help Manual, Release 14.0*. 2011

[27] eFunda. *Failure criteria.* [Online] 07 August 2014.

[28] Lockheed Martin Aeronautics Company. *Structural Repair Manual*, (SMP 583). Lockheed Martin Corporation. 2002.

[29] Lockheed Martin Aeronautics Company. *Sealing and Coating Compound, Corrosion Inhibitive.* Lockheed Martin Corporation. 1998.

[30] Adams, R. D.; Wake, William C. *Structural Adhesive Joints in Engineering*. Chapman & Hall. 1984.

[31] SAE Aerospace. *AMS–S–8802 (Sealing Compound Integral Fuel Tanks)*. SAE International. 1999.
[32] SAE Aerospace. *AS5127/1B (Aerospace Standard Test Methods for Aerospace Sealants)*. SAE International. 1997.
[33] Lockheed Martin Aeronautics Company. *System Peculiar Corrosion Control*, (TO 1C–130A–23). Lockheed Martin Corporation. 2013.

Attachments

Attachment A. Materials Relevant Tables

Table 3.7.6.0(b$_1$). Design Mechanical and Physical Properties of 7075 Aluminum Alloy Sheet and Plate

Specification	AMS 4045 and AMS-QQ-A-250/12																					
Form	Sheet						Plate															
Temper	T6 and T62[a]						T651															
Thickness, in.	0.008-0.011		0.012-0.039		0.040-0.125		0.126-0.249		0.250-0.499		0.500-1.000		1.001-2.000		2.001-2.500		2.501-3.000		3.001-3.500		3.501-4.000	
Basis	S		A	B	A	B	A	B	A	B	A	B	A	B	A	B	A	B	A	B	A	B
Mechanical Properties:																						
F_{tu}, ksi:																						
L	...		76	78	78	80	78	80	77	79	77	79	76	78	75	77	71	73	70	72	66	68
LT	74		76	78	78	80	78	80	78	80	78	80	77	79	76	78	72	74	71	73	67	69
ST	...		...	...	...	...	...	...	...	...	...	...	...	...	...	...	66[b]	68[b]	65[b]	67[b]	61[b]	63[b]
F_{cy}, ksi:																						
L	...		69	72	70	72	71	73	69	71	70	72	69	71	66	68	63	65	60	62	56	58
LT	63		67	70	68	70	69	71	67	69	68	70	67	69	64	66	61	63	58	60	54	56
ST	...		...	...	...	...	...	...	...	...	...	...	...	...	59[b]	61[b]	56[b]	58[b]	54[b]	55[b]	50[b]	52[b]
F_{sy}, ksi																						
L	...		68	71	69	71	70	72	67	69	68	70	66	68	62	64	58	60	55	57	51	52
LT	...		71	74	72	74	73	75	71	73	72	74	71	73	68	70	65	67	61	64	57	59
ST	...		...	...	...	...	...	...	...	...	...	...	...	...	67	70	64	66	61	63	57	59
F_{su}, ksi	...		46	47	47	48	47	48	43	44	44	45	44	45	44	45	42	43	42	43	39	41
F_{bru}^{sec},[c] ksi																						
(e/D = 1.5)	...		118	121	121	124	121	124	117	120	117	120	116	119	114	117	108	111	107	110	101	104
(e/D = 2.0)	...		152	156	156	160	156	160	145	148	145	148	143	147	141	145	134	137	132	135	124	128
F_{bru},[c] ksi																						
(e/D = 1.5)	...		100	105	102	105	103	106	97	100	100	103	100	103	98	101	94	97	89	93	84	87
(e/D = 2.0)	...		117	122	119	122	121	124	114	118	117	120	117	120	113	117	109	112	104	108	98	103
e, percent (S-basis):																						
LT	5		7	...	8	...	8	...	9	...	7	...	6	...	5	...	5	...	5	...	3	...
E, 10^3 ksi	10.3																					
E_c, 10^3 ksi	10.5																					
G, 10^3 ksi	3.9																					
μ	0.33																					
Physical Properties:																						
ω, lb/in.^{3}	0.101																					
C, K, and α	See Figure 3.7.6.0																					

a Design allowables were based upon data obtained from testing T6 temper sheet and from testing samples of sheet, supplied in the O or F temper, which were heat treated to demonstrate response to heat treatment by suppliers. Properties obtained by the user may be lower than those listed if the material has been formed or otherwise cold worked, particularly in the annealed temper, prior to solution heat treatment.

b Caution: This specific alloy, temper, and product form exhibits poor stress-corrosion cracking resistance in this grain direction. It corresponds to an SCC resistance rating of D, as indicated in Table 3.1.2.3.1(a).

c Bearing values are "dry pin" values per Section 1.4.7.1. See Table 3.1.2.1.1.

Table 8.1.2(b). Single Shear Strength of Solid Rivets[a]

Undriven			Driven			Rivet Size							
Rivet Material	F_{su} (ksi) Min	F_{su} (ksi) Max	Rivet Material	F_{su}[b] (ksi)	Rivet Designation	1/16	3/32	1/8	5/32	3/16	1/4	5/16	3/8
						Driven Single Shear Strength, lbs[c]							
5056-H32	24	n/a	5056-H321[d]	28[e]	B[f]	99	203	363	556	802	1450	2290	3275
2117-T4	26	n/a	2117-T3	30[e]	AD	106	217	389	596	860	1555	2455	3510
2017-T4	35	42	2017-T3	38[e]	D	134	275	493	755	1085	1970	3115	4445
2024-T4	37	n/a	2024-T31	41[g]	DD	145	297	532	814	1175	2125	3360	4795
7050-T73	41	46	7050-T731[d]	43[e]	E[h]	152	311	558	854	1230	2230	3520	5030
Monel	49	59	Monel	52[e]	M	183	376	674	1030	1490	2695	4260	6085
Ti-45Cb	50	59	Ti-45Cb	53[e]	T	187	384	687	1050	1515	2745	4340	6200
A-286	85	95	A-286	90[e]	-	317	651	1165	1785	2575	4665	7375	10500

a All rivets must be sufficiently driven to fill the rivet hole at the shear plane. Driving changes the rivet strength from the undriven to the driven condition and thus provides the above driven shear strengths.
b Shear stresses are for the as driven condition on B-basis probability.
c Based on nominal hole diameter specified in Table 8.1.2(a).
d The temper designations last digit (1), indicates recognition of strengthening derived from driving.
e The bucktail's minimum diameter is 1.5 times the nominal hole diameter in Table 8.1.2(a).
f Should not be exposed to temperatures over 150°F.
g Driven in the W (fresh or ice box) condition to minimum 1.4D bucktail diameter.
h E (or KE, as per NAS documents).

Table 8.1.2.2(c). Static Joint Strength of 100° Flush Head Aluminum Alloy (2117-T3) Solid Rivets in Dimpled Aluminum Alloy Sheet[a,b]

Rivet Type	MS20426AD (F_{su} = 30 ksi)								
Sheet Material	2024-T3 2024-T42 2024-T62 2024-T81		2024-T3 2024-T42		2024-T62 2024-T81		2024-T86 7075-T6		
Rivet Diameter, in.	3/32	1/8	5/32	3/16	5/32	3/16	1/8	5/32	3/16
(Nominal Hole Diameter, in.)	(0.096)	(0.1285)	(0.159)	(0.191)	(0.159)	(0.191)	(0.1285)	(0.159)	(0.191)
	Ultimate Strength, lbs								
Sheet thickness, in.:									
0.016	177	...	...	...	...	...	...	...	...
0.020	209	299	...	...	...	...	302	...	...
0.025	217	360	474	...	462	...	383	462	...
0.032	...	388	568	722	596	725	388	596	725
0.040	...	...	596	839	...	862	...	...	862
0.050	...	...	...	862	...	...	...	...	...
Rivet shear strength[c]	217	388	596	862	596	862	388	596	862
	Yield Strength[d], lbs								
Sheet thickness, in.:									
0.016	154	...	...	...	...	...	...	...	...
0.020	184	257	...	...	...	...	257	...	...
0.025	209	315	324	...	324	...	315	410	...
0.032	...	367	430	512	430	512	367	525	640
0.040	...	...	506	644	...	644	...	...	782
0.050	...	...	...	757	...	...	...	...	...
Head height (max.), in.	0.036	0.042	0.055	0.070	0.055	0.070	0.042	0.055	0.070

a These allowables apply to double dimpled sheets and to the upper sheet dimpled into a machine-countersunk lower sheet. Sheet gage is that of the thinnest sheet for double dimpled joints and of the upper dimpled sheet for dimpled, machine-countersunk joints. The thickness of machine-countersunk sheet must be at least one tabulated gage thicker than the upper sheet. In no case shall allowables be obtained by extrapolation for gages other than those shown.

b Test data from which the yield strengths listed were derived and can be found in Reference 8.1.2.2.

c Rivet shear strength from Table 8.1.2(b).

d Permanent set at yield load: the greater of 0.005 inch or 2.5% of nominal diameter.

Table 2.3.1.0(g_2). Design Mechanical and Physical Properties of Low-Alloy Steels

Alloy	4330V	See steels listed in Table 2.3.0.2 for the applicable strength levels					
Specification	AMS 6427	See Tables 2.3.1.0(a) and (b)					
Form	All wrought forms						
Condition	Quenched and tempered[a]						
Thickness or diameter, in.	≤ 2.5	[b]					[c]
Basis	[d]						
Mechanical Properties:							
F_{tu}, ksi	220	125	140	150	160	180	200
F_{ty}, ksi	185	100	120	132	142	163	176
F_{cy}, ksi	193	109	131	145	154	173	181
F_{su}, ksi	132	75	84	90	96	108	120
F_{bru}, ksi:							
(e/D = 1.5)	297	209	209	219	230	250	272
(e/D = 2.0)	385	251	273	287	300	326	355
F_{bry}, ksi:							
(e/D = 1.5)	267	146	173	189	202	230	255
(e/D = 2.0)	294	175	203	218	231	256	280
e, percent:	10	See Table 2.3.1.0(e)					
L	5[a]						
LT							
E, 10^3 ksi	29.0						
E_c, 10^3 ksi	29.0						
G, 10^3 ksi	11.0						
μ	0.32						
Physical Properties:							
ω, lb/in.^{3}	0.283						
C, K, and α	See Figure 2.3.1.0						

a Design values are applicable only to parts for which the indicated F_{tu} has been substantiated by adequate quality control testing.

b For F_{tu} ≤ 180 ksi, thickness ≤ 0.50 in. for AISI 4130 and 8630; ≤ 0.80 in. for AISI 8735, 4135, and 8740; ≤ 1.00 in. for AISI 4140; ≤ 1.70 in. for AISI 4340, 4330V, 4335V, and Hy-Tuf [Quenched in molten salt at desired tempering temperature (martempering)]; ≤ 2.50 in. for AISI 4340, 4330V, 4335V, and Hy-Tuf (Quenched in oil at a flow rate of 200 feet/min.); ≤ 3.50 in. for AISI 4340 (Quenched in water at a flow rate of 200 feet/min.); ≤ 5.00 in. for D6AC (Quenched in oil at a flow rate of 200 feet/min.)

c For F_{tu} = 200 ksi AISI 4130, 8630, 4135, 8740 not available; thickness ≤ 0.80 in. for AISI 8740; ≤ 1.00 in. for AISI 4140; ≤ 1.70 in. for AISI 4340, 4330V, 4335V, and Hy-Tuf [Quenched in molten salt at desired tempering temperature (martempering)]; ≤ 2.50 in. for AISI 4340, 4330V, 4335V, and Hy-Tuf (Quenched in oil at a flow rate of 200 feet/min.); ≤ 3.50 in. for AISI 4340 (Quenched in water at a flow rate of 200 feet/min.); ≤ 5.00 in. for D6AC (Quenched in oil at a flow rate of 200 feet/min.)

d There is no statistical basis (T_{99} or T_{90}) or specification basis (S) to support the mechanical property values in this table. See Heat Treatment in Section 2.3.0.2.

Chemical Composition

The following table shows the chemical composition of aluminium / aluminum 2117-T4 alloy.

Element	Content (%)
Aluminum, Al	94.3 - 97.6
Copper, Cu	2.2 - 3
Silicon, Si	≤ 0.80
Iron, Fe	≤ 0.70
Zinc, Zn	≤ 0.25
Magnesium, Mg	0.20 - 0.50
Manganese, Mn	≤ 0.20
Chromium, Cr	≤ 0.10
Other (each)	≤ 0.050
Other (total)	≤ 0.15

Physical Properties

The physical properties of aluminium / aluminum 2117-T4 alloy are outlined in the following table.

Properties	Metric	Imperial
Density	2.75 g/cm³	0.0994 lb/in³
Melting point	554 - 649°C	1030 - 1200°F

Mechanical Properties

The mechanical properties of aluminium / aluminum 2117-T4 alloy are tabulated below.

Properties	Metric	Imperial
Tensile strength	296 MPa	43000 psi
Yield strength	165 MPa	24000 psi
Elongation at break (@diameter 12.7 mm/0.500 in)	27%	27%
Poisson's ratio	0.33	0.33
Elastic modulus	71 GPa	10300 ksi
Shear strength	193 MPa	28000 psi
Hardness, Brinell (@load 500 kg; thickness 10.0 mm)	70	70
Hardness, Knoop (converted from Brinell hardness value)	93	93
Hardness, Vickers (converted from Brinell hardness value)	81	81
Machinability	50	50

Thermal Properties

The thermal properties of aluminium / aluminum 2117-T4 alloy are tabulated below.

Properties	Metric	Imperial
Thermal expansion co-efficient (@20-100°C/68-212°F)	23.8 µm/m°C	13.2µin/in°F
Thermal conductivity	154W/mK	1070 BTU in/hr.ft².°F

ALLOY 400

MECHANICAL PROPERTIES

////TYPICAL ROOM TEMPERATURE TENSILE PROPERTIES

Condition	Yield Strength 0.2% offset		Tensile Strength		Elongation	Elastic Modulus (E)	
	psi	MPa	psi	MPa	% in 2"	psi	GPa
Annealed	35 000	240	75 000	520	45	26 x 10^6	180
Hot rolled as rolled	45 000	310	80 000	550	30	26 x 10^6	180

//// SHORT TIME ELEVATED TEMPERATURE PROPERTIES

The following table illustrates the short time tensile properties of Alloy 400 at temperatures above room temperature. Low temperature properties are added for comparison.

Temperature		Yield Strength 0.2% offset		Tensile Strength		Elongation
°F	°C	psi	MPa	psi	MPa	% in 2"
70	21	31 000	215	82 000	565	48
200	93	30 000	205	80 000	550	47
400	204	26 000	180	75 000	520	45
600	316	25 000	175	73 000	505	46
800	427	23 000	160	70 000	480	48
1000	538	21 000	145	53 000	370	40

PHYSICAL PROPERTIES

Density
0.318 lb/in³
8.80 g/cm³

Magnetic Permeability
75°F, 200 oersted 1.0002

Specific Heat
0.10 Btu/lb-°F
430 J/kg-°K

Specific Gravity
8.83

Melting Range
°F – 2370-2460
°C – 1300-1350

THERMAL PROPERTIES

Temperature		Mean Linear Expansion[a]		Thermal conductivity[a]		Specific Heat[a]		Electric Resistivity[a,c]	
°F	°C	10^{-6} in/in/°F	10^{-6} cm/cm/°C	Btu/h-ft-°F	W/m-°K	Btu/lb-°F	J/kg-°K	Ω-circ mil/ft	μΩ.m
−320	−200	–	–	–	–	–	–	205	0.360
−300	−180	6.1	11.1	113	16.5	0.050	223	–	–
−200	−130	6.4	11.4	130	18.2	0.078	320	–	–
−100	−70	6.7	12.1	139	19.8	0.088	378	–	–
70	21	–	–	151	22.0	0.102	427	307	0.511
200	100	7.7	14.2	167	24.0	0.105	445	322	0.537
400	200	8.6	15.2	193	26.9	0.110	459	337	0.559
600	300	8.8	15.7	215	30.1	0.114	470	346	0.574
800	400	8.9	16.1	238	33.4	–	–	355	0.587
1000	500	9.1	16.3	264	36.5	–	–	367	0.603
1200	600	9.3	16.6	287	39.4	–	–	379	0.620
1400	700	9.6	17.0	311	42.4	–	–	391	0.639
1600	800	9.8	17.4	335[d]	45.5[d]	–	–	403	0.658
1800	900	10.0[d]	17.7	360[d]	48.8[d]	–	–	415	0.675
2000	1000	10.3[d]	18.1[d]	–	–	–	–	427	0.692

[a] These values also apply to Alloy R-405, the free machining version of Alloy 400.
[b] Annealed material. Between 70°F (21°C) and temperature shown. [c] Annealed material. [d] Extrapolated

Attachment B. Spring Calculus Constants

Thickness 0.2 (Rivet Soli	lbs/in.	in.	psi	in.2
Skin thickness		0,200		
Doubler thickness		0,200		
Fastener diameter		0,156		
E - Modulus Skin			10400000,000	
E - Modulus Fastener			10300000,000	
A				5,000
B				0,800
Spring Constant (General)	260000,000			
Lenght		0,125		
Area				0,019
Spring Constant tension	1580000,212			

Thickness 0.5 (Hi-Lock)	lbs/in.	in.	psi	in.2
Skin thickness		0,200		
Doubler thickness		0,500		
Fastener diameter		0,188		
E - Modulus Skin			10400000,000	
E - Modulus Fastener			29700000,000	
A				1,667
B				0,860
Spring Constant (General)	697487,257			
Lenght		0,125		
Area				0,028
Spring Constant tension	6560529,034			

Thickness 0.2 (Hi-Lock)	lbs/in.	in.	psi	in.2
Skin thickness		0,050		
Doubler thickness		0,200		
Fastener diameter		0,188		
E - Modulus Skin			10400000,000	
E - Modulus Fastener			29700000,000	
A				1,667
B				0,860
Spring Constant (General)	342210,328			
Lenght		0,125		
Area				0,028
Spring Constant tension	6560529,034			

External Tank Drag | Loads | **Spring Constant** | Hi-Lock Elements | Solid Rivets Elements | Bolt Elements | Fitting Elements

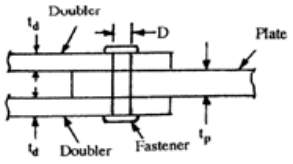

$$k = \frac{E\,D}{[A + B(\frac{D}{t_d} + \frac{D}{t_s})]}$$

where: k – Fastener spring constant (lbs./in.)
E – Modulus of skin and doubler
D – Fastener diameter
t_s – Skin thickness
t_d – Doubler thickness
A – 5 for aluminum fasteners
1.667 for steel fasteners
B – 0.8 for aluminum fasteners
0.86 for steel fasteners

Attachment C. Pylon Fitting Analysis

Data

External Tank	
Wing Pylon Tank Installation Wheight (l	791
Installation Full Wheight (Kg)	4490,564
Installation Full Wheight (Lbs)	9900
Fuel Density	0,7
Capacity (L)	6415,09143
Total Lenght (in.) (fuel)	262,5
Total Lenght (in.)	308,4
Max Diam Ext Tank (in)	45
Height Pylon (in.) Front	22,0472441
Height Pylon (in.) Rear	20,8661417
Distance Btw Centre tank -fix (Front)	44,5472441
Distance Btw Centre tank -fix (Front)	43,3661417
Density 20000 ft (lbs/in3)	3,1805E-06
Density 20000 ft (kg/m3)	0,0880349
Maximum speed at 20000 ft (knot)	320
Maximum speed at 20000 ft (m/s)	164,622222
Maximum speed at 20000 ft (in./s)	6481,18985
Surface (in.2)	1590,43128
Surface (m.2)	1,02608265
Cd	0,81
l/d	6,85333333

Pylon	
Lenght	78,2
Height	21,4566929
Depth	9,84251969
Surface (in.2)	211,187922
l/h	3,64455046
Cd	1,2

Reactions Instalation Weight

	1_Pylon Fix (R	Central Point	2_Pylon F	End Point
Ext. Tank Stations	98,3	131,25	176,5	262,5
Distances	32,95		45,25	
Components_Weight	5728,580563		4171,419	

Drag (External Tank+Pylon)

Drag (lb.in/s2)	102982,2939
Drag (lbf)	3200,787546
R1_Drag	1823,353761
R2_Drag	1823,353761
R1	7551,934324
R2	4171,419437

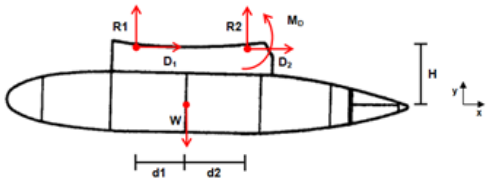

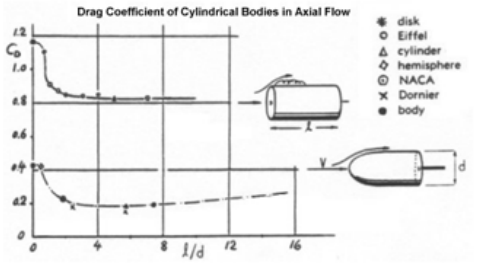

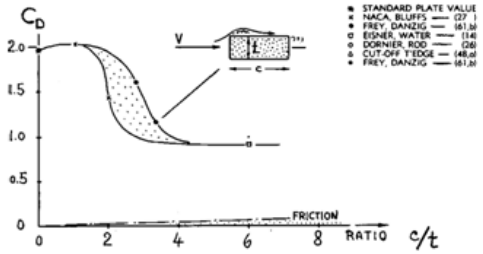

External Tank Drag | Loads | Spring Constant | Hi-Lock Elements | Solid Rivets Elements | Bolt Elements | Fitting Elements | Folha3

Hi-Lock Elements

Load Condition	Elemento	FX	FY	FZ	Force (lbs)	MS_F
Vertical Load n=1 (Static)	131307,000		68,453		69,026	18,601
	131306,000	8,878				
	131331,000		61,536		62,995	20,477
	131330,000	13,480				
	131313,000		26,633		41,056	
	131312,000	31,245				
	131596,000			141,040	141,040	13,683
Vertical Gust Load n= 8.25	131307,000		446,030		449,691	2,009
	131306,000	57,261				
	131331,000		400,150		409,690	2,302
	131330,000	87,897				
	131313,000		172,880		266,487	4,077
	131312,000	202,800				
	131596,000			851,821	851,821	1,431
Banked turn Load n=3	131297,000		142,980		229,994	4,883
	131296,000	180,150				
	131301,000		134,060		237,635	4,693
	131300,000	196,210				
	131305,000		111,440		230,351	4,874
	131304,000	201,600				
	131313,000		23,701		225,270	
	131312,000	224,020				
	131602,000			353,380	353,380	4,860

Fasterner data (MS2002C6)

Fastener diameter	Area (in2)	FU (Lbs)	Fshear_off (Lbs)	Yield Strenght (Psi	Tensile Strenght (Ps	hear Strenght (Ps	E (Psi)
0,188	0,028	2070,874	1352,971	35000,000	75000,000	49000,000	26000000,000

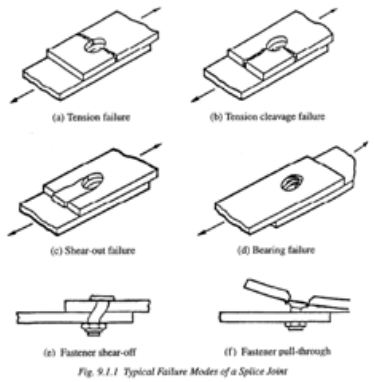

Fig. 9.1.1 Typical Failure Modes of a Splice Joint

Fastener Shear-off load:

$$P_{sot} = F_{su}\left(\frac{\pi D^2}{4}\right) \qquad \text{Eq. 9.2.1}$$

where: F_{su} – Allowable ultimate shear stress of the fastener material from Ref. 9.1.
D – Nominal fastener shank diameter

Bearing

Fitting data Bearing

Load Condition	et Thickness	σbrg (Psi)	1,5σbrg (Psi)	σbru (Psi)	D_rivets (in)	F_bearing_rivet	MS_bearing_rivet
Vertical Load (Static)	0,050	119000,000	178500,000	156000,000	0,188	1462,500	20,188
Gust Load 8.25	0,050	119000,000	178500,000	156000,000	0,188	1462,500	2,252
Banked turn Load n=3	0,050	119000,000	178500,000	156000,000	0,188	1462,500	5,349

$P_{bearing}=MIN(\sigma_{br\text{-}u}\cdot D\cdot t \quad or \quad 1{,}5\cdot\sigma_{br\text{-}y}\cdot D\cdot t)$

Attachment D. Sealants Tests Results

Air content Test

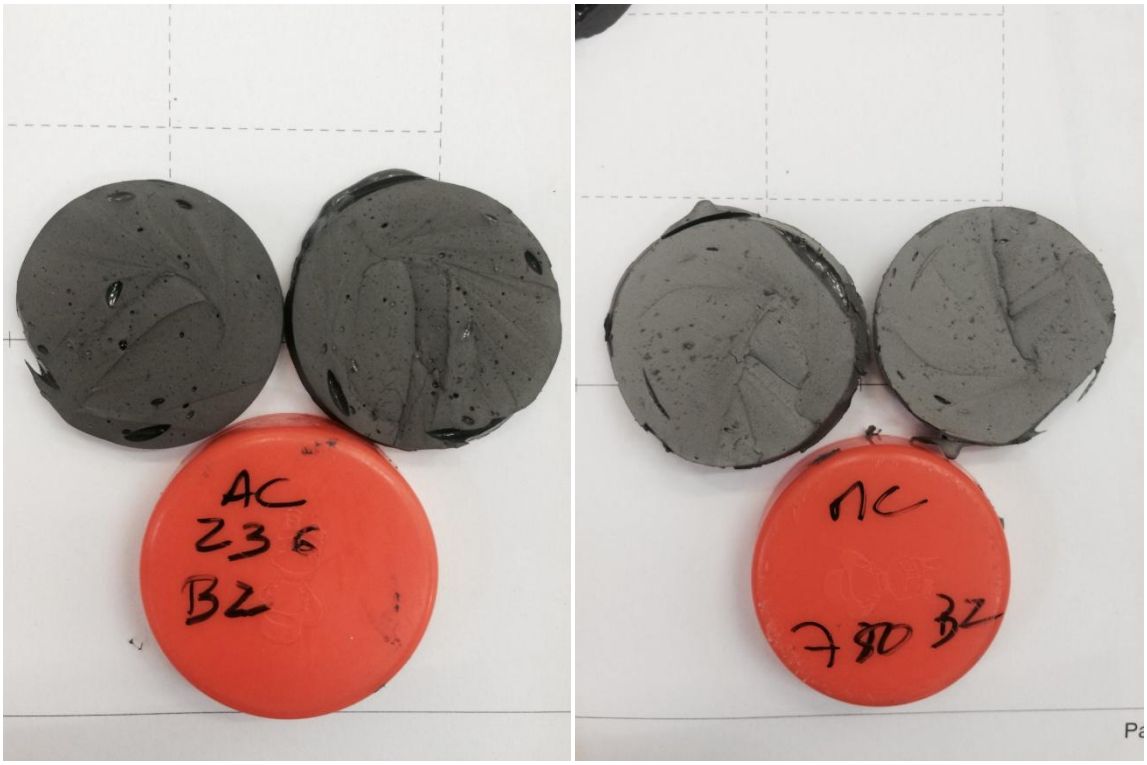

Figure D.1 – AC 236 B2 & MC 780 B2

Figure D.2 – PR 1440 B2 & PS 870 B2

Shear Strength Test Results

Specimen Dimensions:

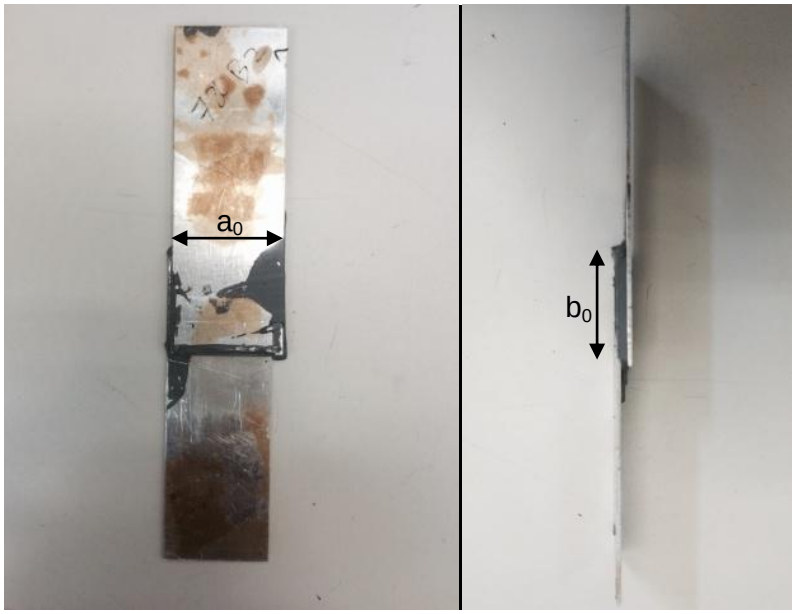

Figure D.3 – Shear strength specimen final assembly and a particular specimen

Product: AC 236 B2

Specimen No.	*a_0 (in)*	*b_0 (in)*	*S_0 (in^2)*	*σ (Psi)*	*Failure Mode*
1	1.006	0.969	0.9748	319.85	Cohesive
2	1.017	0.962	0.9784	331.13	Cohesive
3	0.97	0.974	0.9448	339.96	Cohesive

Table D.1 – Shear strength specimens data and results

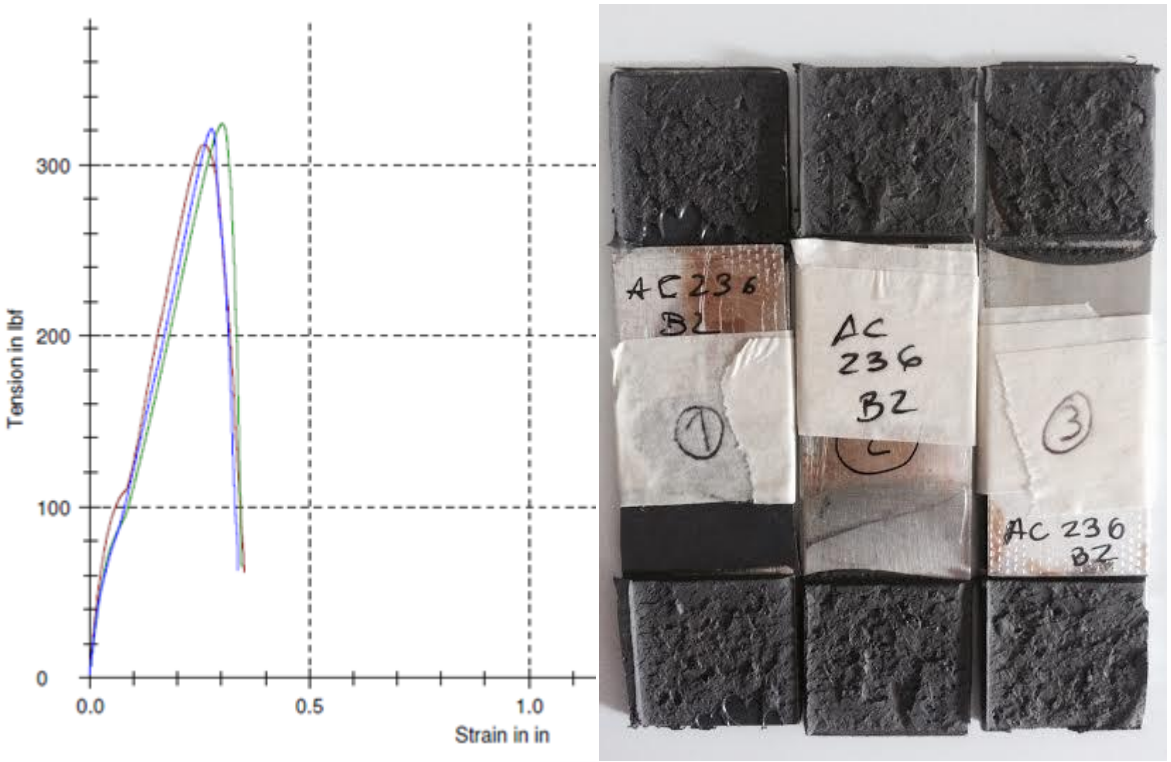

Figure D.4 – Shear strength vs. strain and specimens after test

Product: MC 780 B2

Specimen No.	a_0 *(in)*	b_0 *(in)*	S_0 *(in^2)*	σ *(Psi)*	*Failure Mode*
1	0.977	0.92	0.8988	215.11	Cohesive
2	0.981	0.902	0.8849	200.56	Cohesive
3	0.998	0.911	0.9092	171.47	Cohesive

Table D.2 – Shear strength specimens data and results

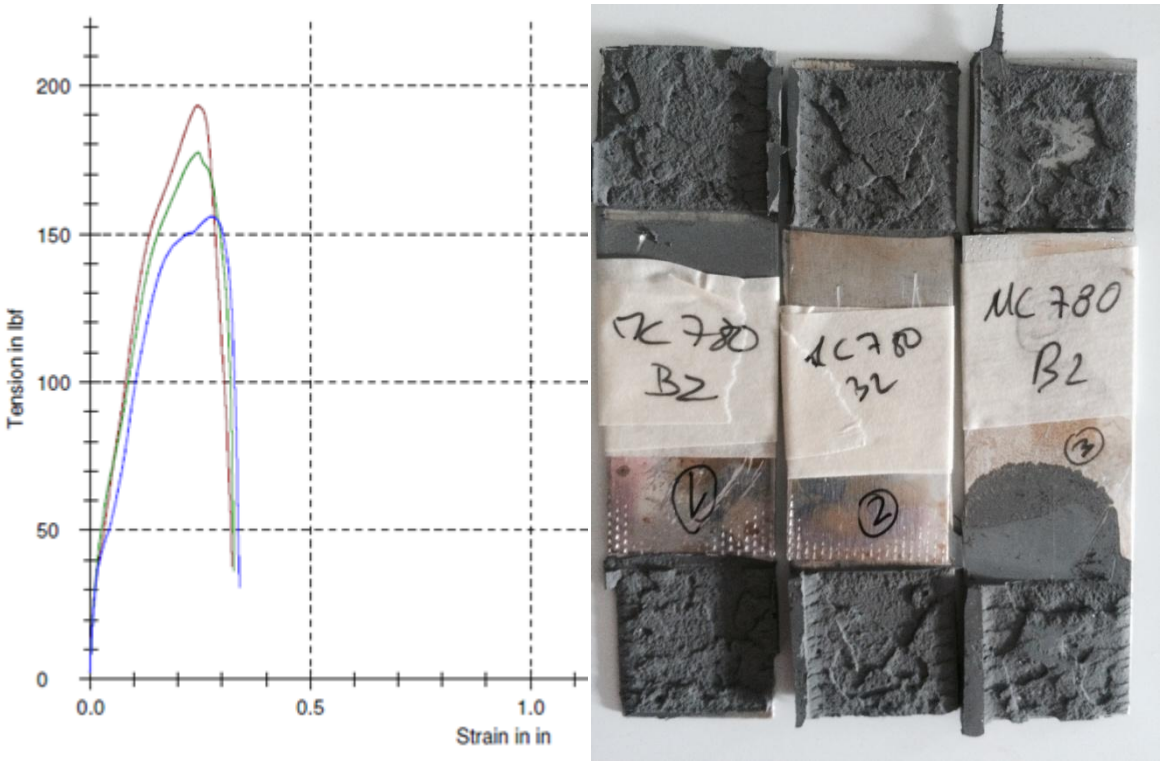

Figure D.5 – Shear strength vs. strain and specimens after test

Product: PR 1440 B2

Specimen No.	a_0 *(in)*	b_0 *(in)*	S_0 *(in^2)*	σ *(Psi)*	*Failure Mode*
1	0.985	0.991	0.9761	278.02	Cohesive
2	1.036	0.975	1.01	328.37	Cohesive
3	0.986	0.973	0.9594	278.91	Cohesive

Table D.3 – Shear strength specimens data and results

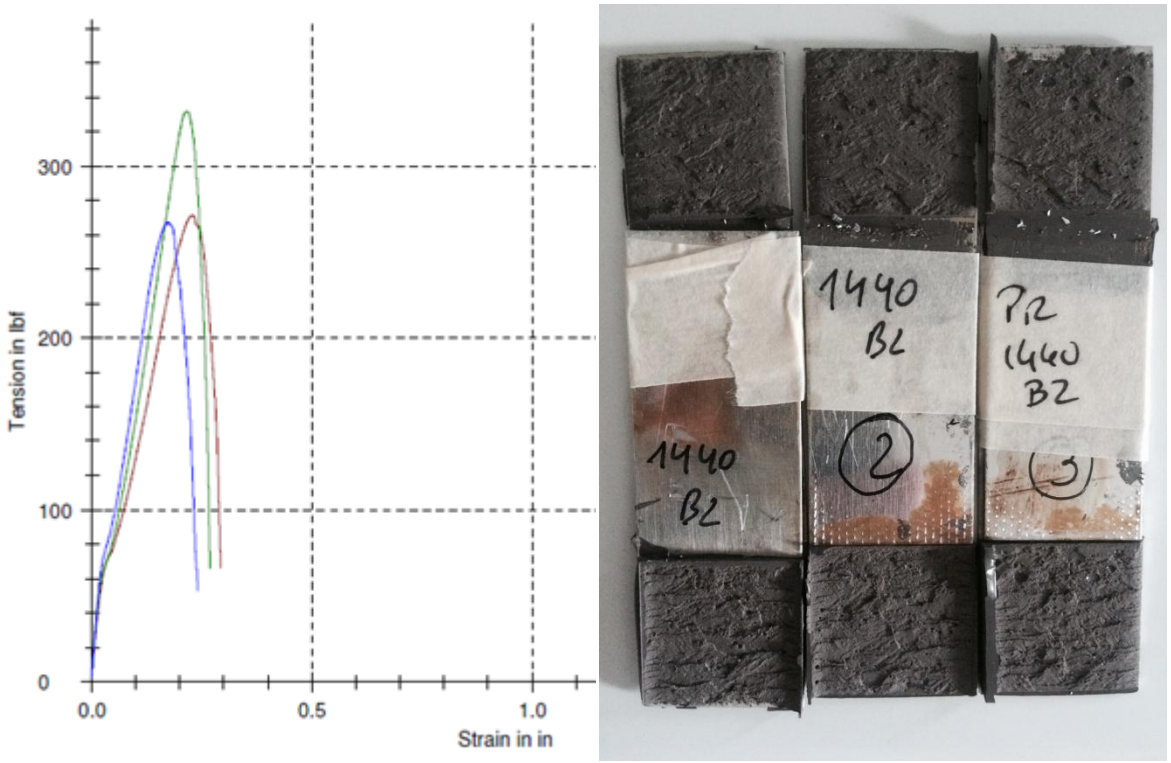

Figure D.6 – Shear strength vs. strain and specimens after test

Product: PS 870 B2

Specimen No.	a_0 *(in)*	b_0 *(in)*	S_0 *(in²)*	σ *(Psi)*	*Failure Mode*
1	0.956	0.936	0.8948	209.52	Cohesive
2	0.982	0.932	0.9152	226.52	Cohesive
3	0.962	0.948	0.912	238.35	Cohesive

Table D.4 – Shear strength specimens data and results

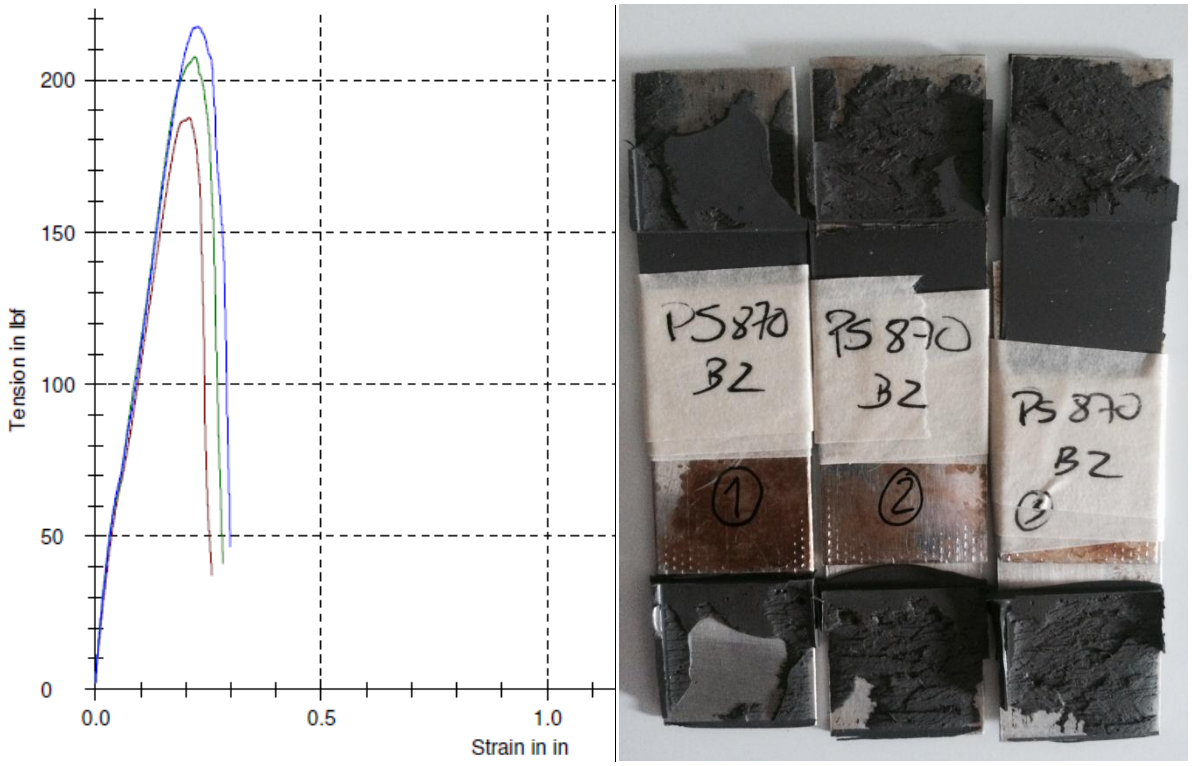

Figure D.7 – Shear strength vs. strain and specimens after test

Peel Strength Test Results

Product: AC 236 B2

Specimen No.	b_0 *(in)*	$F_{max(mean)}$ *(Lbf)*	F_{min} *(Lbf)*
1	1	28,7	3,12
2	1	36,8	3,86

Table D.5 – Peel strength specimens data and results

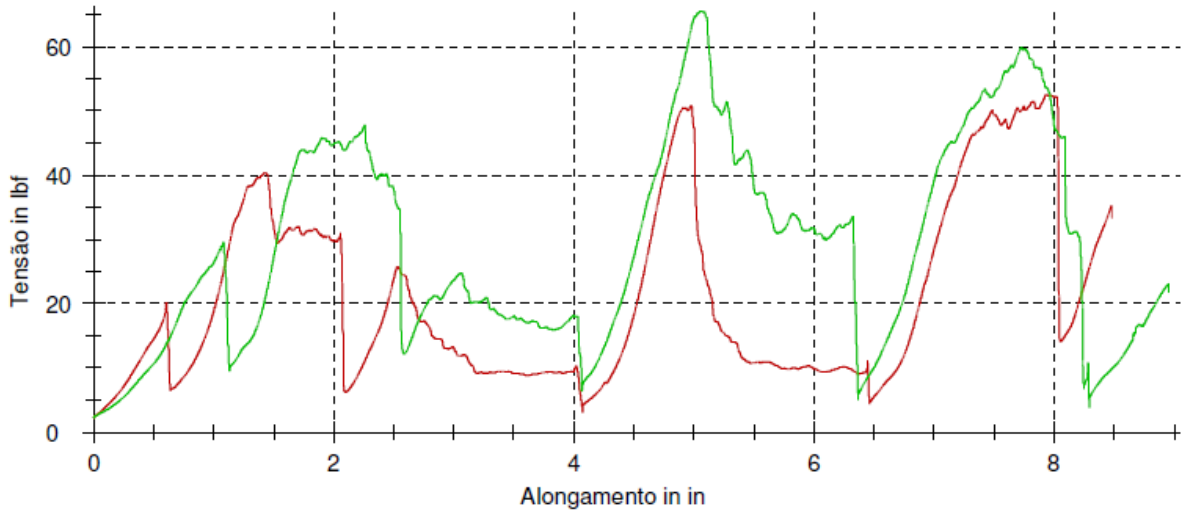

Figure D.8 – Peel strength vs. strain

Product: PR 1440 B2

Specimen No.	b_0 *(in)*	$F_{max(mean)}$ *(Lbf)*	F_{min} *(Lbf)*
1	1	14,7	3,57
2	1	31,4	3,50

Table D.6 – Peel strength specimens data and results

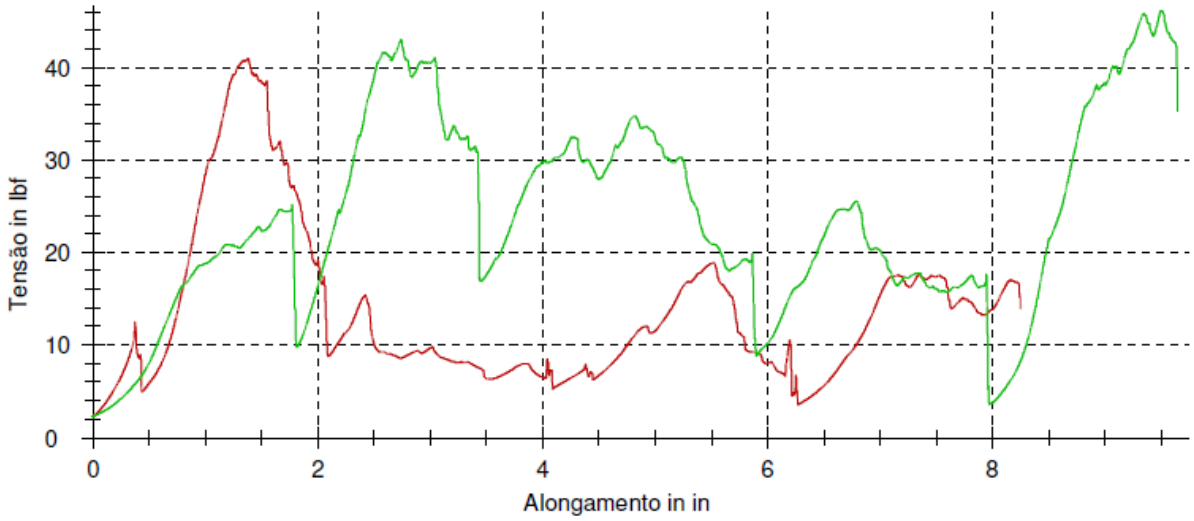

Figure D.9 – Peel strength vs. strain

Product: MC 780 B2

Specimen No.	b_0 *(in)*	$F_{max(mean)}$ *(Lbf)*	F_{min} *(Lbf)*
1	1	14,4	3,83
2	1	13,4	5,46

Table D.7 – Peel strength specimens data and results

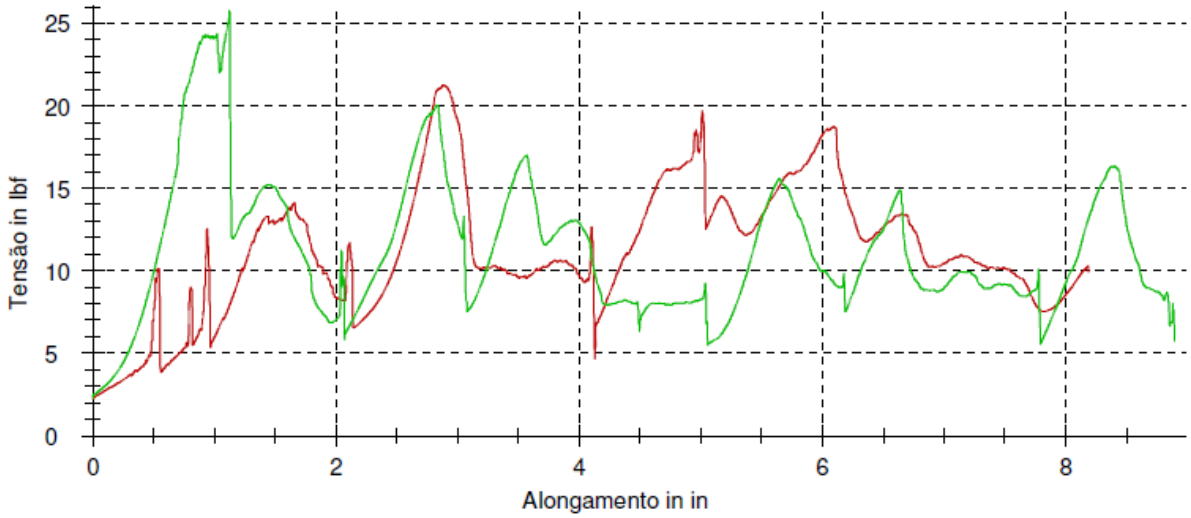

Figure D.10 – Peel strength vs. strain

Example of Peel Strength Test:

Specimen No.	b_0 *(in)*	$F_{max(mean)}$ *(Lbf)*	F_{min} *(Lbf)*
1	1	71,6	22,7

Table D.8 – Peel strength specimens data and results

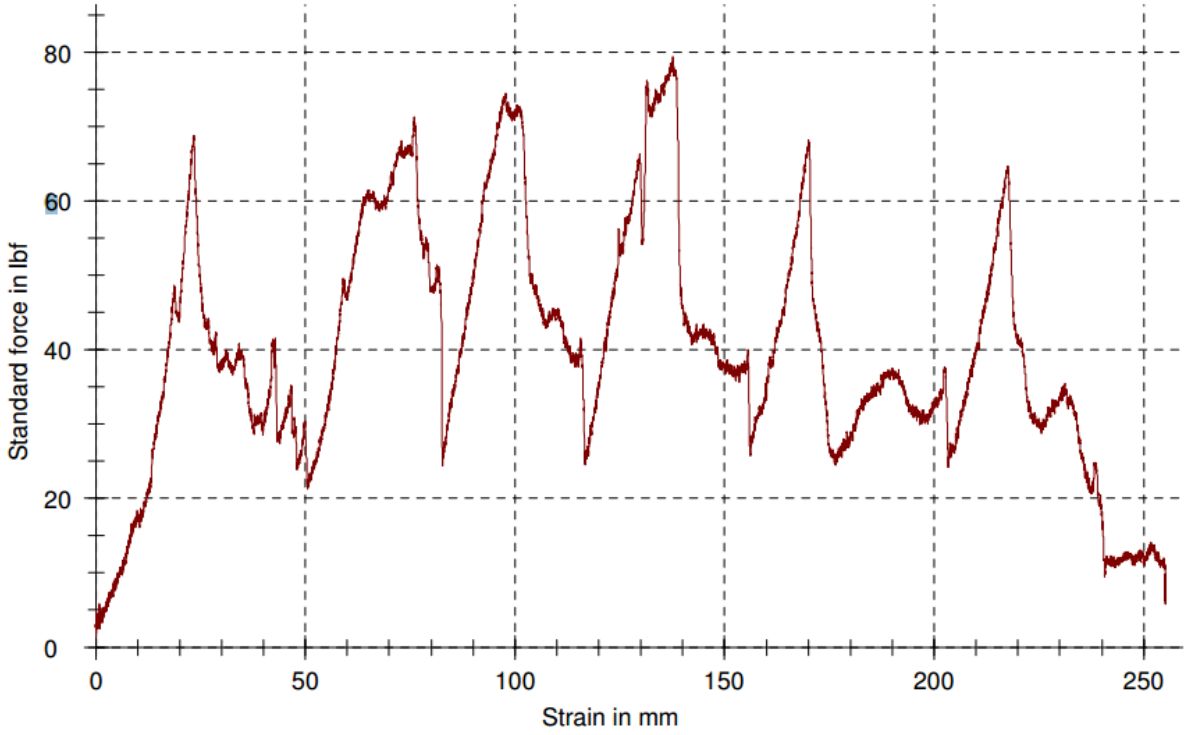

Figure D.11 – Peel strength vs. strain